

UNCLASSIFIED

AD NUMBER
AD463868
NEW LIMITATION CHANGE
TO Approved for public release, distribution unlimited
FROM Distribution authorized to U.S. Gov't. agencies and their contractors; Administrative/Operational Use; APR 1965. Other requests shall be referred to Air Force Materials Laboratory, Wright-Patterson AFB, OH 45433.
AUTHORITY
AFML ltr dtd 23 Jul 1974

THIS PAGE IS UNCLASSIFIED

UNCLASSIFIED

AD 4 6 3 8 6 8

DEFENSE DOCUMENTATION CENTER

FOR

SCIENTIFIC AND TECHNICAL INFORMATION

CAMERON STATION ALEXANDRIA. VIRGINIA



UNCLASSIFIED

NOTICE: When government or other drawings, specifications or other data are used for any purpose other than in connection with a definitely related government procurement operation, the U. S. Government thereby incurs no responsibility, nor any obligation whatsoever; and the fact that the Government may have formulated, furnished, or in any way supplied the said drawings, specifications, or other data is not to be regarded by implication or otherwise as in any manner licensing the holder or any other person or corporation, or conveying any rights or permission to manufacture, use or sell any patented invention that may in any way be related thereto.

463868

AFML-TR-65-115

CATALOGED BY: DDC

463868

DIVALENT RARE-EARTH IONS IN OPTICAL MASER MATERIALS

by

G. J. Goldsmith
H. L. Pinch

RADIO CORPORATION OF AMERICA

TECHNICAL REPORT AFML-TR-65-115

APRIL 1965

AIR FORCE MATERIALS LABORATORY
RESEARCH AND TECHNOLOGY DIVISION
AIR FORCE SYSTEMS COMMAND
WRIGHT-PATTERSON AIR FORCE BASE, OHIO

463868

NOTICES

When Government drawings, specifications, or other data are used for any purpose other than in connection with a definitely related Government procurement operation, the United States Government thereby incurs no responsibility nor any obligation whatsoever; and the fact that the Government may have formulated, furnished, or in any way supplied the said drawings, specifications, or other data, is not to be regarded by implication or otherwise as in any manner licensing the holder or any other person or corporation, or conveying any rights or permission to manufacture, use, or sell any patented invention that may in any way be related thereto.

Qualified users may obtain copies of this report from the Defense Documentation Center.

DDC release to CFSTI (formerly OTS) not authorized.

Copies of this report should not be returned to the Research and Technology Division unless return is required by security considerations, contractual obligations, or notice on a specific document.

DIVALENT RARE-EARTH IONS IN OPTICAL MASER MATERIALS

by

**G. J. Goldsmith
H. L. Pinch**

**AVAILABLE COPY WILL NOT PERMIT
FULLY LEGIBLE REPRODUCTION.
REPRODUCTION WILL BE MADE IF
REQUESTED BY USERS OF DDG.**

FOREWORD

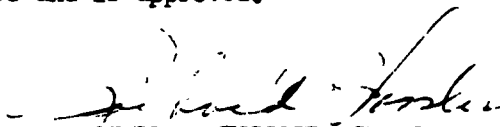
This report was prepared by Radio Corporation of America, RCA Laboratories, Princeton, New Jersey, under USAF Contract No. AF 33(657)-11221. The contract was initiated under Project No. 7371, "Applied Research in Electronic and Magnetic Materials," and Task No. 737101, "Dielectric Materials". The work was administered under the direction of the AF Materials Laboratory, Research and Technology Division, Mr. V. L. Donlan, Project Engineer.

This report covers work conducted from 1 July 1963 to 5 January 1965 in the Materials Research Laboratory, H. W. Leverenz, Director. S. Larach and G. J. Goldsmith were Project Supervisor and Project Engineer, respectively. This report was prepared by G. J. Goldsmith and H. L. Pinch. Other individuals who contributed to the research work reported herein are I. M. Hegyi, A. V. Cafiero, F. K. Fong, Z. J. Kiss, P. N. Yocom, C. H. Anderson, E. S. Sabisky, J. Schwartz, M. M. Hopkins, and R. C. Duncan, Jr.

This report is the Final Report issued under this contract.

Manuscript released by the authors March 1965 for publication as an RTD Technical Report.

This technical report has been reviewed and is approved.


RICHARD J. VOSSLER, Chief
High Energy Physics Branch
Materials Physics Division
AF Materials Laboratory

ABSTRACT

This document represents the third and final report on a study of divalent rare earths in dilute solid solution in hosts suitable for fabrication into optical maser oscillators. The subject matter consists primarily of a description of the final six months' work with summaries and conclusions drawn from the entire eighteen months' investigations. We have attempted to avoid repetition of material reported in the previous Semiannual Progress Reports under this Contract except where the information is germane to current work. As the program progressed, the scope of the effort was continually converged on the materials and problems which appeared to be most critical and which offered the highest probability of success. It will therefore be found that this report concentrates primarily upon the systems BaClF:Ln^{2+} and $\text{ABF}_3\text{:Ln}^{2+}$ (where A = alkali-metal ion, and B = alkaline-earth ion), those compounds selected as best suited to our objectives. The problem is divided into three major categories: reduction of the rare earth from the normal trivalent to divalent; incorporation of the desired ion into the host with retention of the desired valence state; and growth of single crystals of suitable optical quality. The first and third of these categories were satisfactorily solved in many cases, while the second was solved only to a limited extent. It is possible, however, on the basis of these studies to specify in some detail the materials in which, and the conditions under which, this second aspect of the problem can be successfully solved. While most of the studies involved conventional physical and chemical measurements and procedures, some apparatus were designed and constructed which became of sufficiently general utility throughout the laboratories to warrant a brief description of their construction and performance herein. Also included are the relevant calibration measurements necessary for a thorough understanding of the experimental procedures and results.

TABLE OF CONTENTS

<u>Section</u>	<u>Page</u>
I. INTRODUCTION	1
A. Lasers and Divalent Rare Earths	1
B. Hosts	3
C. Reduction of the Rare Earth	4
D. Composition of the Host	9
E. Choice of Rare Earth	10
II. CHEMICAL STUDIES	13
A. Perovskites	13
B. Halofluorides	16
C. The Stability and Retention of Divalent Rare-Earth Ions	24
D. Purification and Growth of Alkaline-Earth Halides	31
III. SPECTRAL STUDIES	33
A. Halofluorides	33
B. Perovskites	66
C. SrCl_2	80
IV. INSTRUMENTATION	85
A. Visible and Near IR Spectrometer	85
B. IR Spectrometer	87
C. Excitation Spectrometer	90
D. Lifetimes	90
E. Light Sources	91
F. Detectors	92
G. Filters	95
H. Calibration	95
V. RECOMMENDATIONS FOR FURTHER WORK	102
A. Growth of Crystals in Sealed Metallic Systems	102
B. Detailed Spectrographic and Metallographic Studies of Crystals Grown under the Above-Mentioned Conditions	102
C. Quenching Studies	103
D. High-Temperature and Molten-State Absorption Spectroscopy	103
E. 5d Fluorescent States, Vibronic Transitions and Color Centers	104
F. Divalent Rare-Earth-Containing Perovskites	104
G. General Rare-Earth Studies	104
REFERENCES	105

LIST OF ILLUSTRATIONS

<u>Figure</u>	<u>Page</u>
1. Energy level scheme for ideal 4-level laser	2
2. Crystal structure of BaClF	17
3. Gradient freeze furnace	20
4. Cooling program for gradient freeze furnace	21
5. Energy level scheme for Dy ³⁺ and Dy ²⁺	34
6. Fluorescence spectrum of Dy ³⁺ in SrCl ₂ at 77°K	36
7. Excitation spectrum of Dy ³⁺ in SrCl ₂ at 77°K with absorption spectrum of DyCl ₃ aqueous solution	37
8. Fluorescence spectrum of "pure" BaClF at 77°K	39
9. Absorption spectra of BaClF pure and BaClF:Dy ³⁺ (O) at 77°K . .	40
10. Fluorescence spectra of BaClF:Dy ³⁺ with varying amounts of oxygen at 77°K	41
11. Fluorescence of BaClF:Dy ³⁺ (O) - residue and crystal at 77°K . .	43
12. Fluorescence spectrum of BaClF:DyOCl at 77°K	44
13. Absorption and excitation spectra of BaClF:Dy ³⁺ (O)	45
14. Fluorescence of BaClF:Dy ³⁺ :Sm ²⁺ (O) under excitation by 2537 Å and 3650 Å	47
15. Fluorescence spectrum of BaClF:Dy ²⁺ at 77°K	49
16. Excitation spectrum for BaClF:Dy ²⁺ at 77°K (Uncorrected). . . .	50
17. Fluorescence of BaCl ₂ :Dy ²⁺ at 77°K	52
18. Energy level scheme for Ho ³⁺ and Ho ²⁺	53
19. Fluorescence spectrum of BaClF:Ho ³⁺ at 77°K	54
20. Fluorescence of BaClF:Ho ²⁺ at 77°K, Hg-lamp excitation	55
21. Excitation spectrum of BaClF:Ho ²⁺ at 77°K (Uncorrected)	56
22. Fluorescence spectrum of BaClF:Ho ²⁺ at 77°K, W-lamp excitation.	58
23. Energy level scheme for Tm ³⁺ , Tm ²⁺	60
24. Fluorescence of Tm ³⁺ in SrCl ₂ at 77°K	61
25. Fluorescence of Tm ²⁺ in various hosts at 77°K	62
26. Fluorescence of BaClF:Tm ²⁺ at 77°K	63
27. Energy level scheme for Sm ³⁺ , Sm ²⁺	64
28. Fluorescence of BaClF:Sm ²⁺ in halofluorides at 77°K	65
29. Crystal structure of ABF ₃ perovskites	68

LIST OF ILLUSTRATIONS (CONT'D.)

<u>Figure</u>	<u>Page</u>
30. Fluorescence spectrum of Nd^{3+} in RbMgF_3 melt, 77°K	68
31. Fluorescence of Nd^{2+} in RbMgF_3 crystal, 77°K	69
32. Fluorescence of Sm in RbMgF_3 melt and crystal, 77°K	72
33. Lifetime of Sm^{2+} in RbMgF_3 , 77°K	74
34. Excitation spectra in $\text{RbMgF}_3:\text{Sm}^{2+}$, 77°K (Uncorrected)	75
35. Fluorescence spectra of $\text{NaMgF}_3:\text{Sm}^{2+}$, 77°K	77
36. Fluorescence of Ho^{3+} in RbMgF_3 , 77°K	79
37. Fluorescence of Dy^{3+} in KCaF_3 , 77°K	81
38. Influence of charge compensation on Tm concentration in SrCl_2 (Nominal concentration, 0.05 mole %)	82
39. Fluorescence of divalent rare earths in SrCl_2 at 77°K	82
40. 5d-band fluorescence in $\text{SrCl}_2:\text{Tm}^{2+}$ at 4.2°K	84
41. Visible and near IR spectrometer	86
42. Tracking and resolution of visible and near IR spectrometer	88
43. IR spectrometer	89
44. Cooled photomultiplier	93
45. Absorption spectrum of 5 cm saturated CuSO_4 solution	96
46. Absorption spectrum of H_2O	97
47. Absorption spectra of Si and Ge filters	98
48. Output calibration of excitation spectrometer	100
49. Spectral sensitivity of 7500 Å-blaze spectrometer and S-1 photomultiplier tube	101

SECTION I

INTRODUCTION

In this introductory section we present a retrospective description of the problem in light of our current information, including a summary of the significant aspects of the work described in the previous two semiannual reports.*

A. LASERS AND DIVALENT RARE EARTHS

Divalent rare earths are most appropriate for the optically pumped 4-level laser system in which the pump light is absorbed in the 4f-5d transitions of the rare earth; a single metastable state in the 4f manifold is then populated; and emission occurs between two 4f levels, the terminal state of which lies more than kT above the ground state (Fig. 1). Rare earths in the divalent state are required in this system because, in contrast to the corresponding isoelectronic trivalent rare earths, the 5d states generally lie in the visible region of the spectrum where they can extract a large fraction of the light from conventional pump sources. In the trivalent species these bands lie far in the ultraviolet beyond the point where pumping sources can reach efficiently and frequently beyond the absorption edge of the host. While these pumping difficulties with the trivalent systems have been overcome in some instances such as in the $\text{CaWO}_4:\text{Nd}^{3+}$ laser¹ where pumping occurs into the large number of 4f-levels of this ion in the visible region of the spectrum, and in the $\text{YAG}:\text{Nd}^{3+}$, Cr^{3+} laser² in which energy transfer occurs between the absorbing states of Cr^{3+} and the Nd^{3+} 4f-levels, the divalent systems represent the most direct analogue of the ideal 4-level laser. As such, they should, in principle, exhibit the highest attainable efficiency. A consideration of the expression of Shawlow and Townes³ for the minimum excess number of atoms in the excited state over those in the terminal state in a Fabry-Perot resonator reveals the necessary additional conditions which must be met for optimized performance. This expression states:

$$n_{\min} = 8\pi^2 e \frac{(1-Q)}{L} v \frac{\Delta v}{v^3} \tau$$

* Footnotes herein refer to Semiannual Progress Report Nos. 1 and 2 issued under Contract No. AF33(657)-11221.

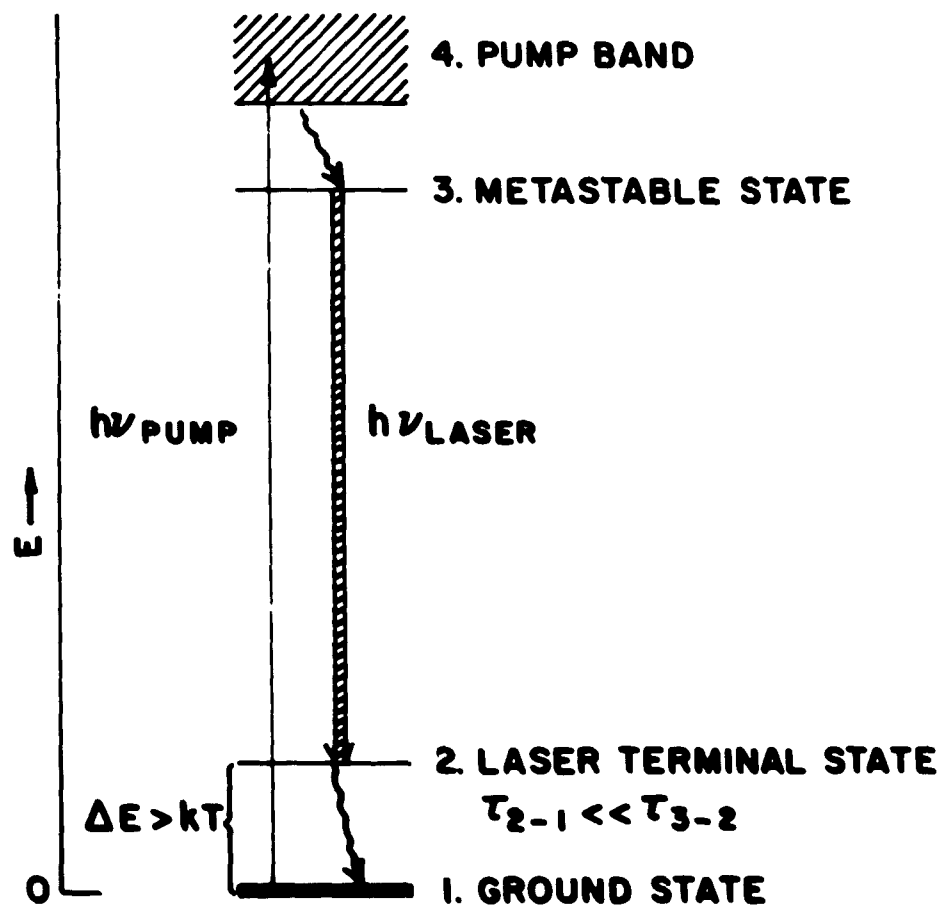


Fig. 1. Energy level scheme for ideal 4-level laser

n_{\min} = minimum excess number of atoms required for oscillation

$\Delta\nu$ = the fluorescent line width

ν = the frequency of oscillation

τ = the radiative lifetime of the state

V = the volume

α = the reflectivity of the ends

L = the length of the oscillator

It is clear from this expression that the ease with which a given system can be made to oscillate is related to minimizing of the product, $(\Delta\nu)\tau$. However, since the attainment of n_{\min} is obviously also related to the rate at which atoms can be excited by the pumping source, then a relatively long lifetime and high absorption coefficient would be desirable. The requirements, in addition to those imposed by the desired level scheme, then become the following:

1. Reasonably long lifetimes, $\sim 10^{-4}$ sec
2. Sharp fluorescence lines
3. High quantum efficiency for the transition of interest
4. Good optical and mechanical quality of the host material

Further, it is important that absorption from the metastable state to levels lying at energies equal to the anticipated laser frequency above it be of low probability. Such absorption would compete with stimulated emission, in effect reducing the number of available ions at any given time. In addition, since in all known real systems only a fraction of the transitions from the pumping levels lead to population of the metastable state, such absorption would prevent achievement of adequate population inversion.

B. HOSTS

There are three major considerations involved in the choice of a suitable host. The first, general for all solid-state optically pumped lasers, is that the host material be obtainable in high optical quality, free of refractive index gradients and scattering centers, that it be mechanically stable to thermal shock, that it be reasonably stable to the atmosphere, and that it not be subject to photochemical decomposition. The second is that it be chemically compatible with divalent rare earths. The third, while not

entirely necessary but a major consideration in the present work, was that there be a singular site for incorporation of the rare earth and that this site not constitute a center of inversion for the crystal. Since the first consideration has not constituted a problem in this work, we need only consider the second two criteria.

The problem of chemical compatibility arises first from the high chemical reactivity of the divalent rare earths. Since, with the exception of Eu and Yb and in some cases Sm, the rare-earth ions are considerably more stable as trivalent ions, they are extremely strong reducing agents. The only cations which are more stable with respect to reduction are those of the alkali metals, the alkaline earths, and possibly Mg^{2+} , Th^{4+} , and Zr^{4+} . Upon addition of reasonable criteria with respect to charge and ion size correspondence, the cations which are by far most favorable, are those of the alkaline earths. Compatible anions include the halides, the oxides, and perhaps the sulfides. However, since experimental studies indicate that the oxides and sulfides inhibit the information of divalent rare-earth ions in many cases, we must consider as the outstanding alternatives alkaline-earth halides and ternary compounds having basically the alkaline-earth halide composition.

The classes of compounds which we have therefore considered are the following: the alkaline-earth fluorides; the alkaline-earth halides other than fluoride; the alkaline-earth halofluorides; and the $A^I B^{II} F_3$ perovskites, where A is an alkali-metal ion and B an alkaline-earth ion. Members of each of these categories have particular advantages and disadvantages, and none meets all criteria equally well. The basis for choice of particular compositions is better understood after consideration of the methods available for attainment of the divalent state.

C. REDUCTION OF THE RARE EARTH

The methods for attainment of the divalent state have been divided into two types which we have designated in situ and a priori, respectively. By in situ methods we mean those techniques in which the rare earth is dissolved in the host as the trivalent ion, and where subsequent treatment of the solid host-impurity system leads to the desired valence state. A priori methods involve reduction of the rare earth prior to or during crystal growth.

1. In Situ Methods

In the compounds of interest the rare earth is introduced substitutionally for a divalent cation. Because of the extra positive charge on the trivalent rare-earth ion, charge compensation must be provided. This may be accomplished by the introduction of an equivalent number of monovalent cations, divalent anions, interstitial monovalent anions, cation vacancies, or combinations of these. The general process which accomplishes reduction involves the introduction of free electrons, which may be captured by the rare earth, accompanied by neutralization of the charge compensator.

The first successful in situ reduction method that was employed is that of photoreduction by intense γ -radiation of the solid. This method has been satisfactory essentially only in the alkaline-earth halides and always leads to a self-limiting level of reduction which is significantly less than 100 percent.

The description of the reduction process is most clear in relationship to $\text{CaF}_2:\text{Ln}^{3+}$, but applies equally well to the other alkaline-earth halides. In these hosts, in the absence of deliberately added charge compensator and charge-compensating impurities, compensation must occur through the introduction of alkaline-earth vacancies and interstitial fluoride ions. Evidence has been found for both types of compensation. In the gamma-ray flux, the crystal is flooded with free electrons. Under steady-state irradiation conditions these electrons are continually being captured and re-excited, the principal activity occurring presumably among the major lattice constituents. Interstitial charge compensators and the rare-earth impurity also act as electron sources (and traps). The trivalent rare earths and the neutral interstitial fluorine atoms are competing traps for a fraction of the free electrons with the F^0 , undoubtedly the trap of higher cross section. Electrons trapped by rare-earth ions which are spatially remote from charge compensators remain divalent primarily because the energy barrier which must be surmounted or penetrated in order to find a site of lower free energy is too high. After irradiation, then, the lattice contains divalent rare-earth ions and an equal number of interstitial fluorine atoms. If lattice defects and impurities such as O^{2-} are also present, it is obvious that other mechanisms will apply.* Whatever the details of the process, however, the

* Semiannual Progress Report No. 1, pp. 49-75.

end result is necessarily a crystal containing rare-earth ions which are metastable with respect to re-oxidation and containing high cross-section traps for free electrons. As a consequence, photoreduced ions are not stable to heat and to absorbed light.

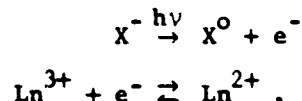
The stability of the reduced ion may be improved substantially by the removal of the neutral charge compensator. One technique for accomplishing this is reduction of the rare earth by exposure of the crystal to alkaline earth metal vapor at elevated temperatures.⁴ In addition to the creation of greater stability, this process also leads to more complete reduction. The mechanism is described in the following manner. At the elevated temperature necessary to produce reasonable vapor pressure of alkaline-earth metal (800°C in the case of Ca), the ionic mobility and diffusion coefficients within the crystal become high. Two different processes can then occur. First, calcium-metal atoms will diffuse into the crystal to be captured at vacancies releasing two free electrons for each site occupied. These electrons are then captured by the rare-earth ion, in principle the only trap available. Second, interstitial fluoride ions will migrate to the surface to react with calcium atoms forming new surface lattice sites also with release of free electrons. If we assume that there are no impurities other than rare earth, only cationic vacancies and interstitial fluoride ions can provide charge compensation. The removal of these defects then must result in total reduction of the rare earth and the absence of their "oxidation products," leading to stability for the reduced rare earth. In practice, however, reduction by this method does encounter some difficulties. Our alkaline-earth halide crystals are not, in general, free of impurities (especially O^{2-}) which act as charge compensators and which occupy lattice sites. While the role of O^{2-} in this reduction process is not well understood, it is evident that it inhibits completion of the reduction. Also, since treatment of CaF_2 with Ca-vapor is a well-known method for the introduction of additive color centers, the process must be controlled very carefully to avoid creation of these centers. Coloration evidently begins to take place long before all the rare-earth ions are reduced.

A second technique which provides for removal of the charge compensator is that of solid-state electrolysis.*^{5,6} In this method the crystal is

* Semiannual Progress Report No. 2, p. 7.

placed between electrodes in a furnace, the temperature of which can be raised to 700°C. When a dc current is passed through the heated crystal, reduction is observed to proceed through the crystal starting at the anode. The process may be pictured as the electric-field-induced migration of the interstitial halide ions to the anode where they become neutralized, and the simultaneous injection of electrons at the cathode. While the interstitial fluoride ions are by far the most mobile ionic species in the crystal, the cationic vacancies presumably are also somewhat mobile and will also drift toward the anode. The removal of the cationic vacancies can be enhanced through the use of Ca metal electrodes.* This method also leads to a far greater degree of reduction than does gamma radiation, but homogeneity is considerably less satisfactory as a consequence of impurities and imperfections in the crystals.

A third type of in situ reduction method in which the charge compensator is removed is that of high-temperature solid-state photoreduction. This procedure is analogous to the molten-state photoreduction process reported previously.** 7 The chemical equations for both processes are



In the usual (room temperature and below) photoreduction experiments with gamma rays on crystals, the oxidized halogen species (X^0 , X_2^- , etc.) remain in the crystal and are strong electron traps for the reionized electron from the Ln^{2+} . In the molten-state photoreduction the oxidized halogens are mobile in the liquid and can be pumped off through the surface. The divalent rare earth is thus quite stable in the resulting crystal. If a crystal with Ln^{3+} is irradiated just below its melting point while under vacuum, then the X^0 produced may have sufficient mobility to diffuse to the surface and be pumped off. Stable Ln^{2+} would result from such a process. As a test of this hypothesis, a $\text{CaF}_2:\text{Dy}^{3+}$ crystal was heated to 1000°C on a molybdenum ribbon in a bell jar vacuum system and irradiated with an unfocused 100-watt low-pressure mercury lamp held about 2 inches from the heated crystal. The irradiation was carried out for several hours. The crystal was rapidly cooled in the absence of the radiation. Very weak Dy^{2+} emission was found. The

* E. Sabisky, Unpublished work.

** Semiannual Progress Report No. 2, p. 7.

solid-state process is much less efficient than the molten-state photoreduction which produced very high concentrations of Ln^{2+} under conditions of somewhat lower uv flux. If the crystal had been heated closer to the melting point of CaF_2 (1360°C), the mobility of the X^0 species would be increased and a larger concentration of Ln^{2+} may have resulted. Crystal growth and annealing under irradiation may be the answer to the problem of retention of divalent rare earths.

The in situ reduction techniques depend of course on our ability to incorporate trivalent rare earths into the lattice. Further, assuming the mechanisms described herein do apply, these methods will result in the reduction of rare earths only if charge compensation is achieved through vacancies or interstitial halide ions. This latter point is confirmed in the case of $\text{SrCl}_2:\text{Tm}^{3+}$ compensated by Na^+ in which photoreduction was found not to take place while it occurs readily in "uncompensated" crystals. The particular advantages of the in situ methods lie in the fact that, since the rare earth is already incorporated in the crystals, one is no longer concerned with oxidizing impurities which may be present in the ambient environment. Further, because the solid material is treated well below its melting point, such auto-oxidation processes as disproportionation are much less likely to take place.

2. A Priori Methods

While in situ reduction offers many advantages, it is limited to those hosts which can incorporate significant concentrations of trivalent rare earth ions. The compounds which have become of particular importance in these studies, the halofluorides and the perovskites, are among those which accommodate only negligible quantities of the trivalent species even in the presence of an excess of cationic charge compensator. The divalent rare-earth ions, on the other hand, will substitute readily at the alkaline-earth sites in these compounds, and hence the a priori methods become important.

These reduction techniques are entirely analogous to those of familiar solution chemistry save in one instance where gamma radiation is employed. However, because of the high reactivity of the divalent rare earths, reduction must be carried out in the molten host compound and special attention must be paid to the elimination of oxidizing agents such as oxygen, hydroxyl ion, hydrogen halide gases, and transition metal ions. Purification procedures

were worked out for the constituents of the host and the host itself as described in Section II of this report and in the previous two Semiannual Reports on this contract. The reducing agents are either alkaline-earth metal or rare-earth metal added in sufficient excess to combine with residual oxidizing impurities and to inhibit disproportionation. The latter reducing agent has been preferred because it participates in a self-limiting process, while the alkaline-earth metal can reduce the rare earth to the metallic state.

A second technique is that of photoreduction in the molten state with removal of the gaseous reaction products. This method proved far more efficient than solid-state photoreduction, requiring two orders-of-magnitude less gamma-dosage for equivalent reduction. It was also found to be possible to achieve photoreduction by means of ultraviolet radiation under these conditions.*

With each of these techniques it was possible to prepare polycrystalline samples of a number of host materials containing concentrations of rare earth which were entirely adequate for spectroscopic studies. In most instances, however, when the materials were held molten for periods of time necessary to obtain large single crystals, all traces of divalent rare earth vanished. A study directed toward the understanding of this phenomenon and toward means for circumventing it constituted a large portion of the work over the past six months. Details of this study will be found in the sections of this report which follow.

D. COMPOSITION OF THE HOST

The compounds which we have considered as meeting the chemical criteria described in Section I.B. above are listed in Table 1. Since we are concerned with optimizing performance, we have imposed, in addition to the chemical criteria, the requirement of a non-centrosymmetric site for the rare earth in most instances. This requirement arises from the La Porte selection rule which states that in the free atom, transitions between states of the same parity (as is the case for the $4f-4f$ transitions in rare earths) may take place only through magnetic dipole or electric quadrupole interactions, and only an operator of even parity may cause a transition. These interactions

* Semiannual Progress Report No. 2, p. 7.

are intrinsically weak and lead to very long-lived radiative states where nonradiative processes can predominate. The free atom selection rules are maintained in very weak crystalline fields and in centrosymmetric (local) environments. An unsymmetrical electric crystal field will relax this selection rule and allow the shorter lived and more intense electric dipole transitions to take place.

Of the compounds under consideration, BaBr_2 , having the lowest symmetry, meets this latter criterion exceptionally well and there has been, over the past three years, a continuing study of it. It has two serious disadvantages: it is highly hygroscopic, and its resistance to thermal shock is so poor that no crystals have survived laser testing.

In spite of its cubic symmetry, SrCl_2 has been of considerable interest, initially because of its desirable crystallization properties and later because of the particular behavior of a metastable $4f^{n-1}5d$ state in Tm^{2+} contained in it.* This material is also hygroscopic.

Of the noncubic materials, BaClF and the noncubic ABF_3 compounds present the best compromise with regard to crystal stability in the ambient atmosphere, resistance to thermal shock, and attainable crystal quality. The chief disadvantage of these compounds, as pointed out above, is the requirement that divalent rare earths must be introduced through a priori techniques.

Miscellaneous compounds of the BaZrF_6 type, which on fundamental grounds should meet all the criteria well, presented crystal preparation problems so formidable as to require their abandonment early in the study.

E. CHOICE OF RARE EARTH

The initial requirement placed on the rare earth is, of course, that in the divalent state it exhibit observable $4f-4f$ transitions of suitable sharpness and that the transition $4f^{n-1}5d \rightarrow 4f^n$ be efficient. We have arbitrarily imposed the additional practical limitation that the long wave limit for the fluorescent transitions not exceed 3μ since this constitutes a reasonable limit for analysis and detection with conventional spectrographic equipment.

According to McClure and Kiss,⁸ Gd^{2+} , Ce^{2+} , and Tb^{2+} are immediately ruled out because these ions have a $5d$ ground-state configuration and, hence, it would not be possible to find $4f-4f$ transitions in them. Nd^{2+} and Pr^{2+} ,

* Semiannual Progress Report No. 2, p. 28, and p. 83 of this report.

TABLE 1
HOST SYSTEMS FOR DIVALENT RARE-EARTH IONS

Compound	Structure	Melting Point (°C)	Transition Point (°C)	Remarks
<u>ALKALINE-EARTH HALIDES</u>				
MgF ₂	tetragonal	1266	920	Lattice may be too small for Ln ²⁺
MgCl ₂	rhombohedral	708		Very hygroscopic
CaCl ₂	orthorhombic	772		Very hygroscopic
SrCl ₂	cubic	873		Short liquid range
BaCl ₂	orthorhombic	960		Very hygroscopic
MgBr ₂	hexagonal	700	645	Solid-solid transition
CaBr ₂	orthorhombic	742		Very hygroscopic
SrBr ₂	tetragonal	657		Very hygroscopic
BaBr ₂	orthorhombic	857		Solid-solid transition
MgI ₂	hexagonal	decomposes		Very hygroscopic
CaI ₂	hexagonal	779		Very hygroscopic
BrI ₂	(SrI ₂ type)	538		Very hygroscopic
BaI ₂	orthorhombic	711		Very hygroscopic
<u>MIXED FLUORIDES</u>				
BaZrF ₆	?	953		High vapor pressure of ZrF ₄ on melting
<u>HALOFLUORIDES</u>				
CaClF	planar tetragonal	incongruently melting		Slightly hygroscopic
SrClF	planar tetragonal	990 (approx.)		Stable and nonhygroscopic
BaClF	planar tetragonal	1021		Stable and nonhygroscopic
BaBrF	planar tetragonal	965		Deteriorates in time
<u>PEROVSKITES</u>				
NaMgF ₃	orthorhombic	1030		Stable and nonhygroscopic
KMgF ₃	cubic	1091		Stable and nonhygroscopic
RbMgF ₃	rhombohedral	923		Stable and nonhygroscopic
KCaF ₃	cubic	1020		High vapor pressure of KF on melting
RbCaF ₃	cubic	1110		High vapor pressure of RbF on melting

according to our studies, have either 5d ground states in the hosts of interest, or 5d-levels which lie so low in energy as to be of no interest. Remaining in the first half of the rare-earth series are Sm^{2+} , which is of great interest, and Eu^{2+} , which, in principle, should be suitable but in practice exhibits only broad-band 5d fluorescence. Of the remaining ions in the second half of the series, Dy^{2+} , Ho^{2+} , Er^{2+} , and Tb^{2+} have transitions which should lead to laser action, while Yb^{2+} is of no value having f^{14} configuration. All of the useful ions in this half of the series emit principally beyond $1\ \mu$ with the exception of the red 5d emission in $\text{SrCl}_2:\text{Tm}^{2+}$.^{*} Chemical considerations have dictated that we focus on Sm^{2+} , Tm^{2+} , Dy^{2+} , and Ho^{2+} .

^{*} Semiannual Progress Report No. 2, p. 20 and p. 83 of this report.

SECTION II

CHEMICAL STUDIES

The alkali -- alkaline-earth fluoride perovskites and the alkaline-earth halofluorides satisfy many of the requirements of a host material for a laser with divalent rare-earth impurities. Most of the members of both of these classes of compounds can be controllably grown from the melt, provide a unique lattice site for the incorporation of divalent rare earth, and are stable and nonhygroscopic. The divalent rare earths exhibit very high fluorescence efficiencies in these hosts.

A. PEROVSKITES

The perovskites were extensively studied by Klasens and coworkers⁹ and by Thoma.¹⁰ The compound ABF_3 will have the cubic perovskite structure (Fig. 29) if a tolerance factor, $t = 1.09(R_A + R_F) / 0.94 \sqrt{2} (R_B + R_F)$, lies between 0.9 and 1.1. R_A , R_B , and R_F are the ionic radii of the A, B, and F ions, respectively. For values of t close to or slightly greater than the limiting values, the compounds formed have distorted perovskite (generally noncubic) structures. However, many of the compounds with a tolerance factor within the prescribed limits are pseudo-cubic, and the symmetry about the divalent ion will be slightly distorted. For example, $RbSrF_3$ with $t = 0.93$ was found¹¹ to be biaxial with indices of refraction, $N_\chi = 1.396$ and $N_\gamma = 1.400$. When t is much outside the tolerance limits, no compounds are formed. The perovskites prepared are listed in Table 2.

The nonhygroscopic starting materials such as NaF , MgF_2 , and CaF_2 were sufficiently pure as purchased and required no preliminary purification. KF was prepared from the carbonate and concentrated hydrofluoric acid and precipitated as either $KF \cdot 2H_2O$ or $KF \cdot HF$. Both the dihydrate and the hydrofluoride salt were vacuum-dried before use. Rubidium was purchased as the fluoride or the carbonate and was treated in the same way as was the potassium salt. Equimolar quantities of the appropriate alkali fluoride and alkaline-earth fluorides, and the trivalent rare-earth fluoride impurity were mixed together, placed in a platinum or pure nickel boat, and melted under a HF gas flow in a monel reactor tube. The HF gas was started while the materials were at room

TABLE 2
PEROVSKITES STUDIED UNDER THIS CONTRACT

Compound	Melting Temperature	Structure Type	t
NaMgF ₃	1030°	orthorhombic	0.917
KMgF ₃	1091°	cubic	1.05
KCaF ₃	1020°	cubic	0.915
KMgF ₃ ·KCaF ₃	980°	cubic	-
RbMgF ₃	923°	rhombohedral	1.12
RbCaF ₃	1110°	cubic	0.980
* KCaF ₃ and KMgF ₃ form a continuous solid solution with a flat minimum at the equimolar compound. ⁴			

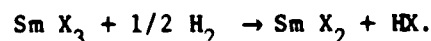
temperature so that fluorination was carried out at all temperatures. Fluorination was continued beyond the time that all traces of water ceased to appear in a Teflon exit tube. In many cases, the procedure was repeated to insure a material as free of oxide as possible. Dried ultra-pure hydrogen gas was flushed through the system before the system was cooled. The molten salt was cooled in this hydrogen flow to remove dissolved HF gas.

The purified perovskites were then grown by either the gradient freeze or the Czochralski method. Little work was done on NaMgF₃ and KMgF₃ since preliminary work with RbMgF₃ indicated that the small cationic sizes in the former compounds offered little hope for the incorporation of Ln³⁺. Of the other perovskites which were grown, only RbMgF₃ gave clear uniform crystals. The rest, KCaF₃, KCaF₃·KMgF₃, and RbCaF₃ yielded white, opaque, and inhomogeneous polycrystalline growths. These compounds continuously coated the walls of the Czochralski apparatus with white deposits of KF or RbF, which are the scattering inclusions found in the grown polycrystals. The reasons for the stability of molten RbMgF₃ are not known. Although the melting point of RbMgF₃ is the lowest of the perovskites examined, with a corresponding decrease in RbF pressure, this alone does not account for the stability. KCaF₃·KMgF₃, for example, has a vapor pressure at the melting point of RbMgF₃, if one assumes Raoult's Law behavior for both systems.

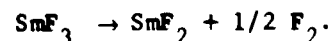
RbMgF₃ was grown in a gradient freeze furnace with a gradient of 25°C/in. and a cooling rate of 10°C/hour. Large clear fragments were easily obtained from high-density graphite boats. Most of the larger crystals were grown by the Czochralski technique. Vertical pulling rates of 0.25 to 0.5 cm/hour and

rotation of 14 rpm were used; crystals averaging 0.75 cm in diameter, 3 to 4 cm long (weighing approximately 15 gm) were grown from seeds or pointed molybdenum rods. RbMgF_3 has a rhombohedral unit cell with dimensions $a = 5.585 \text{ \AA}$, and $\alpha = 70^\circ$. The direction of growth was along the [111] axis.

The major problems encountered with this material were concerned with the incorporation and reduction of the rare-earth ions. The solubility of Ln^{3+} in RbMgF_3 is extremely low. Crystals were pulled with increasing amounts of Ho^{3+} or Dy^{3+} added to the Czochralski pot, the concentrations increasing from an initial 0.01 mole percent to greater than 1 mole percent. In none of the crystals was the characteristic fluorescence of either Ho^{3+} or Dy^{3+} seen. Arc emission spectroscopy and mass spectrometric analysis showed that the rare earths were present to about 20 ppm atomic, which was evidently below the fluorescent detection limit for these ions in this host. Rare-earth metal, Ho or Dy, was added to the respective heavily doped residues to produce divalent rare earth. Only minute amounts of trivalent ions were seen in fluorescence in the pulled crystals, and the residues showed little or no divalent ions. Part of the difficulty in reduction may arise from the presence of oxidizing impurities in the flowing gas stream used in the Czochralski apparatus. Helium and helium-hydrogen flow rates of about 30 liters/hour were used. However, the perovskites in general are hosts in which reduction of rare earths appear to be an unfavorable process. The behavior of Sm in these hosts is illustrative. Trivalent Sm impurity in a wide variety of hosts (BaClF , BaBr_2 , SrCl_2 , BaZrF_6 , and CaF_2) is almost completely reduced when the host and the Sm impurity are fused together in hydrogen. The reaction can be written as



Weller, Axe, and Pettit¹² found that occasionally as much as 40% of the Sm^{3+} is reduced to Sm^{2+} in the absence of any deliberately added reducing agent in $\text{CaF}_2\text{:Sm}$, a process which they wrote as



In the perovskites, fusion under hydrogen produces relatively little Sm^{2+} . Significant concentrations of divalent Sm must be produced in these hosts by the addition of samarium metal. The other rare-earth ions also show a

resistance to reduction in the perovskites. The compounds with larger alkaline earths, such as KCaF_3 , readily incorporate Ln^{3+} . Pieces of a pulled opaque polycrystal of $\text{KCaF}_3:\text{Dy}^{3+}$ were irradiated with γ -rays or heated in calcium metal vapor. Color centers were formed in the irradiated sample, but no reduction of the rare earth by either process took place. Treatment of the $\text{RbMgF}_3:\text{Dy}^{3+}$ crystal pulled from the melt highly concentrated with $\text{Dy}^{3+} + \text{Dy}^0$, with Ca or Mg vapor did not produce Dy^{2+} or visible coloration of the crystal.

The difficulty of reduction of the rare earth in the perovskites remains a puzzle. The different modifications of the crystal structure show the same behavior. It would be of interest to know in more detail what is occurring in the molten state. In the Czochralski apparatus the rare-earth metal was observed reacting vigorously with the melt. After apparent solution took place, the melt became quiet and clear. Upon solidification, the metal was found dispersed on the bottom, trivalent rare-earth fluorescence was found, with very little divalent fluorescence. These hosts may favor the disproportionation reaction (see Section II.C.) or the metal may dissolve in these hosts without much reaction with the trivalent. The use of high-temperature absorption spectroscopy would aid immensely in answering these questions. The overall behavior of the perovskites is similar to that of the sulfides. In both classes of compounds, europium is readily made divalent, while the reduction of Sm^{3+} is marginal and the other rare earths remain trivalent.

B. HALOFLUORIDES

Preliminary preparations indicated that BaFCl was easier to grow as single crystals than BaFBr , SrFCl , or CaFCl . The single-crystal growth of BaFCl itself is quite complicated; therefore, most of the effort was restricted to this material. Representative smaller crystal sections of the other hosts doped with rare earths were, however, prepared for evaluation. These host crystals all grow as layer structures; that is, all similar atoms are in one plane, with two adjacent planes of Cl atoms having such weak bonds between them that a very easy cleavage plane results. Because of this easy cleavage plane, the crystalline material is micaceous, and the growth of optically clear single crystals is difficult. In Fig. 2, the crystal structure is drawn in such a way (Cl atoms chosen as edges of the unit cell) that the

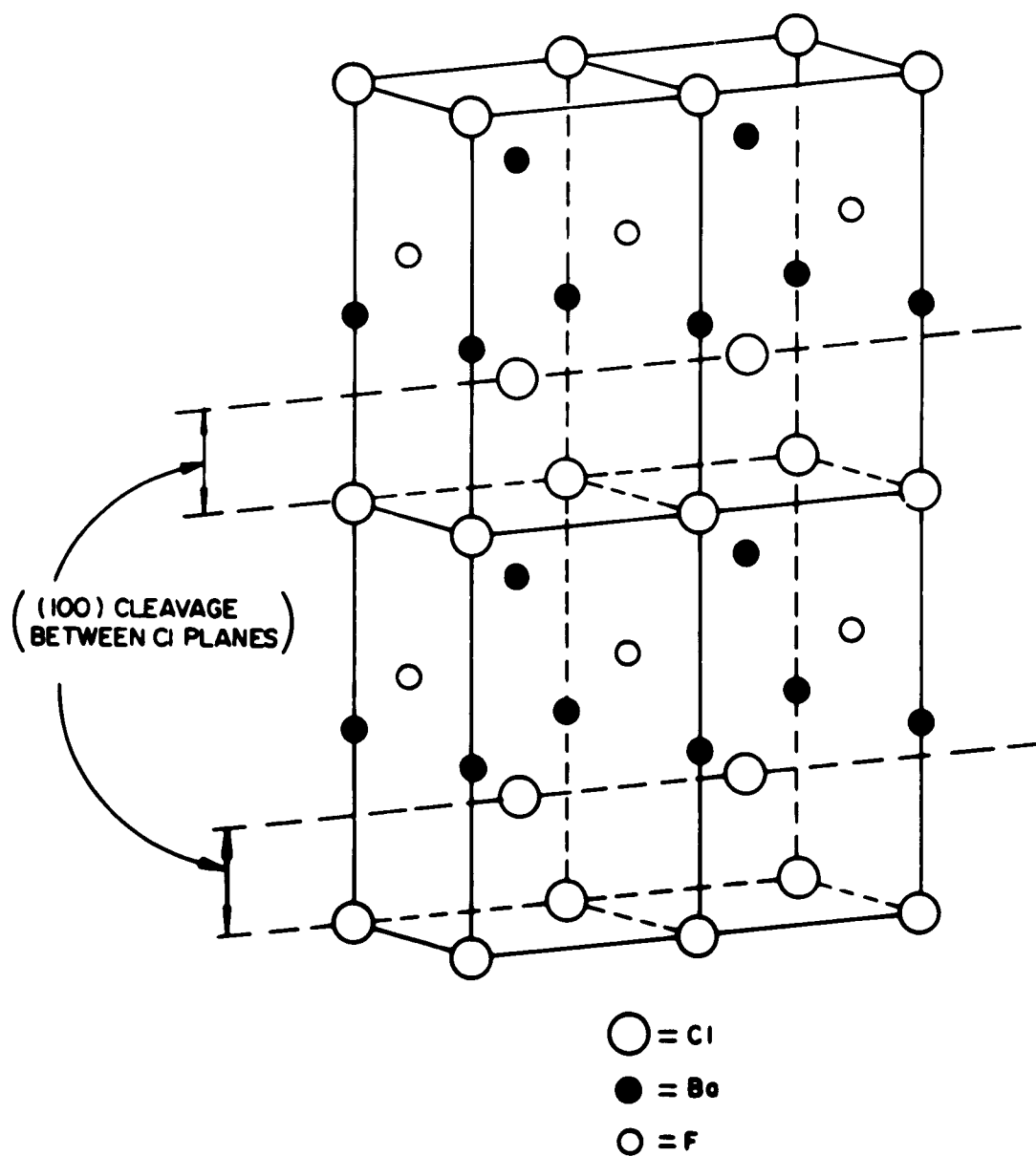


Fig. 2. Crystal structure of BaClF

two adjacent Cl planes of easy cleavage and the layer position of the other atoms are clearly illustrated relative to one another. In Table 3, pertinent data are tabulated of the findings of a single-crystal x-ray study.

The best optical-quality crystals were grown by the gradient freeze method. A gradient of at least $30^{\circ}\text{C}/\text{in.}$, and a slow cooling rate of about $0.6^{\circ}\text{C}/\text{hour}$ were found necessary to obtain optically clear crystals. For lower gradients and faster crystallization rates the crystals became translucent, because of the numerous twinings and slippage in the easily cleaved (100) planes.

Figure 3 shows the furnace used and its temperature gradient. The quartz tube enclosure with the crucible in position during crystal growth in a hydrogen atmosphere is also illustrated. The bottom of the growth crucible is located at 1020°C for BaFCl . The temperature gradient rises linearly for about 4 inches up the crucible to a temperature of 1150°C , giving a gradient of about $32^{\circ}\text{C}/\text{in.}$ The rate of cooling the furnace using a West Instrument Disk Programmer is illustrated in Fig. 4. The plotted temperature is the temperature at the tip of the crucible as a function of time during the crystal growth period. At the start of the crystal preparation the temperature is 1020°C at the tip of the crucible. The furnace temperature is programmed down linearly for nine days to a temperature 890°C at the tip of the crucible, thus giving a $0.6^{\circ}\text{C}/\text{hour}$ decrease in temperature. A check has shown that the gradient remains in the range of $30^{\circ}\text{C}/\text{in.}$ during this lowering. By this procedure the freezing point travels up the crucible so that with the $0.6^{\circ}\text{C}/\text{hour}$ lowering of temperature and the $30^{\circ}\text{C}/\text{in.}$ gradient it takes 50 hours to freeze one inch, or in one hour 0.02 in. of crystal freezes out. After nine days, the temperature is lowered at a faster rate, as shown in Fig. 4. The crystal is removed about 14 days after the start of the program.

The crystals were grown in graphite crucibles of two sizes, the larger, 1-1/4 in. O.D., 6 in. long with a 1/16-in. wall having a 45° cone on its end, and the smaller, with a 3/4 in. O.D. of same length and wall thickness, with a 60° cone tip. The crucibles were machined from a special-grade, high-density graphite (Grade ZTA) obtained from the National Carbon Company. This was the only available graphite that was found satisfactory as crucible material. The crucible was loaded with the material to about the full height of the 6-in. length; however, upon melting, the final height of the crystal was about 4 in.

TABLE 3
PbFCl STRUCTURES (TETRAGONAL)

Space Group: $D_{4h}^7 - P_{4/mmm}$

<u>BaFCl</u>			
Lattice constants:		$a = 4.380 \text{ \AA}$	
		$c = 7.212 \text{ \AA}$	
Distance between Cl-Cl planes:		3.74 \AA	
Atoms positions:			
2F	$3/4, 1/4, 0; 1/4, 3/4, 0$		
2Ba	$1/4, 1/4, z; 3/4, 3/4, \bar{z};$	$2Z_{Ba} = 0.205$	
2Cl	$1/4, 1/4, z; 3/4, 3/4, \bar{z};$	$2Z_{Cl} = 0.355$	
<u>BaFBr</u>			
Lattice constants:		$a = 4.503 \text{ \AA}$	
		$c = 7.441 \text{ \AA}$	
Distance between Br-Br planes:		3.88 \AA	
Atoms positions:			
2F	$3/4, 1/4, 0; 1/4, 3/4, 0$		
2Ba	$1/4, 1/4, z; 3/4, 3/4, \bar{z};$	$2Z_{Ba} = 0.191$	
2Br	$1/4, 1/4, z; 3/4, 3/4, \bar{z};$	$2Z_{Br} = 0.349$	
<u>SrFCl</u>			
Lattice constants:		$a = 4.140 \text{ \AA}$	
		$c = 6.595 \text{ \AA}$	
Distance between Cl-Cl planes		3.50 \AA	
Atom positions:			
2F	$3/4, 1/4, 0; 1/4, 3/4, 0$		
2Sr	$1/4, 1/4, z; 3/4, 3/4, \bar{z};$	$2Z_{Sr} = 0.200$	
2Cl	$1/4, 1/4, z; 3/4, 3/4, \bar{z};$	$2Z_{Cl} = 0.355$	

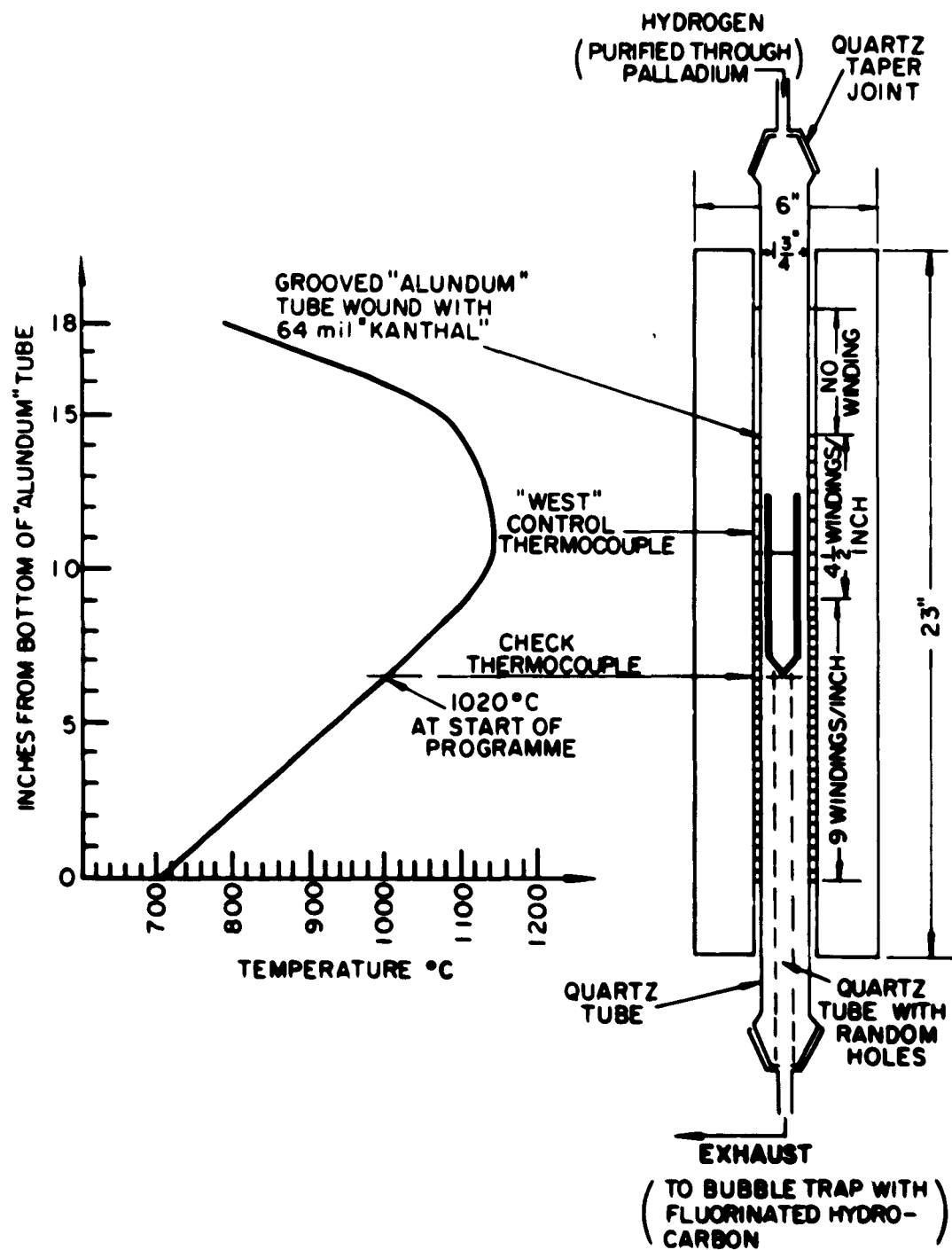


Fig. 3. Gradient freeze furnace

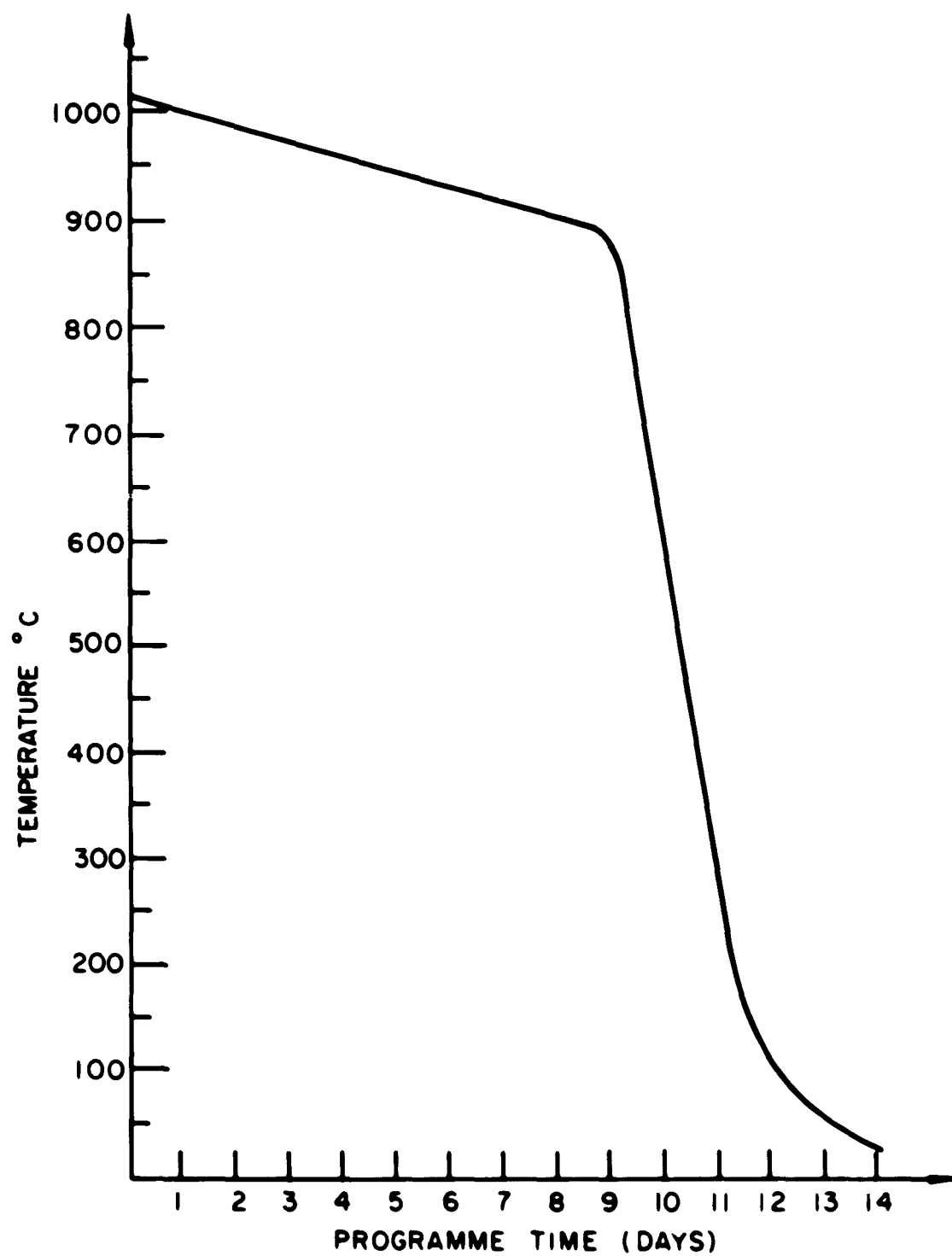


Fig. 4. Cooling program for gradient freeze furnace

The large crucible was used to grow crystals in a pure hydrogen atmosphere (H_2 purified through Pd), and the smaller crucible was used to grow crystals in a vacuum. The vacuum growth was carried out by sealing the loaded crucibles in evacuated quartz ampoules with initial vacua in the range of 10^{-4} to 10^{-5} torr.

The graphite crucible was satisfactory for most of the preparations made. However, only the Sm rare-earth impurity could be extensively reduced to the +2 valence state with hydrogen, while other rare earths such as Dy and Ho were reduced with hydrogen only very slightly. It was necessary to try a more drastic reduction reaction such as a reaction with free metal. An illustrative reaction would be



This reaction could not be performed in graphite since the rare-earth metals react with graphite, forming carbides. The only suitable material is molybdenum. Several molybdenum crucibles were made and a few crystals were grown. The crucibles were 6 in. long, 1 in. in diameter with a 45° cone tip; the side walls were 0.015 in. thick. The crucibles were difficult to construct since the cone tip had to be machined from a solid molybdenum rod, and the upper tube had to be welded from sheet stock. The tube was then welded onto the cone. Because of the difficulty in welding, only a few leakfree crucibles were constructed.

The pure $BaCl_2$, $BaBr_2$, or $SrCl_2$ used as raw material for the crystal growth had to be purified, since material of sufficient purity could not be purchased. The BaF_2 was purchased from Harshaw Chemical Company as optical-grade crystalline sections, which had been prepared by melting a large batch of the purest powder available, and then picking out from the frozen melt portions which were optically clear. To purify the $BaCl_2$, $BaBr_2$, or $SrCl_2$, reagent-grade material was dissolved in distilled water and extraneous insoluble material was filtered out. The filtrate was then recrystallized and heated above its melting point in a platinum crucible in air to burn out organic matter. This is a necessary step, since all sources of these salts contained soluble organics, which were entrapped during crystallization from water. The air-heated salt was dissolved in distilled water and recrystallized again. The material was then dehydrated in a vacuum oven. The anhydrous

salt was melted (at 1000°C) in an atmosphere of pure H₂ (purified through Pd) and anhydrous HCl gas. The rare-earth impurity was introduced at this stage of the preparation either as the chloride or the oxide. Organic contaminants were removed from the HCl gas by passing it over a quartz tube containing quartz rings at 850°C. The salt was heated in the H₂-HCl gas stream in a high-density ZTA graphite boat, 6 in. long, 1-1/4 in. high with 1/8-in. wall thickness contained in a demountable quartz tube to well above its melting point for about 6 hours. The material was then broken up, and heated again the same way. This procedure was repeated four times to obtain suitably pure material. A satisfactory process previously described,* in which the material is melted in a quartz container with a fritted bottom through which the gases are bubbled into the molten salt, was also used. For the best optical-quality crystals, however, it was necessary to HCl-treat the salt at least once more in a graphite boat. After thorough HCl treatment of the purified salt plus impurity, a molar equivalent of BaF₂ was added for the preparation of the barium halofluoride. This charge was then melted in a high-density ZTA graphite boat in pure hydrogen at 1050° and cooled to room temperature in hydrogen, after which it was loaded into the cone-tipped growth crucible. If the growth was to be done in hydrogen, the crucible was positioned in the furnace and the quartz tube flushed thoroughly with purified hydrogen. The gas was flowed from top to bottom of the furnace with all gas connections of glass or metal. For vacuum-grown crystals the crucible contained in the evacuated quartz ampoule was positioned in the furnace. The furnace was then turned on, and when the bottom end of the growth crucible was above the melting point of BaClF (1020°) the temperature controller was set at 1020°C, and the furnace was allowed to come to equilibrium overnight. The programmer lowered the furnace temperature at the rate of 0.6°C/hour for 9 days, and then at a faster rate as previously described. The crystals could easily be withdrawn from the graphite growth crucibles by gentle tapping to allow reuse.

Thus, single crystals were grown of the hosts BaFCl, BaFBr, SrFCl, and CaFCl, undoped and doped with various rare-earth impurities. Large optical-quality single-crystal sections (at least 3/8 x 3/8 x 2 in.) of BaFCl, and BaFCl:Sm²⁺, and smaller sections of optical quality in the range of 1/4 x 1/4 x 3/4 in. of all the other materials were obtained.

* Semiannual Progress Report No. 2, p. 4.

Attempts were also made to incorporate trivalent rare-earth ions, but in all cases the solubility of these cations was so low that only traces could be obtained, too low for lasing properties. By compensating with oxygen using LnOCl rather than LnCl_3 , however, the solubility of the rare-earth impurity can be increased in the host (see Section III.A.2a). Attempts to compensate the 3+ rare earths with K^+ cations to increase their solubility was also attempted, but was not successful. Using the above-mentioned growth procedure, the various optical-quality crystals were prepared and are enumerated in Table 4.

BaClF was also grown by the Czochralski method under conditions similar to those used for RbMgF_3 . The seeds were obtained from gradient freeze prepared crystals. The Czochralski method required very pure material and, in addition to the purification normally given to the BaClF starting materials, the BaClF was also given a rapid gradient freeze treatment. The top portion of the boule, which often appeared frosty due to impurities or nonstoichiometry, was discarded, and the lower portion was used as the Czochralski charge. Crystals prepared by the Czochralski method are listed in Table 5.

In the experiments with rare-earth metal and BaClF , the metal again reacted vigorously with the molten salt. Unlike the case of RbMgF_3 , the molten BaClF did not become clear, but a fluctuating network of dark lines following the liquid turbulence patterns persisted throughout the period of crystal growth.

C. THE STABILITY AND RETENTION OF DIVALENT RARE-EARTH IONS

The reoxidation of divalent rare-earth ions is the main obstacle to the successful preparation of these optical masers. This is true to some extent for the case of the in situ reduced ions and is almost the complete statement for the case of the a priori reduced ions. The crystals in which Ln^{2+} has been produced by in situ methods generally require a post-reduction annealing to achieve uniform optical and mechanical properties. Rarely has the Ln^{2+} survived the annealing step. Even Sm^{2+} has been found to reoxidize as a result of annealing. While the a priori methods yield the required concentrations of Ln^{2+} in rapidly quenched samples, only in a few rare instances has Ln^{2+} been found in a crystal after the long periods of time at elevated temperatures necessary for proper crystal growth. An understanding of the

TABLE 4

Crystal No.	Composition* (In Moles)
Vacuum-Grown Crystals (Graphite Crucible in Evacuated Quartz Ampoule)	
LP-2	BaFCl
LP-3	BaFBr
L-17A	BaFCl:0.01 SmCl ₂
L-18B	BaFCl:0.00075 TmCl ₃
L-20A	BaFCl:0.001 DyCl ₃
L-24	BaFCl:0.001 NdCl ₃
L-30	BaFCl:0.001 SmCl ₂
L-31	BaFCl:0.01 NdCl ₃ :0.01 KCl
L-32	BaFCl:0.01 DyCl ₃ :0.01 KCl
L-40	BaFBr:0.01 SmBr ₂
L-41	BaFCl:0.005 SmCl ₂
L-42	BaFBr:0.005 SmBr ₂
L-45	BaSrF ₂ Cl ₂ :0.01 SmCl ₂
L-49	BaFCl:0.001 DyCl ₃ :0.005 Dy (metal)
L-52	CaFCl:0.0025 HoCl ₃
L-59	SrFCl:0.0025 HoCl ₃
L-52	BaFCl:0.0025 HoCl ₃ in graphite
Hydrogen-Grown Crystals (Graphite Crucible)	
L-55	SrFCl:0.005 SmCl ₂
L-58	BaFCl:0.005 SmCl ₂
L-61	BaFCl:0.0025 HoCl ₃
L-64	BaFCl:0.01 HoCl ₃
L-67	SrFCl:0.01 DyCl ₃
L-71	BaFCl:0.01 DyOCl:0.01 DyCl ₃
Hydrogen-Grown Crystals (Platinum-Lined Crucible)	
L-60	SrFCl:0.01 HoCl ₃ :0.005 Ho (metal)
L-63	BaFCl:0.01 DyCl ₃ :0.005 Dy (metal)
Hydrogen-Grown Crystals (Molybdenum Crucible)	
L-66	SrFCl:0.01 DyCl ₃ :0.005 Dy (metal)
L-70	BaFCl:0.05 DyCl ₃ :0.025 Dy (metal)

* Represents dopant added, but due to segregation during crystal growth dopant concentration decreases, and final concentrations are smaller.

TABLE 5
CRYSTALS PREPARED BY CZOCHRALSKI METHOD

CRYSTAL	REMARKS AND OBSERVATIONS
BaClF (pure)	Crystals are similar to gradient freeze crystals. Some micaceous cleavage. Broad-band emission (see Section III.A.2a).
BaClF:Sm ²⁺ (0.01m%)	Grown with 2% H ₂ in He gas flow to reduce Sm ³⁺ . Crystal is clear, has strong Sm ²⁺ fluorescence, no Sm ³⁺ .
BaClF:Sm ²⁺ (0.5m%)	Grown with 2% H ₂ in He gas flow. Crystal is yellow-orange, but is lighter than the residue. Sm ²⁺ fluorescence is very strong.
BaClF:Ho	Total Ho is 0.1 mole % with HoF ₃ and Ho metal added. Crystal quality is very poor and is deep-blue due to color centers. Filaments of Ho metal dispersed throughout crystal. Ho ³⁺ fluorescence, almost no Ho ²⁺ emission in crystal, some in pot.
BaClF:Tm	Total Tm is 0.6 mole % with TmF ₃ +Tm metal added. Crystal quality is poor; many bubbles and inclusions. The color is blue-green on outside with pink core. This is due to color centers. Some metal inclusions. Very weak Tm ²⁺ emission, some Tm ³⁺ in crystals. More Tm ²⁺ emission from pot. Considerable Sm ²⁺ contamination, probably from Tm metal.
BaClF:DyOCl	Broad-band emission and little Dy ³⁺ emission (see Section III.A.2).

mechanisms through which this reoxidation occurs is necessary if suitable host crystals with divalent rare earths are to become a reality.

Reoxidation may be caused by the presence of oxidizing impurities, such as oxygen, water, the halogens, carbon dioxide, hydroxyl ions, the various hydrogen halides and more readily reducible metallic ions, Group II B or transition metal ions. These are present to some extent in the starting materials themselves, are adsorbed onto the surface of the materials during handling, and are in the inert gases used during preparation and purification. Consider the case of a priori reduction prior to Bridgman growth. If stoichiometric amounts of reducing agent, as rare-earth metal or alkaline-earth metal, were added, the above-mentioned impurities are more readily reduced than Ln^{3+} , and the extent of reduction is correspondingly decreased. Some of these impurities may also be introduced during Bridgman growth by the sealing off of the quartz ampoules, the outgassing of the quartz and crucibles into the evacuated sealed ampoules, and the attack of the melt or crystal on the quartz containers. An estimate of the contribution to the impurity level due to the degassing of quartz can be made from previously published data. Ekstrom and Weisberg¹³ found that greater than 10^{18} molecules were desorbed from an acid-cleaned, partially prebaked quartz tube, 2 cm i.d. and 30 cm long (approximately 200 cm^2 inner surface area), which was heated to 1100°C for a 15-hour period.

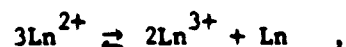
Mass spectrometric examination showed that more than 80% of the desorbed species were of an oxidizing nature. Quartz tubes of comparable surface area were used in our Bridgman growth, and longer periods of time at high temperatures were involved. The pressure in a sealed quartz tube held at 1000°C was found to increase by an order of magnitude or more as the time was increased from 10 to 80 hours.¹⁴ A suitable estimate of the impurities due to the degassing of quartz is 10^{-5} moles, and since water and oxygen are the main impurities about 2×10^{-5} moles of divalent ions could be oxidized to the trivalent state. The average melt was a dilute solution of rare earth ranging in concentration from 0.005 to 0.1 mole percent, and the quantities of rare earth varied from 10^{-6} to 10^{-3} moles. Thus, from one source of impurity alone a good fraction of the divalent ions can be lost during growth. The sum total of impurities from all sources may be sufficient to oxidize completely the small quantities of divalent rare earth.

The loss of divalent rare earth produced by a priori reduction in materials heated in the Czochralski apparatus was undoubtedly due to oxidation. Crystals of BaClF, for example, which were pulled in this apparatus fluoresced very strongly in the broad-band emission characteristic of oxide contamination. The large flow of helium sweep gas and the numerous seals and joints make it difficult to exclude oxidizing impurities from this apparatus.

The loss of divalent rare earth from crystals as the result of annealing may also be due to oxidation. The source of oxidation may be internal in that OH⁻ or HX may be occluded or dissolved in the crystal, or the oxidizing agent may be in the external environment in which the crystal is being annealed. At high temperatures, an electron may be readily ionized from the Ln²⁺ and subsequently combine with the internal OH⁻ or HX to produce O²⁻ or H. The electron may also migrate through the crystal and react at the surface. In either case, Ln³⁺ results. Several crystals of CaF₂:Sm²⁺ and SrF₂:Sm²⁺, with the Sm reduced by hydrogen during Czochralski growth were annealed at 1200°C in recrystallized alumina tubes under a dynamic vacuum of 10⁻⁸ torr. The crystals became much paler in color as a result of the annealing, indicating a loss of Sm²⁺. Thermodynamically, Sm²⁺ is a stable ion, and the loss of Sm²⁺ could only have occurred through direct oxidation.

The foregoing discussion indicates the need for further improvement in the techniques of material preparation and handling to reduce the concentration of oxidizing impurities to levels which will not significantly affect the concentration of divalent rare-earth ions. It is of interest to note that in the most carefully prepared samples in which BaClF was grown under a highly purified hydrogen flow, divalent rare earths were obtained.

Another way in which reoxidation could occur is through an auto-oxidation reduction mechanism or disproportionation of the Ln²⁺ itself. This process,



is the reverse of the a priori method of reduction using metallic rare earth. In a previous report,* this mechanism was described in detail and was emphasized rather strongly. There is much evidence for disproportionation from studies on the pure rare-earth halides. In the Pr-PrCl₃ system, Druding and Corbett¹⁵ found that the phase PrCl_{2.3} (approximately PrCl₂·PrCl₃)

*Semiannual Progress Report No. 2, p. 3.

was stable above 594°, but that below this temperature apparent disproportionation to Pr and PrCl₃ took place. On the other hand, in the Nd-NdX₃ systems¹⁶ the phases NdCl₂, NdCl_{2.27}, NdCl_{2.37}, and NdI₂ were stable at low temperatures and as little as 3 mole percent Nd in Pr_{1-X}(Nd_X)Cl_{2.3} stabilized the PrCl_{2.3} phase. The existence of Pr²⁺ in the molten chloride was also clearly indicated from vapor pressure measurements of PrCl₃ above solutions of Pr and PrCl₃.¹⁷ From a thermodynamic study of the NdCl₂-NdCl₃ system, Polyachenok and Novikov¹⁸ calculated that NdCl₂ should be stable above 227°K (-46°C) and should disproportionate into NdCl₃ and Nd below this temperature. Using the same value of the entropy of disproportionation obtained from the Nd system for the other rare earths and making other rough approximations they estimated ΔH° and ΔF° for the disproportionation reaction for the other rare earths. Using these data the temperatures below which the divalent state is unstable were calculated, and the results are shown in Table 6.

TABLE 6
ESTIMATED INSTABILITY TEMPERATURES FOR DISPROPORTIONATION
FOR DIVALENT RARE-EARTH IONS

Rare-Earth Ion	T _{inst} (K)
La	8550
Ce	7550
Pr	2300
Nd	227*
Pm	(-)
Sm	(-)
Eu	(-)
Gd	8600
Tb	7860
Dy	1465
Ho	1800
Er	533
Tm	(-)
Yb	(-)
* Calculated from thermodynamic measurements. (-) indicates a negative temperature.	

Thus, above T_{inst} the divalent state is favored; below this temperature disproportionation occurs. For the case of a solid with a rare-earth impurity (0.05 mole percent, for example) the nearest neighbor distance between rare-earth ions is from 15 to 20 lattice distances depending on the host, if one assumes uniform rare-earth distribution. For disproportionation to occur, a given divalent ion must capture over these long distances two electrons which were thermally ionized from other Ln^{2+} . The details of this process were presented previously* and are summarized below.

It was postulated that at elevated temperatures the electron combined with an anion vacancy through a tunneling process and the resultant Ln^{3+} was stabilized by combination with an anionic interstitial. The electron was transferred through the crystal by exchange hopping and through the mobile anion vacancy. Disproportionation occurred when two such electron-vacancy complexes were captured by a divalent ion. In view of the dilute nature of the solid solution and the low free electron density, the recapture process is equivalent to a three-body collision, a not very probable event. The disproportionation process should therefore proceed very slowly under these conditions, and the divalent state should be stable in a frozen-in equilibrium in dilute solid solutions.** Thus, disproportionation should be negligible in hosts whose melting point is above the T_{inst} . The melting points of the hosts used lie between 1200° and 1400°K. Taking account of the uncertainties in T_{inst} in Table 6, one sees that in addition to the well-known Yb^{2+} , Eu^{2+} , and Sm^{2+} , the ions Nd^{2+} , Er^{2+} , and Tm^{2+} should be quite stable; Dy^{2+} and Ho^{2+} represent marginal cases of stability, and the other rare earths should be unattainable in the divalent state. The estimated T_{inst} for Pr is 2300°K. The temperature at which $\text{PrCl}_{2.3}$ disproportionated, found from phase studies,¹⁵ was 590°C (867°K), a substantially lower value than the rough estimate. Corbett† also found a congruently melting DyCl_2 in the Dy-DyCl_3 system which is stable at room temperature. The stable compound, TmI_2 , isostructural with YbI_2 , has also been reported.¹⁹ We have attempted to prepare with little success Nd^{2+} , Tm^{2+} , Pr^{2+} , and Dy^{2+} in various hosts whose melting temperatures are above the measured, calculated, or estimated temperatures of disproportionation. In view of the argument that disproportionation temperature is much

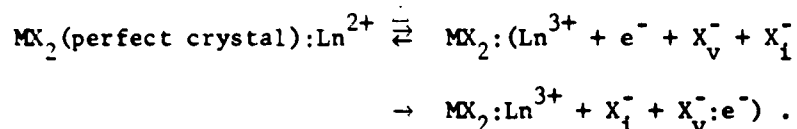
* Semiannual Progress Report No. 2, p. 3.

** The $\text{PrCl}_{2.3}$ disproportionation was described as "rather sluggish,"¹⁵ thus indicating that this reaction is slow even in the pure rare-earth systems.

† J. D. Corbett, Iowa State University, unpublished data.

below the melting point of the host, disproportionation does not seem to be a likely mechanism for the loss of Ln^{2+} .

An alternate possible reoxidation mechanism not subject to the objections which were raised against disproportionation is that of electron trapping by the host. Consider a solid containing Ln^{2+} at a high temperature. If re-oxidation is not due to disproportionation or oxidizing impurities, then the thermally ionized electron from the reaction $\text{Ln}^{2+} \rightarrow \text{Ln}^{3+} + e^-$ must be captured at some other type of site. An obvious candidate for such site is an anionic vacancy. The anionic vacancy concentration is quite high in alkaline-earth halides at temperatures near the melting points. Solid-state electrolysis studies indicated that the anions were significantly more mobile than were the cations, and thus the majority of the thermally produced vacancies will be anionic (anti-Frenkel type). The process can be represented by the following equations:



X_V^- and X_I^- are anionic vacancies and interstitials. An electron captured in this manner constitutes a color center and should absorb light in the visible region of the spectrum. Crystals of $\text{CaF}_2:\text{Dy}^{2+}$ which were annealed were colorless. The particular color centers formed in this way and influenced by the presence of Ln^{3+} impurities may absorb in the uv. It is known²⁰ that color centers in CaF_2 produced by irradiation are different from those produced additively by a Ca vapor bake. Recently, Fong* has found color centers in $\text{CaF}_2:\text{Dy}$ and $\text{CaF}_2:\text{Tm}$ at 3300 Å and 2300 Å, which are associated with the thermal bleaching of γ-ray-reduced Dy^{2+} and Tm^{2+} . A study of the absorption behavior with cycling of the oxidation states of rare earths in these hosts is very much in order. If such electron traps exist, then it might be possible to obtain Ln^{2+} by emptying the traps with energetic radiation.

D. PURIFICATION AND GROWTH OF ALKALINE-EARTH HALIDES

Essential to many of these investigations is the attainment of high purity of the crystalline hosts. While specific purification procedures are

* F. K. Fong, North American Aviation Science Center, unpublished work.

described in the appropriate sections, a general method which was employed both for purification of starting materials and for the preparation of crystals of simple salts such as SrCl_2 is discussed here. The example given is for $\text{SrCl}_2:\text{Tm}$ since it is a promising system, but the procedures are applicable in general to the chlorides and bromides of all the alkaline earths.

The starting material is reagent grade $\text{SrCl}_2 \cdot 6\text{H}_2\text{O}$. The salt is used as purchased or is dissolved in distilled water, filtered to remove insoluble impurities and recrystallized as the hexahydrate. The $\text{SrCl}_2 \cdot 6\text{H}_2\text{O}$ is dehydrated in a vacuum oven to remove the major portion of the water of hydration. The dried salt, the required amount of TmCl_3 , and possibly NaCl or KCl as charge compensator are rapidly transferred to a special quartz tube fitted with a medium pore quartz frit.* Purified argon is passed through the salt supported on the frit while it is heated to $\sim 400^\circ\text{C}$ for further dehydration. Dried and cracked (to remove hydrocarbons) HCl gas is then sent through the frit and salt while the temperature is raised to above the melting point (875°C). The HCl is bubbled through the molten solution for several hours. The molten salt is then flushed with argon and vacuum filtered through the quartz frit into a Bridgman growth ampoule which is then sealed off under vacuum. The sealed ampoule is placed in a vertical Stockbarger furnace with the tip at the bottom of the upper zone held at 900°C . The lower zone is at 800°C and the growth gradient, 20° to $30^\circ\text{C}/\text{inch}$. The SrCl_2 is lowered at the rate of 1 in./day into the lower zone and the crystal, cooled from 800°C to room temperature over a period of three days.

The resulting single crystal is clear and strain-free. Occasionally, the top was white and optically scattering, perhaps from the segregation of a high concentration of oxide or other impurities. The thulium impurity was reduced to the divalent state by either γ -irradiation, calcium metal vapor baking, or solid-state electrolysis.

* Semiannual Progress Report No. 1, p. 4.

SECTION III

SPECTRAL STUDIES

A. HALOFLUORIDES

1. Introduction

With respect to structure and chemical stability, the halofluorides appear to be ideal host substances. However, there have been extremely difficult problems associated with the fabrication of a successful laser. Leaving aside, for the present, the special case of Sm^{2+} , the central problems have been the growth of satisfactory crystals and incorporation of divalent lanthanides in concentrations sufficiently high to lead to laser action. Procedures for satisfactory crystal growth have now been worked out and are described elsewhere in this report (Section II.B.). Incorporation continues to present serious difficulties. In view of the uncertainty about the extent to which the divalent rare earth disproportionates during crystal growth and because of the attractive aspects of in situ reduction by radiation, electrolysis, or cationic vapor treatment, we have investigated the conditions under which trivalent rare earth can be introduced substitutionally in halofluorides. For this study, we chose Dy^{3+} as the impurity ion and BaClF as the host material. Dysprosium was selected as the active impurity; first, because Dy^{2+} in CaF_2 has yielded a particularly successful laser system with good cw operating characteristics and very low threshold. It would be anticipated that the advantages of having this ion in a host of low symmetry such as the halofluorides should result in even greater efficiency of operation. Second, as a chemical probe for the study of oxidation-reduction characteristics of rare earths and of incorporation, Dy, lying in chemical activity about midway between the difficult-to-reduce and easy-to-reduce rare earths, is expected to exhibit typical chemical behavior.

2. Dysprosium

The energy level scheme for trivalent dysprosium (f^9) is illustrated in Fig. 5. The most prominent fluorescence occurs from the $^4\text{F}_{9/2}$ state to the $^6\text{H}_{15/2}$ and $^6\text{H}_{13/2}$ levels, yielding visible blue and yellow light, respectively. The high intensity of the $^4\text{F}_{9/2} \rightarrow ^6\text{H}_{13/2}$ fluorescence transition found in most hosts indicates that, given an efficient method for pumping, this ion

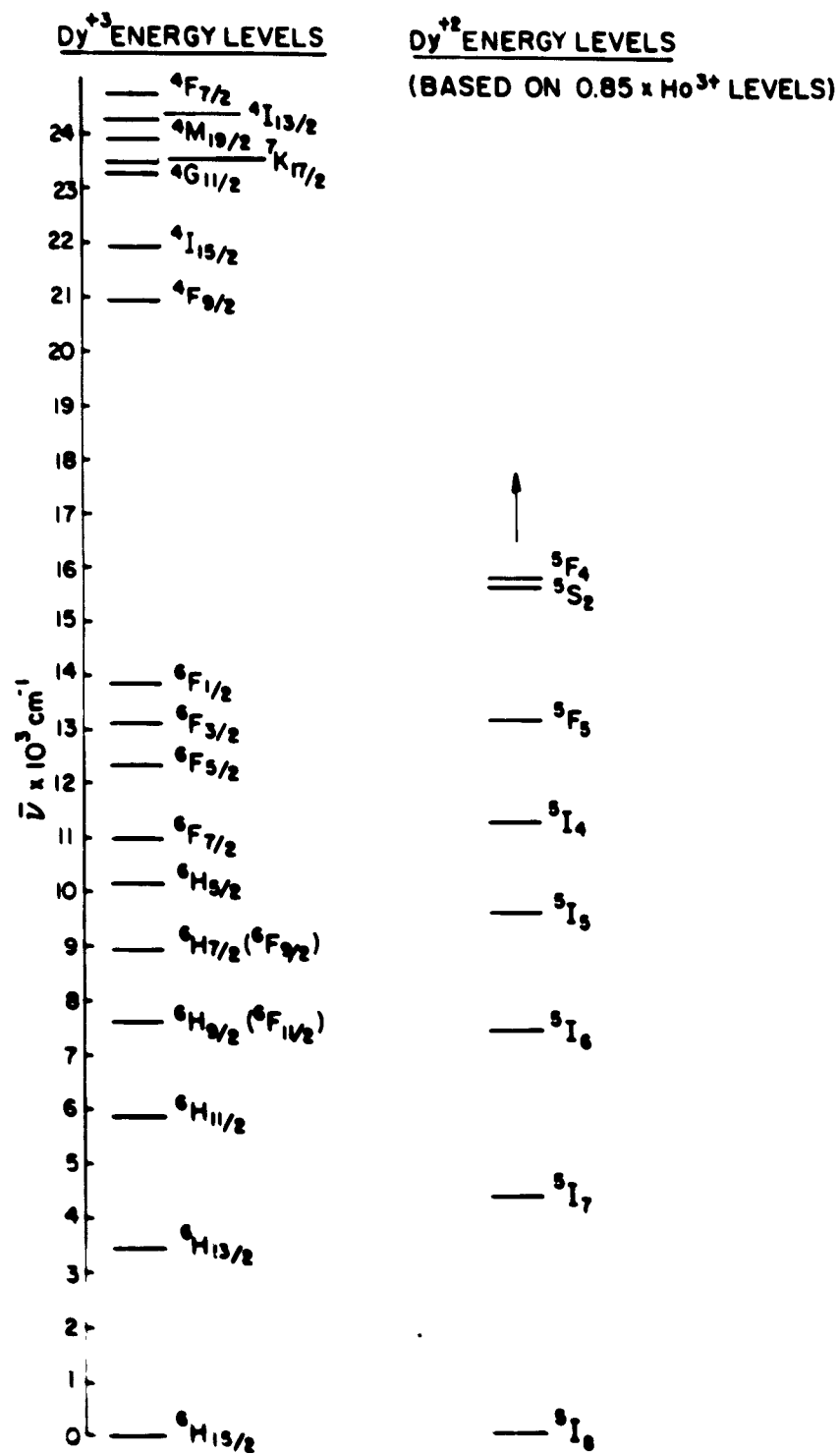


Fig. 5. Energy level scheme for Dy³⁺ and Dy²⁺.

would be suitable for use in a 4-level visible laser. From the point-of-view of this study, however, these transitions serve only as analytical probes for following the oxidation-reduction process and for studying incorporation.

Dy^{2+} is isoelectronic with Ho^{3+} , and the energies corresponding to the 4f levels can be derived from those of Ho^{3+} through the use of the factor 0.85 to account for the lowered nuclear charge as suggested by McClure. This yields the level scheme for the transitions of interest illustrated in Fig. 5. In CaF_2 , laser action occurs between $^5\text{I}_7$ and the crystal field components of $^5\text{I}_8$. It is either a three-level or a four-level system depending on the temperature of operation,²¹ the output occurring in the infrared near 2.4 μ . These transitions may be employed for unambiguous identification of the presence of the divalent species.

In a typical alkaline-earth-halide host such as SrCl_2 , trivalent dysprosium, at a nominal concentration of 0.05 mole percent, behaves in the expected manner. Under excitation by 3650-Å Hg light it fluoresces from the 4f states, primarily from the $^4\text{F}_{9/2}$ level to the $^6\text{H}_{13/2}$ and $^6\text{H}_{15/2}$ levels of the ground state, yielding emission in the yellow and blue regions of the spectrum (Fig. 6).^{*} The excitation spectrum resembles closely the absorption spectrum for an aqueous solution of Dy Cl_3 (Fig. 7).

In contrast to this behavior, single crystals of BaClF , into which we have tried to introduce Dy^{3+} during growth, do not fluoresce upon excitation by 3650-Å radiation. In many samples, fluorescence, characteristic of Dy^{3+} , is found upon excitation with 2537-Å Hg radiation, while in others, under similar conditions of excitation, this emission is nearly totally obscured by an intense broad fluorescence band in the yellow-green spectral region. The excitation spectrum for the Dy^{3+} emission (e.g., for the $\text{Dy}^{3+} \text{ } ^4\text{F}_{9/2} \rightarrow ^6\text{H}_{13/2}$ transition) is not characteristic of absorption into the 4f manifold of the dysprosium ion as in $\text{SrCl}_2:\text{Dy}^{3+}$, but rather consists of a broad, slightly structured band extending from 3500 Å to higher energies. Samples of "pure" (i.e., undoped) BaClF also fluoresce under 2537-Å Hg excitation exhibiting a fluorescence band shifted slightly to shorter wavelengths compared with that of the Dy-doped crystals.

^{*} In Fig. 6, the intense emission in the vicinity of 7000 Å is from a trace of Sm^{2+} contamination in this particular specimen. The intensity of the Sm^{2+} fluorescence is indicative of the generally greater efficiency of the divalent rare-earth species.

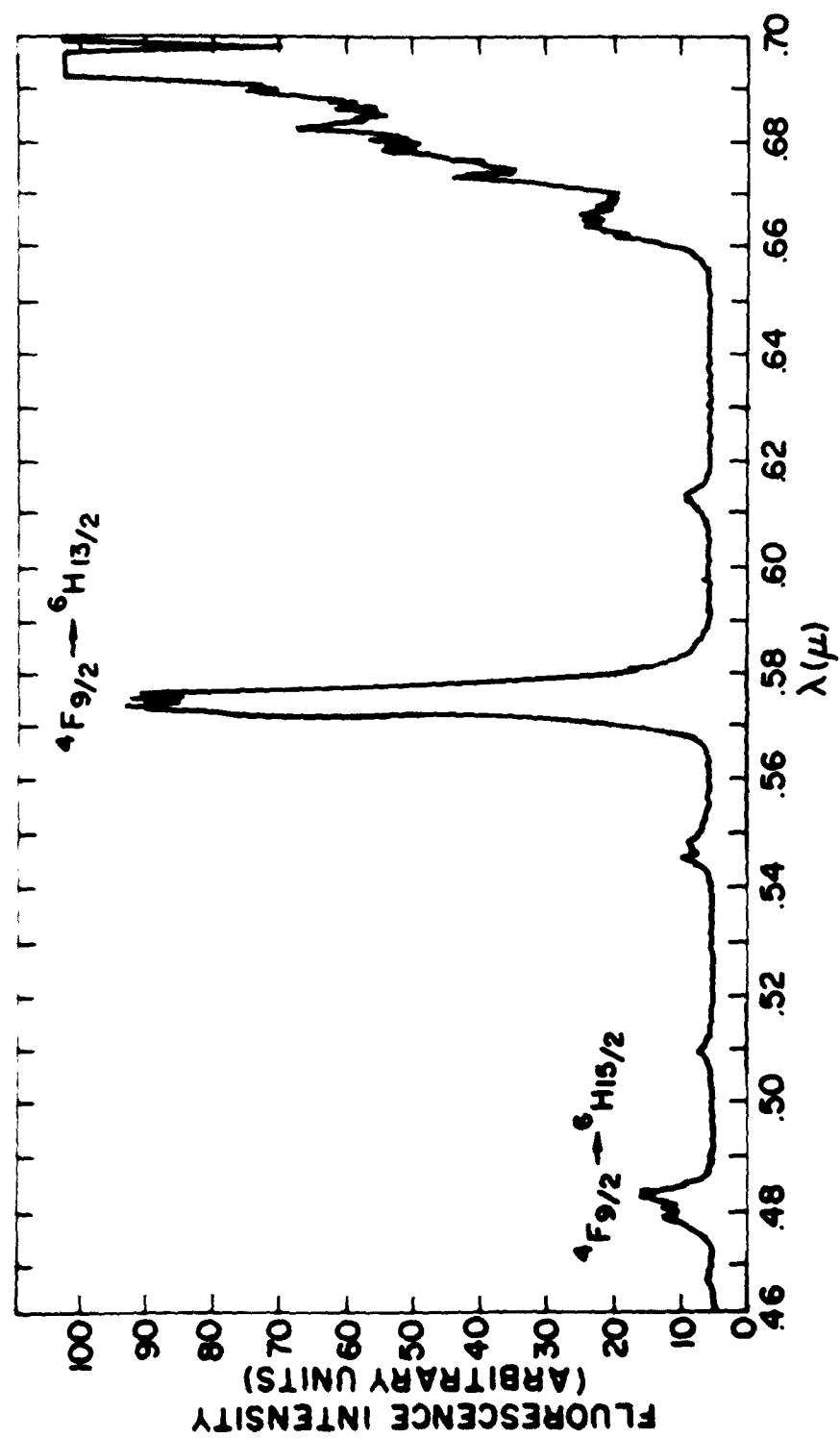


Fig. 6. Fluorescence spectrum of Dy^{3+} in SrCl_2 at 77°K

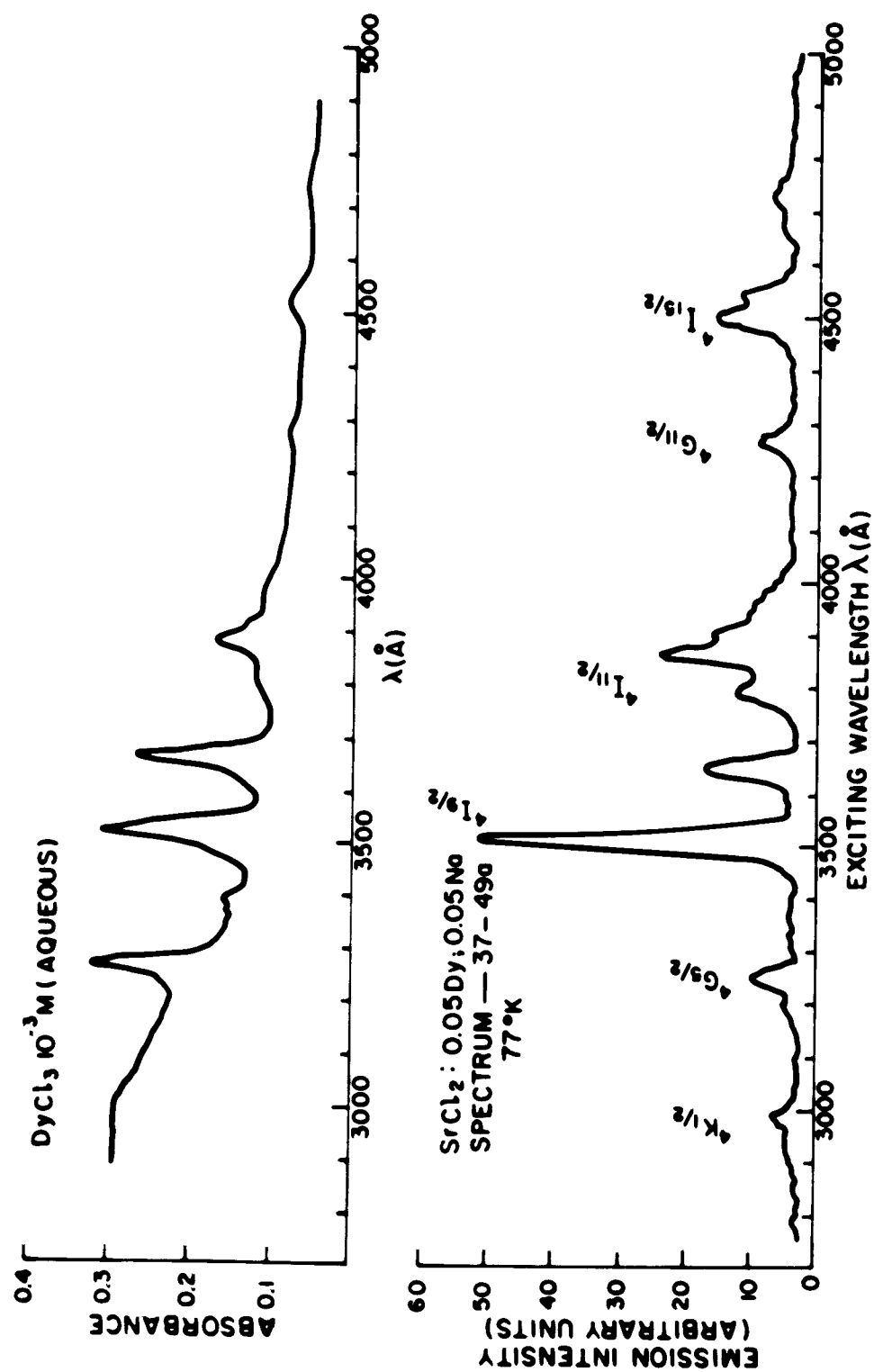


Fig. 7. Excitation spectrum of Dy^{3+} in SrCl_2 at 77°K with absorption spectrum of DyCl_3 aqueous solution

a. Optical Characteristics of the Host - Considering first the host, while the absorption spectrum of BaClF, known to be free of impurities, has not been observed, from analogy with the behavior of other alkaline-earth-halide compounds such as SrCl₂, the absorption caused by band-gap transitions would not be expected to occur at wavelengths longer than about 2000 Å. The samples of "pure" BaClF which exhibit visible fluorescence under 2537-Å excitation (Fig. 8) begin to absorb noticeably at about 3500 Å (Fig. 9), even in extremely thin layers and, are absorbing strongly at 2000 Å. Therefore, it must be concluded that this observed absorption-luminescence in "pure" material is a consequence of the presence of unspecified impurities. Because of the high stability of alkaline-earth oxides and the difficulty of removing them once formed, it can be assumed that a major contributor to these absorbing states is oxide. In samples containing Dy³⁺ as indicated by the fluorescence spectrum and known to be contaminated with oxide (e.g., sample L-65) absorption in the range 2000 Å to 3500 Å is even more intense (Fig. 9).

b. Dy³⁺ in BaClF - The absence of excitation or of observable 4f-4f absorption in the Dy³⁺-doped samples can be interpreted as the consequence either of a very low Dy³⁺ concentration resulting from segregation during growth or that for some unaccountable reason the 4f-4f transitions are improbable in this particular host. The observations suggest that the Dy³⁺ enters the host substitutionally for Ba²⁺ and that charge compensation is brought about by the substitution of O²⁻ for fluoride or chloride. Since DyOCl is isostructural with BaClF, and since efficient energy transfer occurs between the uv absorption band and the 4f fluorescent levels, a significant number of the Dy³⁺ sites are most likely associated with O²⁻ as a nearest neighbor. Further evidence for this conclusion is seen in Fig. 10 which shows the splitting of the ⁴F_{9/2} → ⁶H_{13/2} transition with increasing O²⁻ concentration. Curve A (sample L-63) was taken from a sample which contained 1 mole percent Dy added as DyCl₃ plus a slight excess of Dy metal. The crystal was contained in a platinum-lined graphite crucible and grown in a purified H₂ atmosphere by the gradient freeze method described elsewhere in this report (Section II.B.). Curve B (sample L-65) was prepared in the same manner, except that a molybdenum crucible was employed for growth. During the crystallization period a small fraction of the melt leaked through a crack in the molybdenum crucible and attacked the quartz protective tube, presumably releasing some O₂ into the

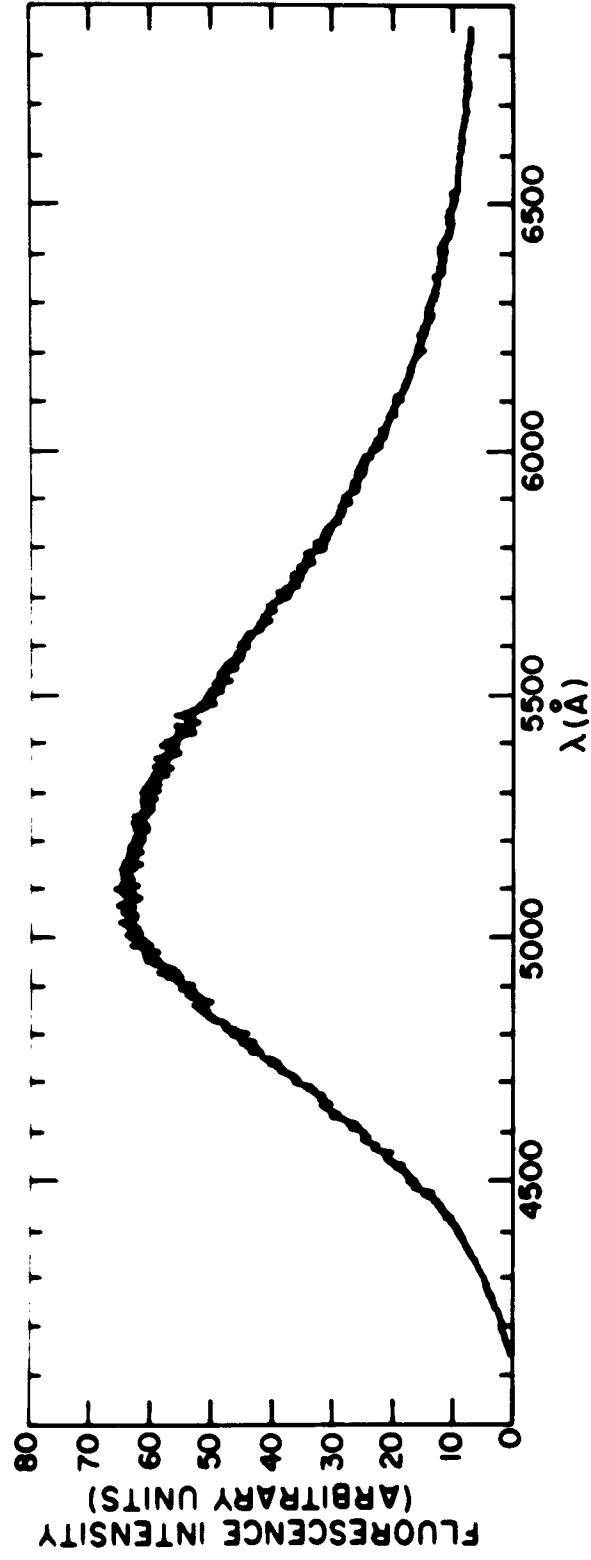


Fig. 8. Fluorescence spectrum of "pure" BaClF at 77°K

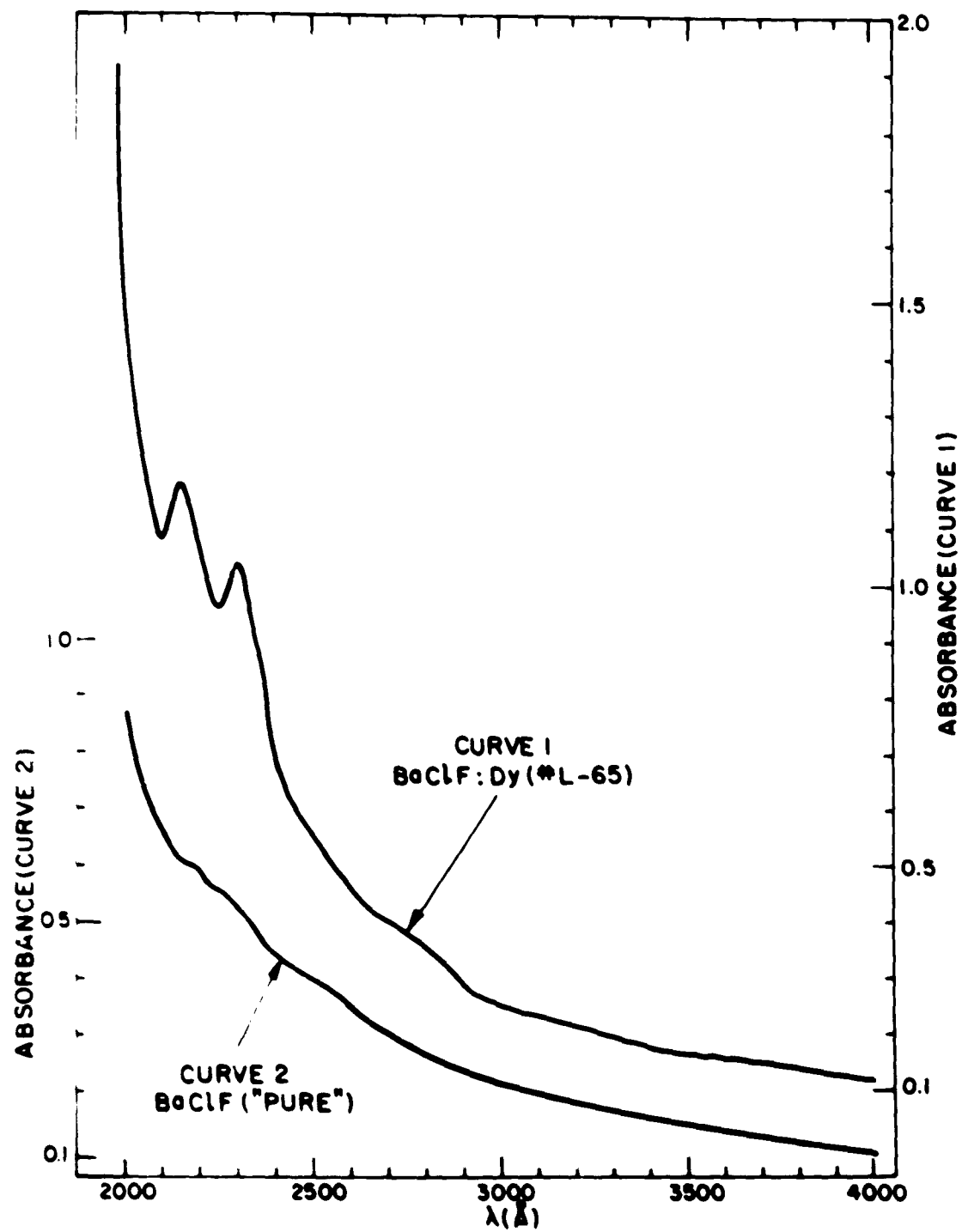


Fig. 9. Absorption spectra of BaClF: Dy³⁺ (O) at 77°K

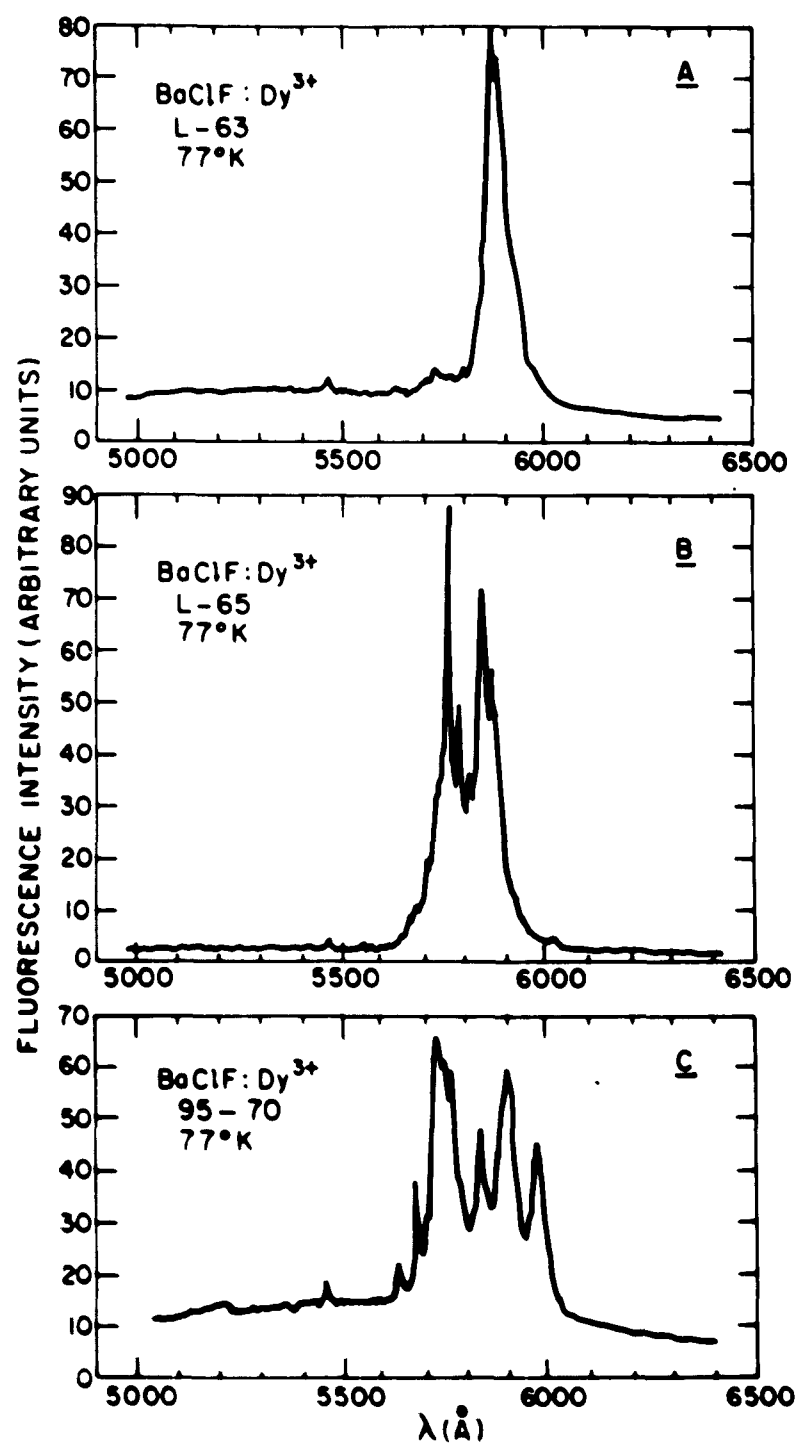


Fig. 10. Fluorescence spectra of BaClF:Dy^{3+} with varying amounts of oxygen at 77°K

H₂ stream. Curve C represents a sample (95-70) which was prepared with the identical mole fraction of Dy, but in this case the rare earth was added as DyOCl. The increased splitting with increased oxygen concentration is indicative either of increased site multiplicity or of the influence of nearest neighbor (pair) interaction. To gain further information concerning the nature of the Dy³⁺ environment, sample (95-70) was diluted 10:1 with pure BaClF and a crystal grown by the Czochralski method in an atmosphere of purified H₂ and He. Fluorescence spectra of the crystal and of the residual material are shown in Fig. 11. It will be noted that no significant change has occurred in the lines ascribed to the Dy³⁺ $^4F_{9/2} \rightarrow ^6H_{13/2}$ transition. There appears, however, a broad band underlying these lines. The line-to-band relative intensity is decreased in the crystalline material relative to the residue, indicating segregation of the Dy³⁺ into the residue. The origin of this band is not known at present, but it should be noted that the fluorescence band (Fig. 8) of pure BaClF is also of similar nature, but shifted at peak intensity toward the violet. Dilution of the original (95-70) material by one order of magnitude without significant change in the Dy³⁺ splittings is satisfactory evidence that the splittings are not caused by Dy³⁺ - Dy³⁺ interactions but rather are a consequence of site multiplicity probably brought about by O²⁻ charge compensation lying either as a nearest neighbor to a Dy³⁺ substituted Ba²⁺ lattice site or at some point removed from the rare-earth ion.

Since the Czochralski technique in this material favors the removal of the impurity ion from the crystal concentrating it in the melt, a single experiment was performed in which a large crystal containing 5.0 mole percent DyOCl was grown by the Bridgman technique in the hope that, if segregation were to occur, it would appear as a concentration gradient in the final crystal. This procedure yielded a large crystal of good optical quality. No fluorescence was excited by 3650-Å light as in previous specimens, and a yellowish-white fluorescence was produced by 2537-Å illumination. The resulting fluorescence spectrum (Fig. 12) shows only a trace of structure attributable to Dy³⁺ and an extremely intense band, thus confirming the conclusion that the band is associated with O²⁻ in the lattice. An absorption study of a thick (5-mm) segment of this crystal shows some similarity to the corrected (see Section IV of this report) excitation spectrum for Dy³⁺ $^4F_{9/2} \rightarrow ^6H_{13/2}$ fluorescence in more dilute samples (Fig. 13) and no absorption in the 4f-4f

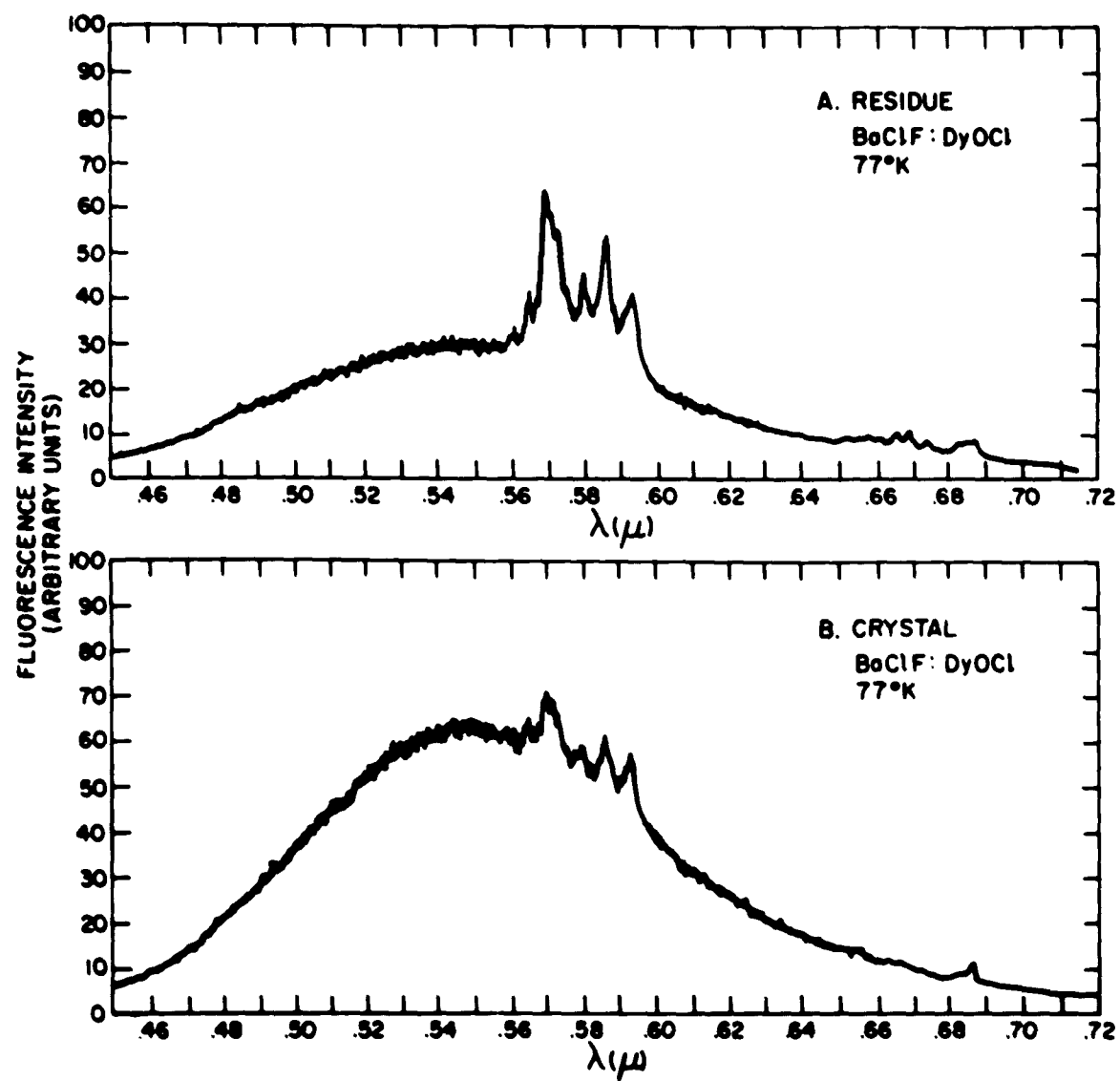


Fig. 11. Fluorescence of BaClF:Dy³⁺ (0) - residue and crystal at 77° K

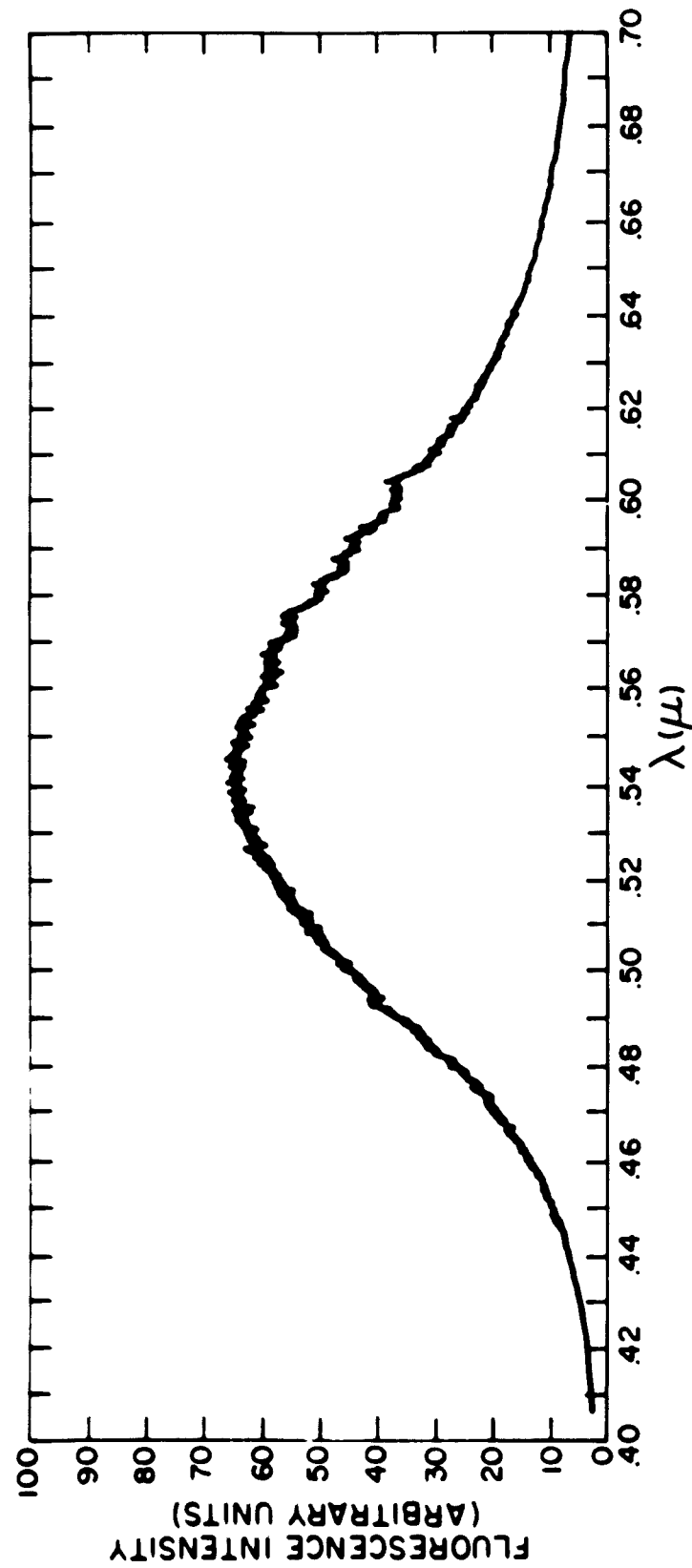


Fig. 12. Fluorescence spectrum of BaClF:DyOCi at 77° K

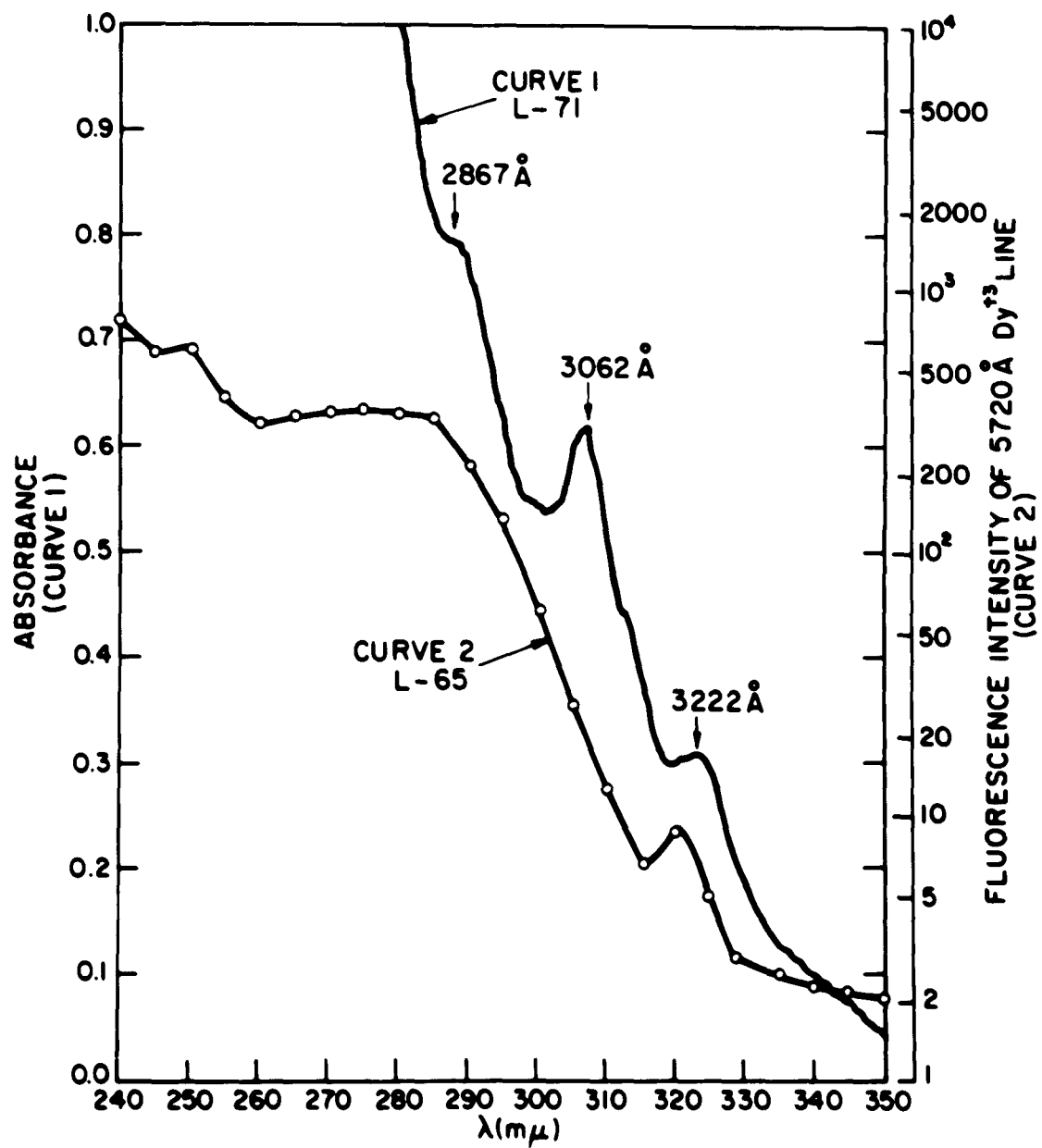


Fig. 13. Absorption and excitation spectra of BaClF:Dy³⁺ (0)

states. Because of the nature of an excitation spectrum, it is not anticipated that perfect correspondence necessarily will be found with absorption studies. The agreement, however, satisfactorily indicates that excitation of the Dy^{3+} is via the O^{2-} absorption bands.

One further experiment provides additional evidence that the trivalent rare earth can only be incorporated in association with oxide as a charge compensator. (Previous attempts at cationic charge compensation resulted in no significant increase in rare-earth concentration.) The initial objective of this experiment was to produce material having divalent rare earth. This aspect of the results will be discussed later. The crystal was grown with a concentration of 5 mole percent Dy^{3+} added as the chloride and free metal to carefully purified starting materials in a molybdenum crystallization tube. The melt froze in the form of a thick single crystalline shell surrounding and floating on a polycrystalline residue. Excitation at 3650 \AA produces in both the single-crystal portion and the polycrystalline residue fluorescence characteristic of the Sm^{2+} contamination (arising evidently from traces of Sm in the Dy metal), but no Dy^{3+} emission. Upon irradiation at 2537 \AA , the Sm^{2+} emission is suppressed and a weak Dy^{3+} line appears (Fig. 14). The structure of the Dy^{3+} lines appears to indicate a very low oxide concentration which is consistent with the conditions under which the material was prepared. The low intensity of the Dy^{3+} emission is a consequence of its low solubility in BaClF in the absence of oxide charge compensation.

These observations suggest strongly, then, that trivalent rare earth may be substituted in significant concentrations in BaClF only in the presence of oxide charge compensation. In its absence, the Dy^{3+} is precipitated in non-incorporated forms of DyF_3 or DyCl_3 , both of which do not fluoresce and hence are not observed by fluorescence techniques.

In view of this conclusion and in view of the fact that oxide-associated rare earths cannot be reduced in situ, it is clear that reduction must be carried out by chemical or photochemical methods in the molten phase during crystal growth. If the results of the Sm^{2+} (Section III.A.5.) experiments can be generalized to all rare earths, then the divalent species should incorporate much more readily than does the trivalent. This suggests that successful crystals can be fabricated from highly purified starting materials by pulling a crystal from a melt heavily doped with rare-earth salt and

FLUORESCENCE INTENSITY (ARBITRARY UNITS)

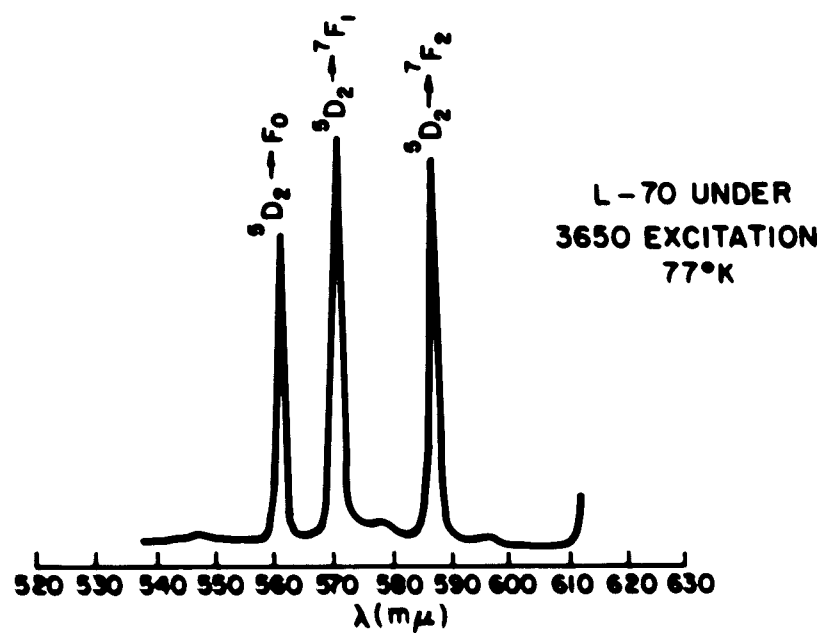
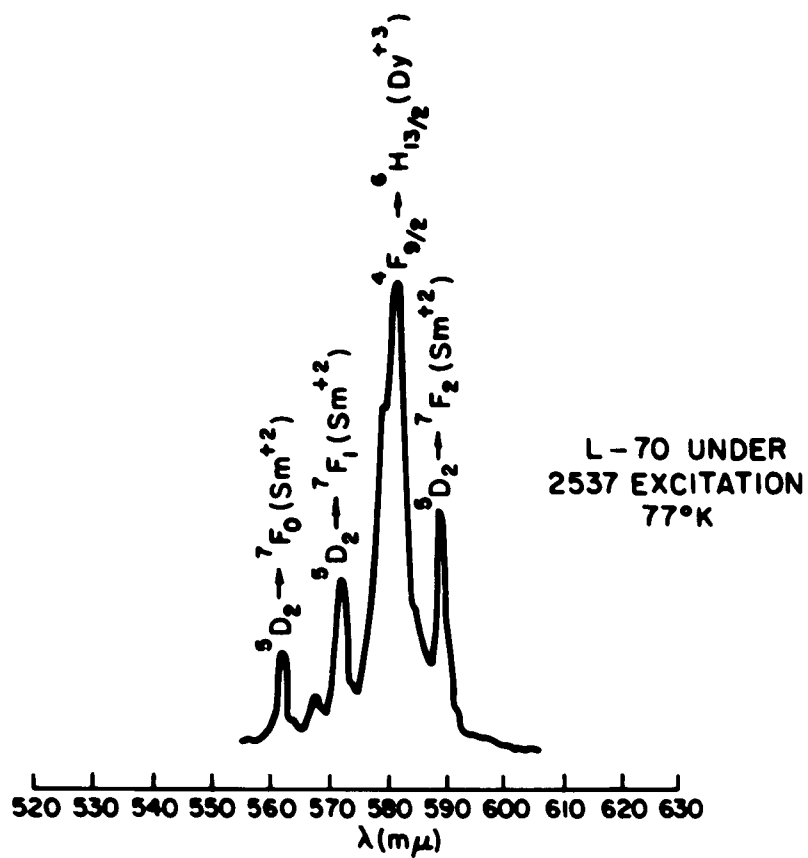


Fig. 14. Fluorescence of $\text{BaClF:Dy}^{3+}:\text{Sm}^{2+}$ (O) under excitation by 2537 Å and 3650 Å

rare-earth metal. The crystallization system must be entirely free of oxygen- and hydroxyl-producing materials and must be sufficiently tight to prevent any diffusion of oxygen or water vapor into it.

c. Dy²⁺ in BaClF - Fluorescence, characteristic of Dy²⁺ has been observed in a number of BaClF samples treated under a variety of conditions. The spectrum (Fig. 15) consists of several groups of lines, each of which corresponds within reasonable limits to a predicted transition based on the Ho³⁺ spectrum (Fig. 5). The excitation spectrum for this emission (Fig. 16) is composed roughly of five bands extending downward in wavelength from about 7500 Å to 4300 Å. Presumably, these bands represent transitions between the 4f and the 5d states.

The most intense of the emission lines at ~ 1.4 μ arises from the ⁵I₆ → ⁵I₈ transition. Its intensity is more than an order of magnitude greater than any of the other emission groups. It consists of three sharp lines at 6974, 7016 and 7067 cm⁻¹, arising probably from ground-state splitting since similar splittings of ~ 50 cm⁻¹ are also observed between major components of the ⁵I₇ → ⁵I₈ transition near 2.4 μ and the ⁵I₅ → ⁵I₈ transition near 1.08 μ (not shown on the figure).

This characteristic divalent fluorescence is observed in the following BaClF:Dy samples:

- (a) Quenched samples treated with Dy metal.
- (b) One crystal grown in the presence of Ba metal.
- (c) The starting material for sample L-70 in which no reduction attempt was made.
- (d) Crystal L-70 grown in molybdenum with Dy metal in H₂ atmosphere.
- (e) Crystal L-63 grown in platinum-lined graphite boat in H₂ atmosphere.

In general, there are no significant differences among the fluorescence spectra of these samples. The fact that divalent dysprosium appears in samples treated with no deliberately added reducing agent indicates that under appropriate conditions adequate concentration of Dy²⁺ can be incorporated. In none of these preparations has the Dy²⁺ concentration been sufficiently high to indicate that lasers could be fabricated with the exception of the quenched samples where crystal quality was too poor.

In this discussion, we have not considered the question of disproportionation. This aspect of the problem is discussed elsewhere in this report (Section II.C.). It is of interest, however, to point out that in sample L-70,

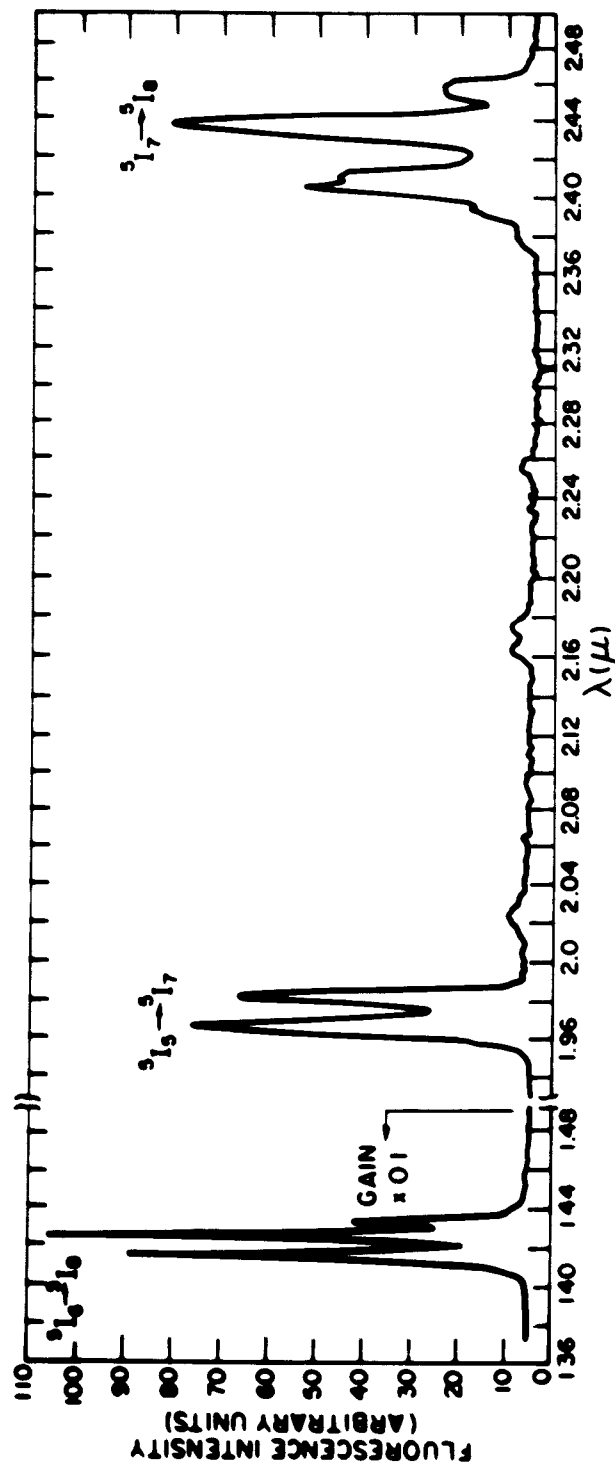


Fig. 15. Fluorescence spectrum of BaClF:Dy²⁺ at 77°K

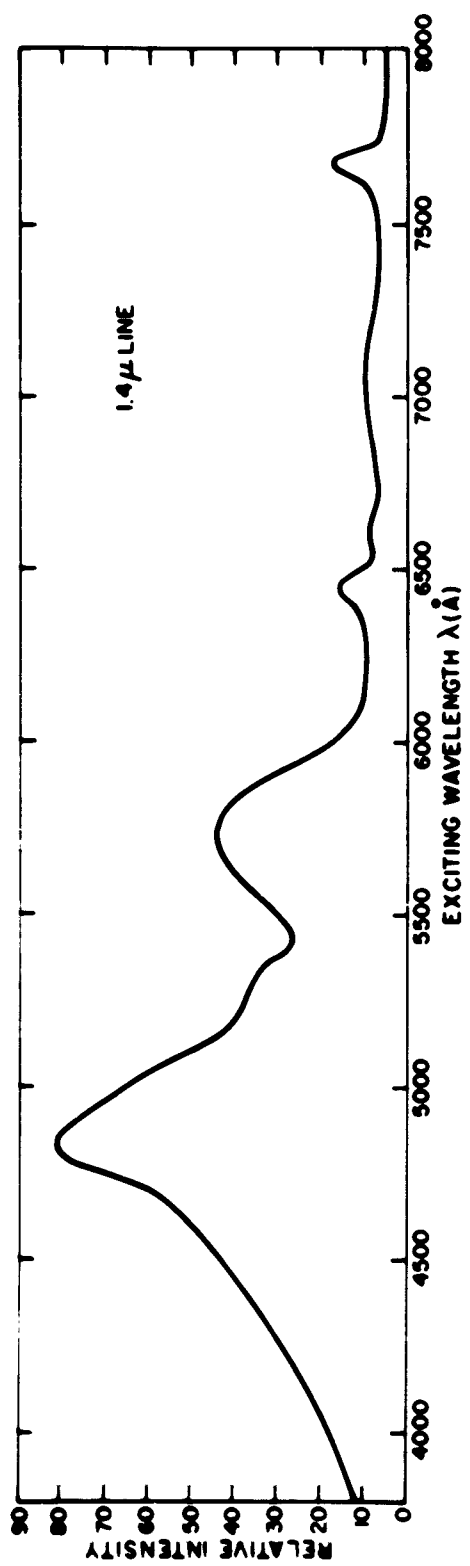


Fig. 16. Excitation spectrum for BaClF:Dy²⁺ at 77°K (Uncorrected)

from the fluorescence analysis, very little trivalent dysprosium was detected while the divalent concentration was substantial. Were disproportionation occurring in the solid phase, relatively large concentrations of the trivalent species would be expected to be present. This result, then, argues against the disproportionation hypothesis.

d. Dy²⁺ in BaCl₂ - In considering the question of "spontaneous" reduction (i.e., those cases where the divalent ion is detected in samples in which no reducing agent has been employed during preparation), the possibility of "extraction" of the divalent ion into one of the residual constituents of the BaClF host arises from small deviations from stoichiometry. The spectrum of divalent dysprosium in BaF₂ is well known and does not resemble the spectra which we have found. We therefore examined the behavior of this ion in BaCl₂. The sample was a polycrystal which had been reduced by uv radiation in the molten state. The fluorescence is intense and the spectra of the ⁵I₇ → ⁵I₈ transition and of the ⁵I₅ → ⁵I₈ transition (Fig. 17) are significantly different from that of the BaClF samples. We therefore can conclude that the spectrum that we have attributed to Dy²⁺ in BaClF is indeed that.

3. Holmium

Holmium in BaClF behaves in a manner similar to that of dysprosium. The solubility of the trivalent species is low in the absence of oxide, and energy transfer occurs between the oxide-associated states and the emissive states of Ho³⁺. The energy level scheme for Ho³⁺ and that of Ho²⁺ derived from the Er³⁺ isoelectronic system are illustrated in Fig. 18. Upon excitation with 2537-Å light, BaClF:Ho fluoresces in three groups of lines which can be identified as arising from the transitions, ⁵F₃ → ⁵I₈, ⁵F₄(⁵S₂) → ⁵I₈, and ⁵F₅ → ⁵I₈. An additional group of lines does not correspond to any obvious transition in Ho³⁺ but does correspond to the ⁵D₂ → ⁷F₁ transition in Sm²⁺ which is known to be present as an impurity (Fig. 19).

Fluorescence which can be identified as arising from the transition ⁴I_{13/2} → ⁴I_{15/2} in Ho²⁺ has been observed in several samples of BaClF:Ho. In those materials which have been reduced with Ho metal and then quenched, the spectrum contains two groups of lines, one at 5100 cm⁻¹ and the other centered about 5400 cm⁻¹ (Fig. 20). The former exhibits a broad excitation spectrum extending to beyond 1 μ in the infrared to about 4000 Å in the violet (Fig. 21a).

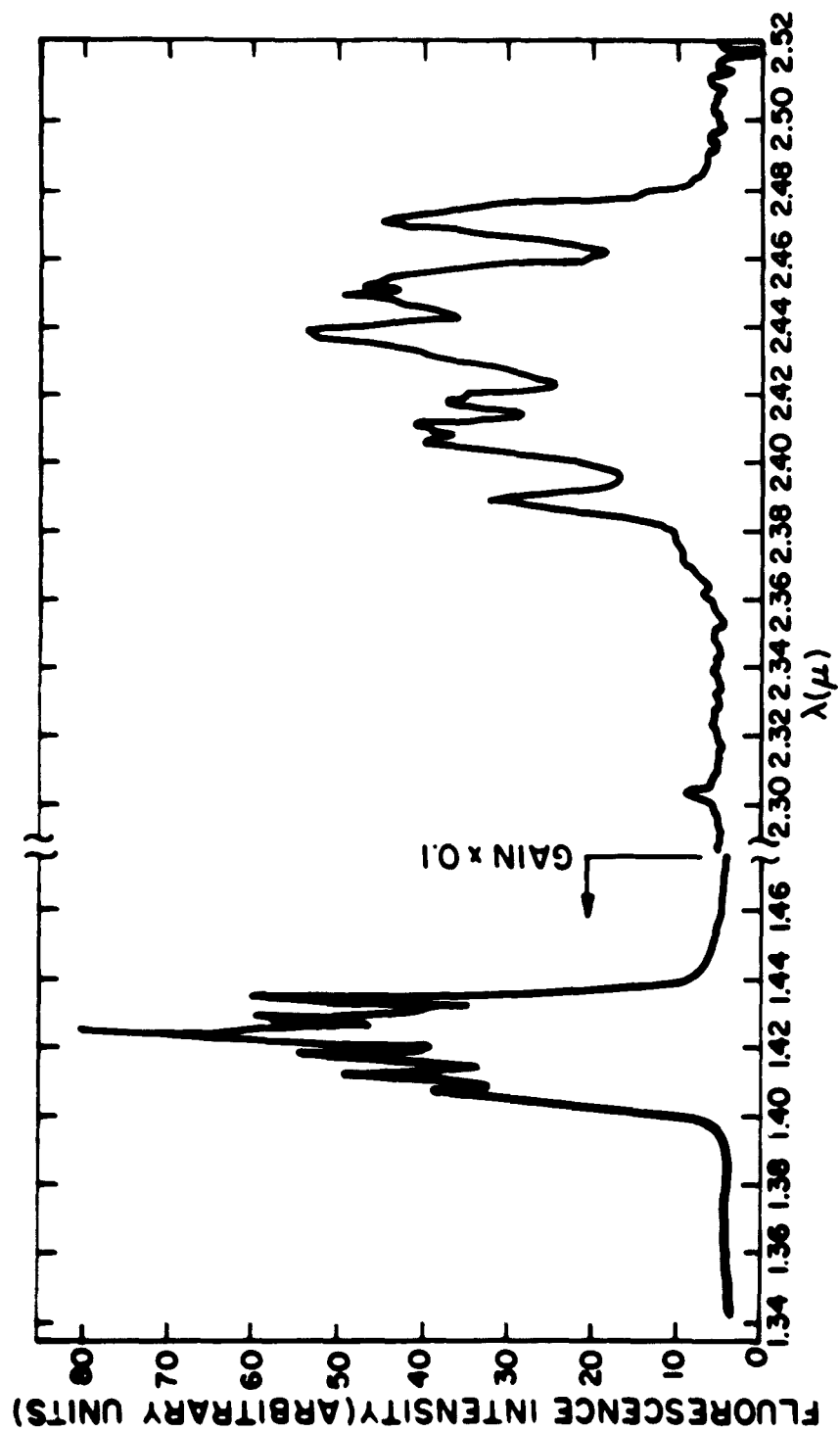


Fig. 17. Fluorescence of $\text{BaCl}_2:\text{Dy}^{2+}$ at 77°K

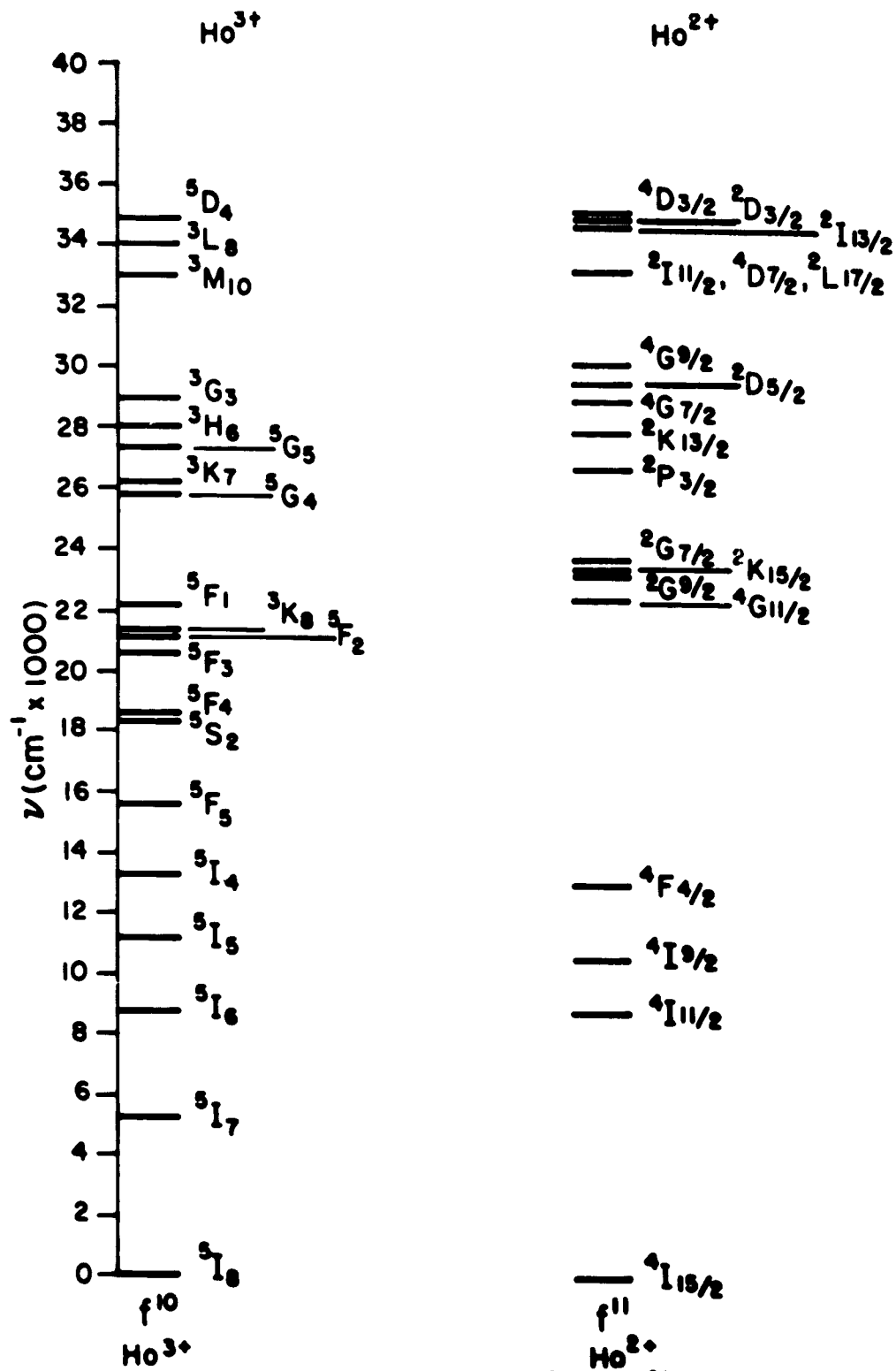


Fig. 18. Energy level scheme for Ho³⁺ and Ho²⁺

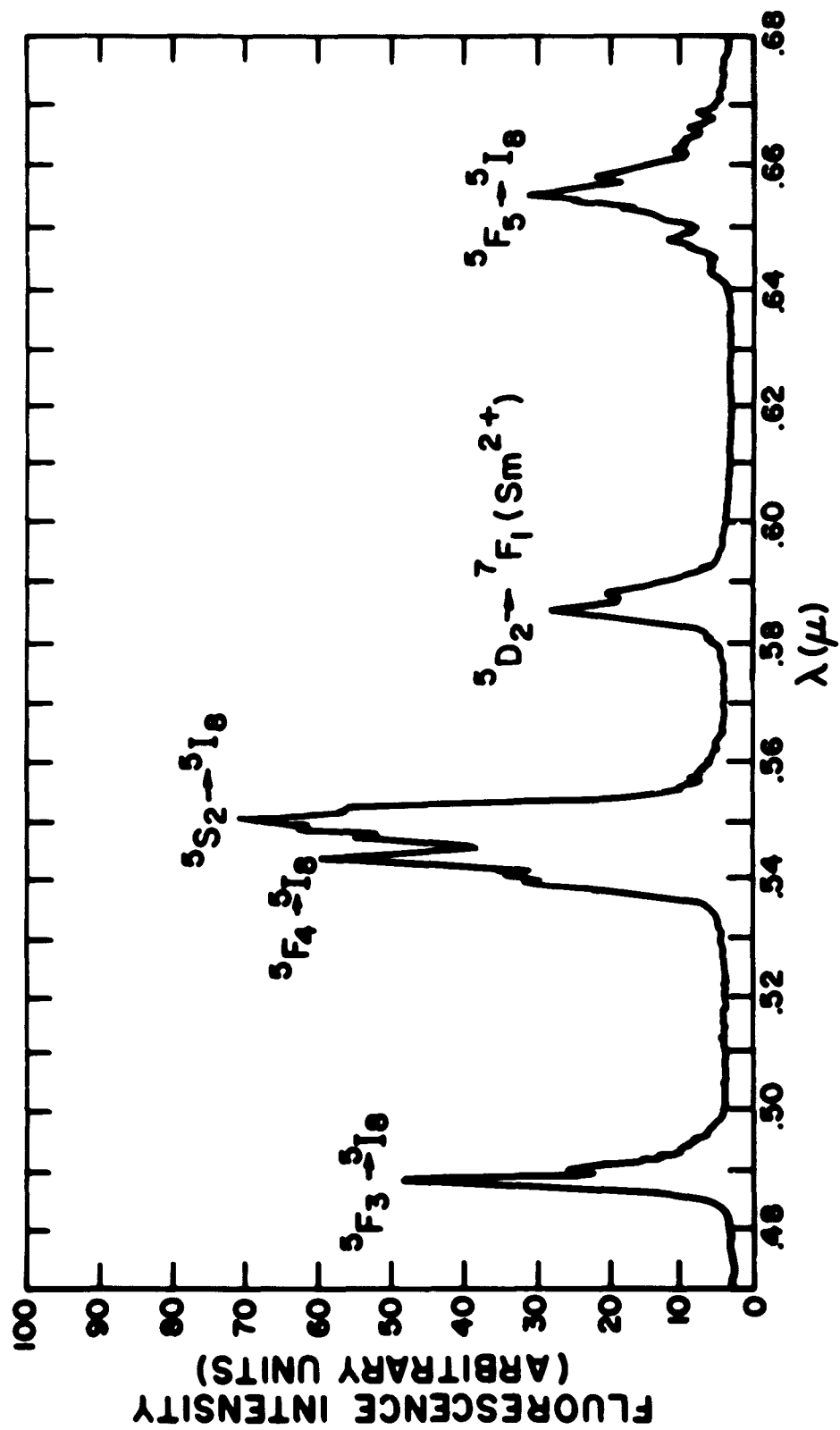


Fig. 19. Fluorescence spectrum of BaClF:Ho³⁺ at 77°K

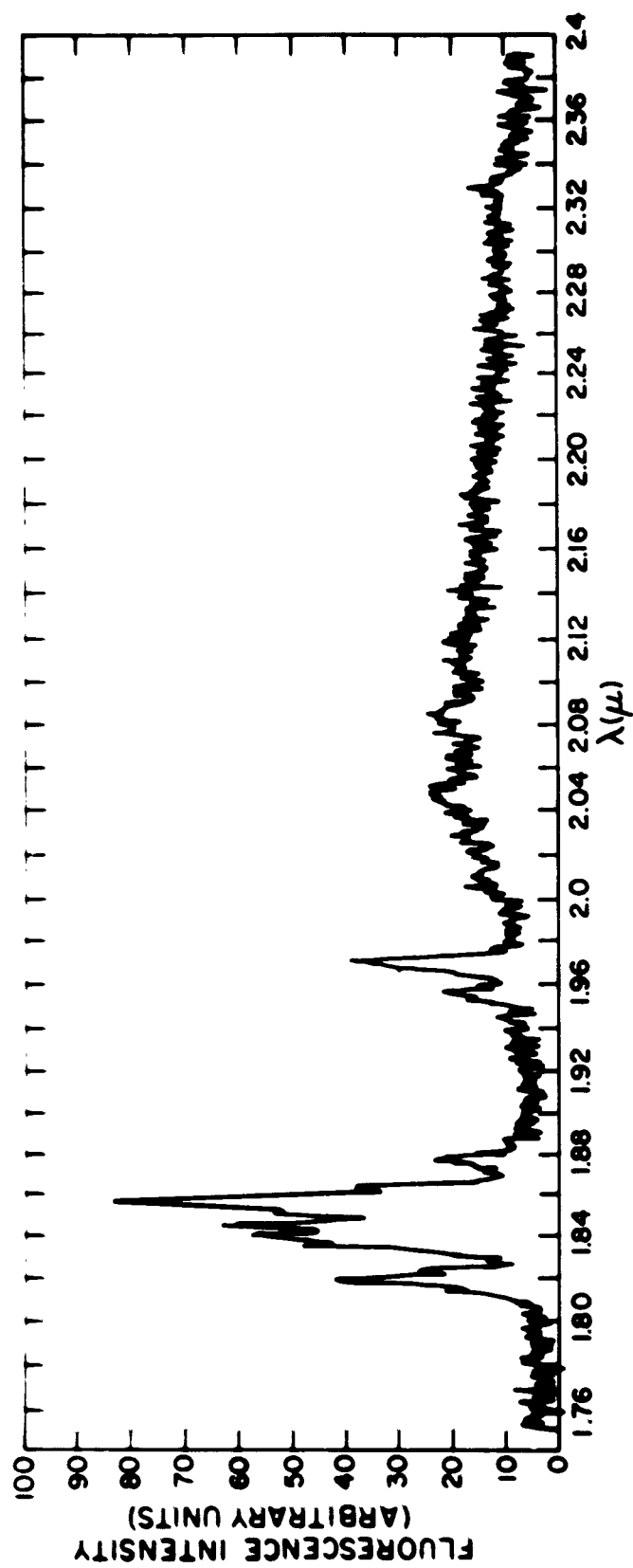


Fig. 20. Fluorescence of BaClF:Ho^{2+} at 77°K , Hg-lamp excitation

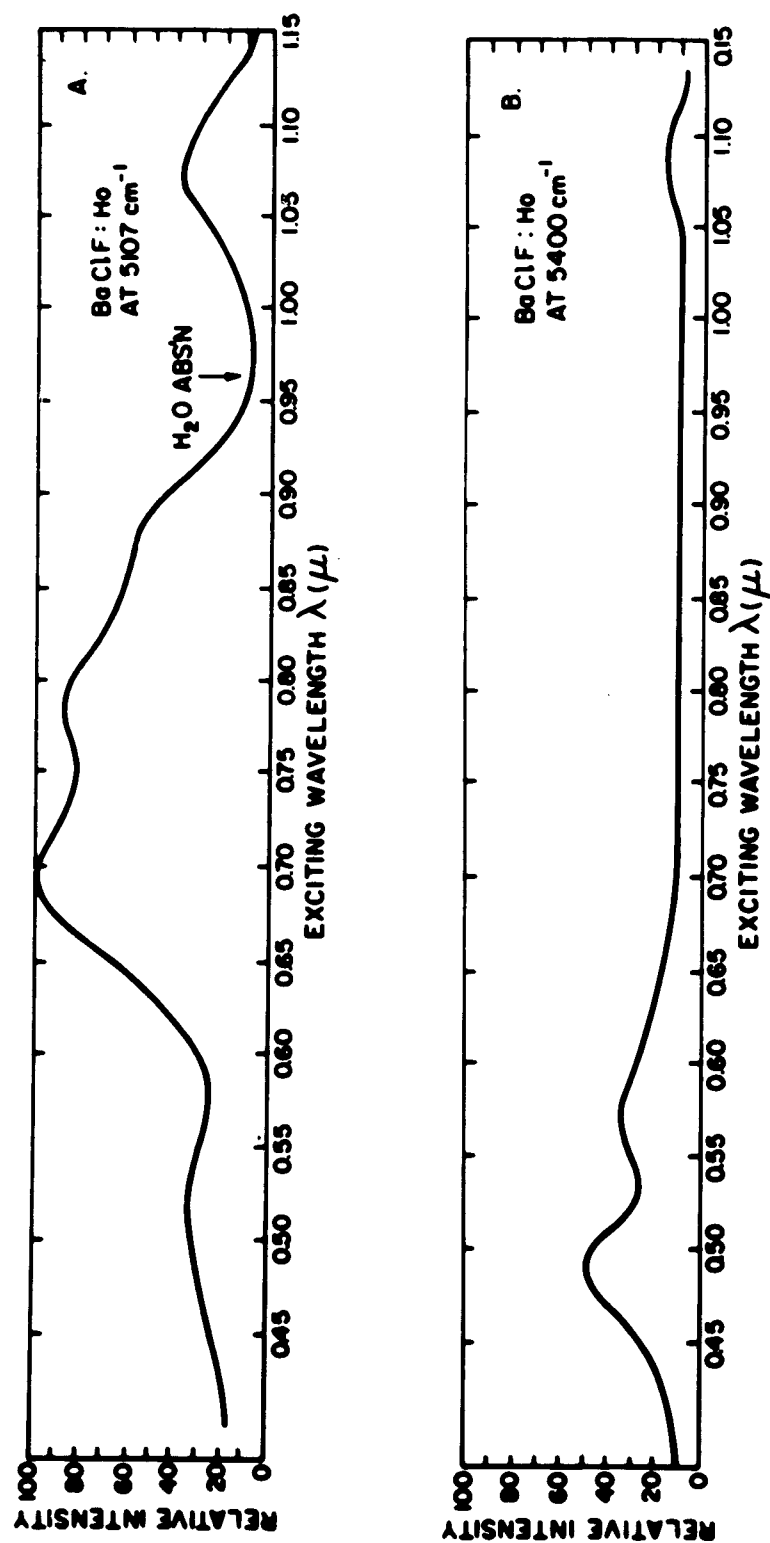


Fig. 21. Excitation spectrum of BaClF:Ho²⁺ at 77°K (Uncorrected)

The latter set of lines appears on excitation between about 6300 Å and 4000 Å (Fig. 21b). This accounts for the relatively high intensity of the higher energy group in Fig. 20, where excitation was by Hg light, rich in blue-green. Under excitation by tungsten light, the higher energy pair of lines is suppressed, and under the higher resolution possible with the greater fluorescence intensity the lower energy pair is better resolved. Furthermore, the group at 4900 cm⁻¹ is also suppressed and a third line evidently related to the 5100 cm⁻¹ pair emerges (Fig. 22). These three lines at 5110 cm⁻¹, 5076 cm⁻¹, and 4885 cm⁻¹ agree reasonably well with the crystal field components of the transition $^4I_{13/2} \rightarrow ^4I_{15/2}$ in Ho²⁺ which are calculated to lie near 5240 cm⁻¹.

Further confirmation of this assignment is derived from a study of samples L-62 and L-61, both of which were prepared from the same BaClF composition containing initially 0.25 mole percent of Ho³⁺. Sample L-62 was grown into a single crystal while contained in a graphite crucible enclosed in a quartz ampoule evacuated to 10⁻⁴ torr and sealed. This crystal fluoresces strongly on excitation with 2537-Å light, yielding the expected Ho³⁺ spectrum (Fig. 18). In the range between 1 μ and 3 μ no fluorescence is observed either with 2537-Å or 3650-Å excitation. Sample L-61 was grown into a single crystal while contained in a graphite boat surrounded by a flowing stream of purified H₂. This crystal exhibits no detectable Ho³⁺ fluorescence on excitation with 2537 Å or 3650 Å, but intense fluorescence in the 1.98-μ region similar to that shown in Fig. 19 upon excitation with the Hg lamp.

There are two significant consequences of these results. First, the influence of residual oxygen in enhancing the solubility of trivalent lanthanides is demonstrated in the relative fluorescence intensity of Ho³⁺ between the sample which was grown in a sealed system containing residual air as well as a source of oxygen in the quartz ampoule. Second, that reduction of Ho³⁺ to Ho²⁺ occurs in the presence of H₂, and graphite-provided oxygen is eliminated. Further, the divalent ion is dissolved readily in the growing crystal. Holmium appears to be reduced more readily than does Dy under similar conditions which is not consistent with the relative reducibility as derived from the work of Polyachenok and Novikov.¹⁸

The absence of Ho³⁺ in sample L-61 with measurable amounts of Ho²⁺ present supports the view that disproportionation is not taking place in the

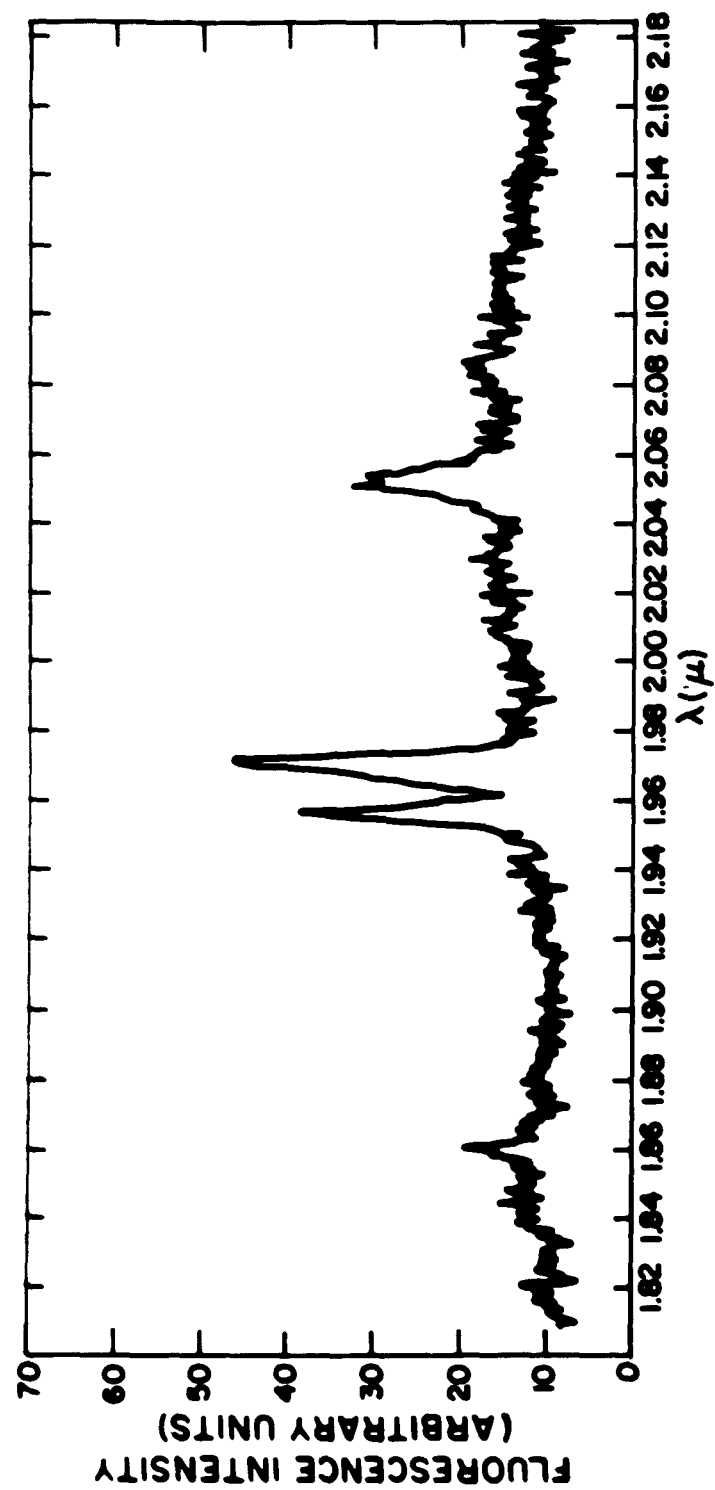


Fig. 22. Fluorescence spectrum of BaClF:Mo²⁺ at 77° K, W-lamp excitation

solid state. However, since the crystal was maintained in hydrogen as it was cooled, it is also possible that disproportionation was inhibited by the reducing action of the hydrogen.

4. Thulium

Trivalent thulium (see Fig. 23), in many hosts, fluoresces in the blue, green, red, and infrared regions of the spectrum, with the blue transition $^1D_2 \rightarrow ^3H_4$ predominating. This transition in $\text{SrCl}_2:\text{Tm}^{3+}$ is illustrated in Fig. 24. We have not, however, observed any fluorescence attributable to Tm^{3+} in the halofluorides, presumably because of the low solubility of this species. Further, no Tm^{3+} fluorescence is excited upon irradiation by 2537-Å light, indicating that the energy transfer mechanism operative in the Dy^{3+} and the Ho^{3+} systems does not obtain here.

Divalent thulium (f^{13}) exhibits the relatively simple energy level scheme illustrated in Fig. 23, having a $^2F_{7/2}$ ground state and $^2F_{5/2}$ first excited state of the 4f levels. Fluorescence occurs between the crystal field components of the 4f levels in the vicinity of 1.1 μ , the details of the spectrum depending upon the host (Figs. 25 and 26). In BaClF , the spectrum (Fig. 26) consists of a pair of sharp lines separated by 33 cm^{-1} with some weaker structure on the low energy side of the lines corresponding probably to vibrational transitions. The relatively small splitting of the major lines represents splitting of the $^2F_{7/2}$ level and is indicative of a relatively weak crystal field. As a consequence of the small splitting of the ground state, Tm^{2+} in BaClF will function as a four-level laser only at temperatures near that of liquid helium.

5. Samarium

Divalent samarium in BaClF has been studied in detail over the past three years and is reported in a number of Technical Reports issued by these laboratories.^{23,24} The energy level scheme for Sm^{2+} is illustrated in Fig. 27 and the fluorescence spectrum in halofluorides in Fig. 28. Because of the ease with which Sm^{3+} can be reduced, it is possible to incorporate large concentrations of Sm^{2+} in BaClF and to attain good crystal quality.

In spite of the high fluorescence efficiency, small spectral linewidth, and satisfactory crystal quality, Fabry-Perot resonators fabricated from this material do not exhibit laser action. While we have not explored the reasons

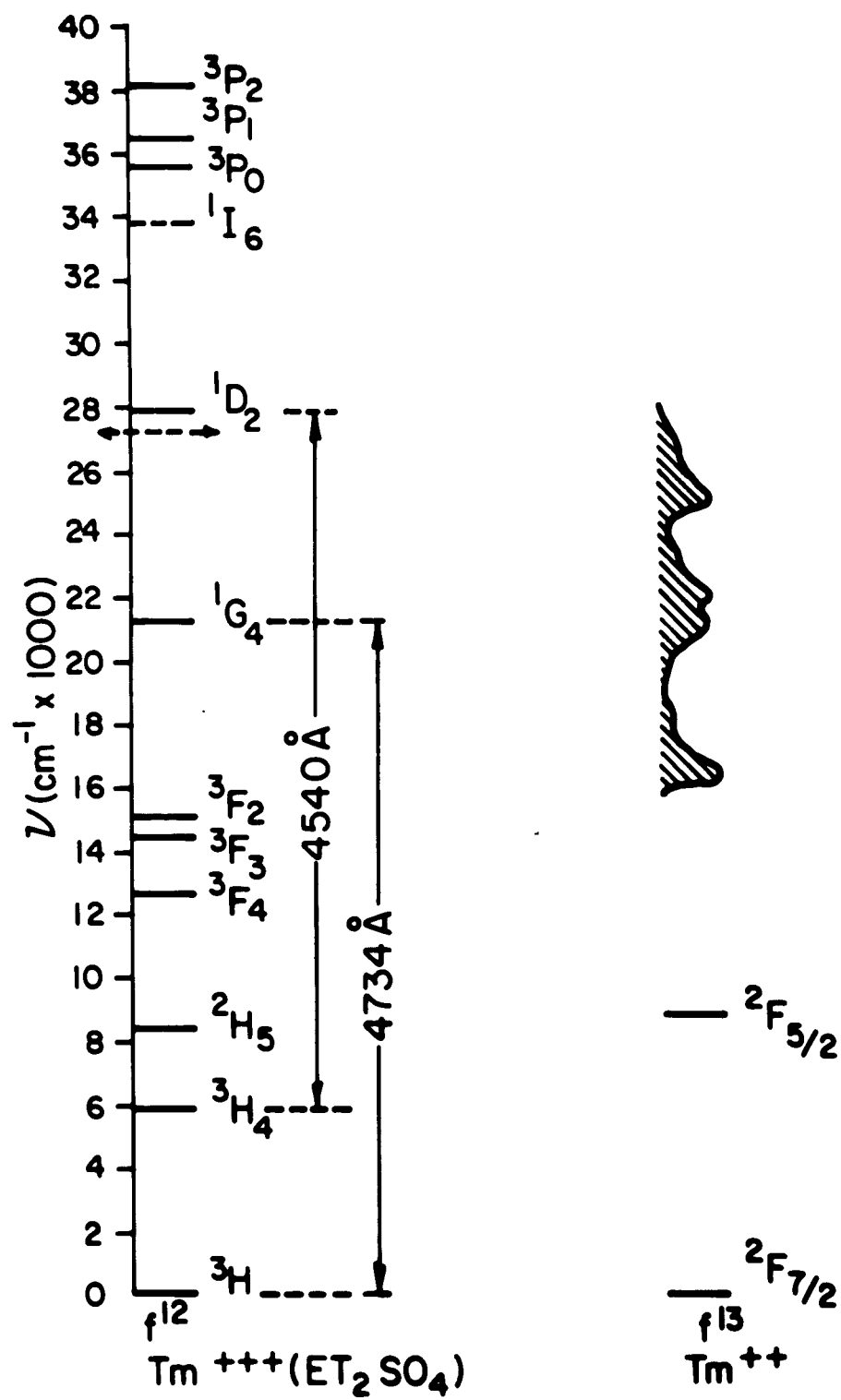


Fig. 23. Energy level scheme for Tm^{3+} , Tm^{2+}

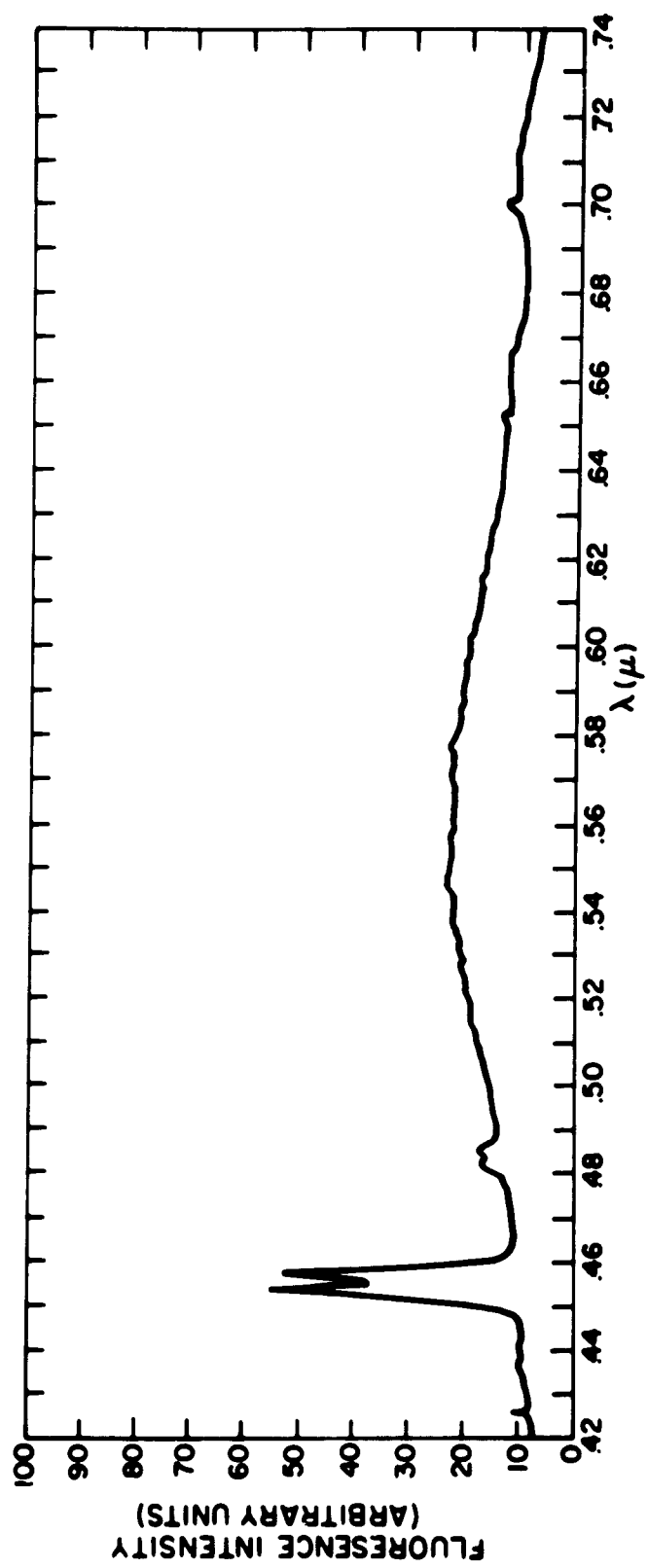


Fig. 24. Fluorescence of Tm^{3+} in $SrCl_2$ at $77^\circ K$

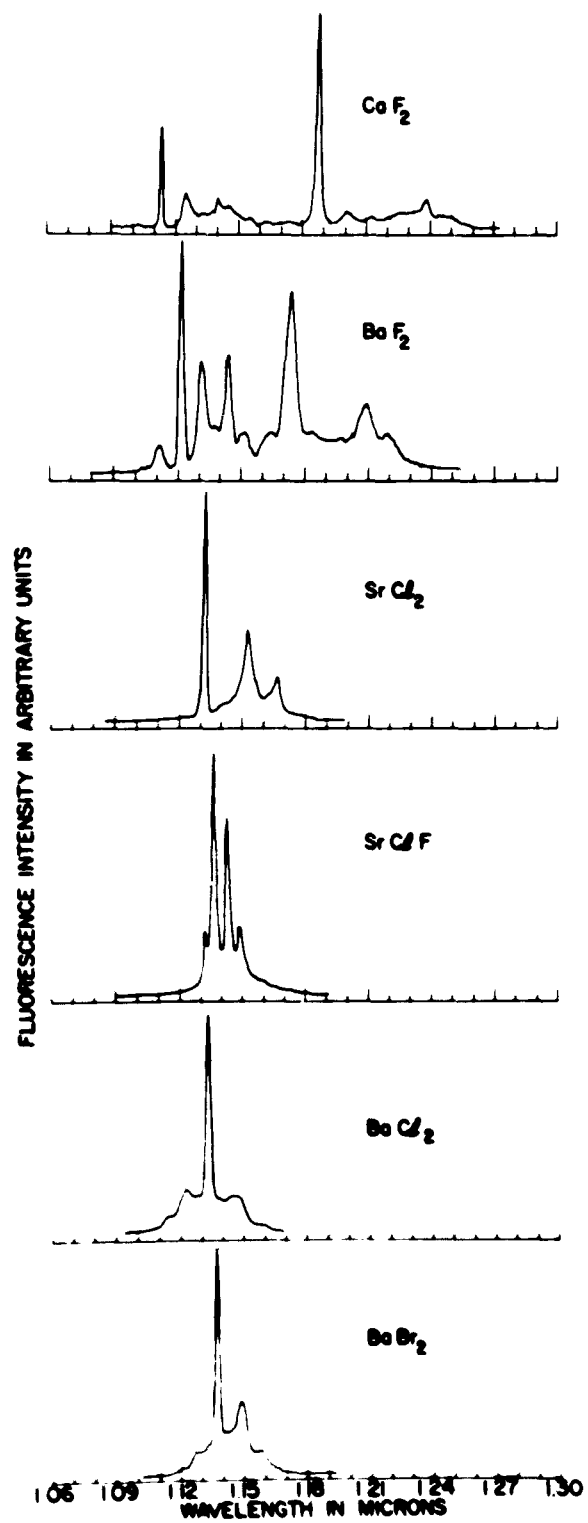


Fig. 25. Fluorescence of Tm^{2+} in various hosts at 77°K

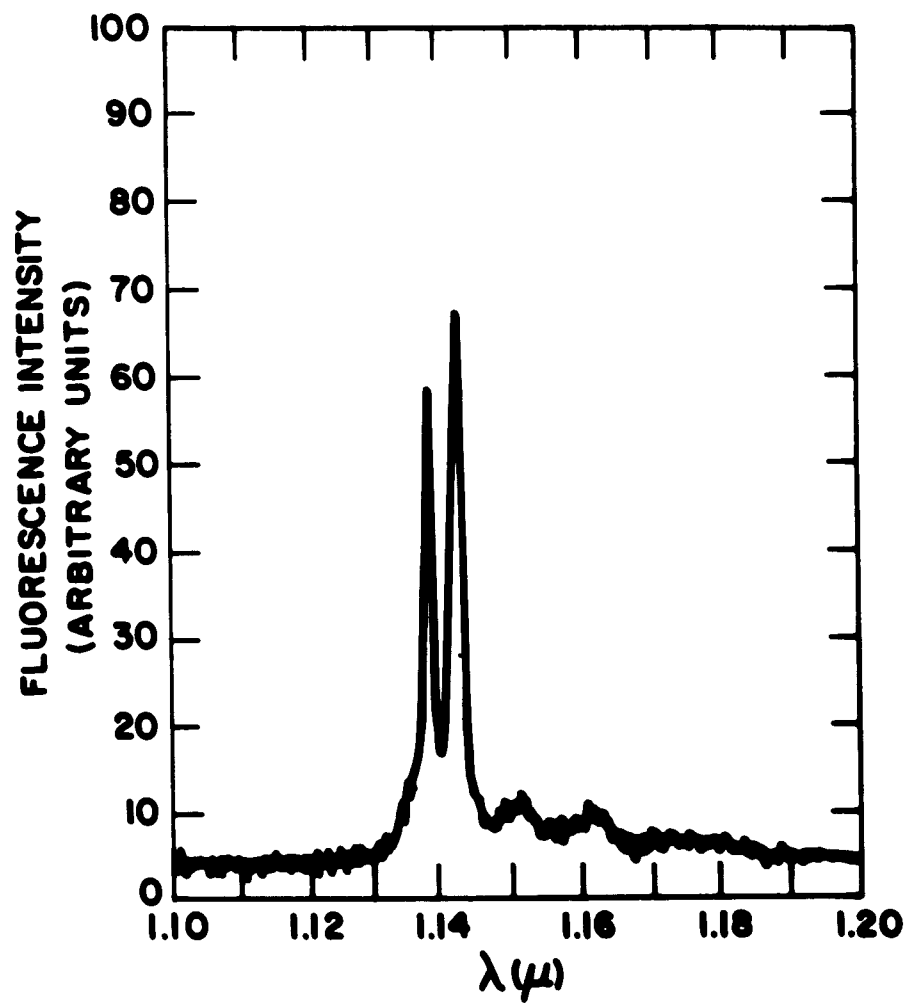


Fig. 26. Fluorescence of BaClF:Tm²⁺ at 77 K

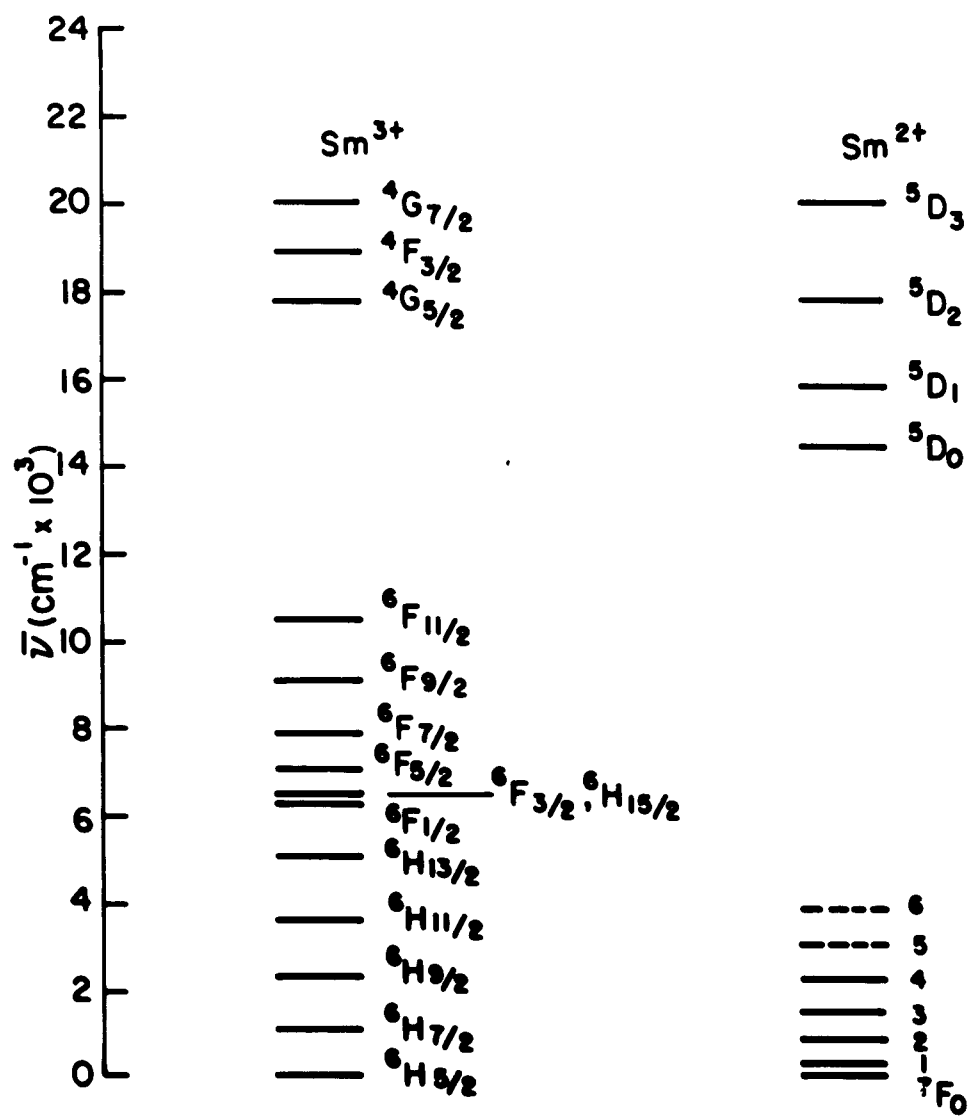


Fig. 27. Energy level scheme for Sm^{3+} , Sm^{2+} .

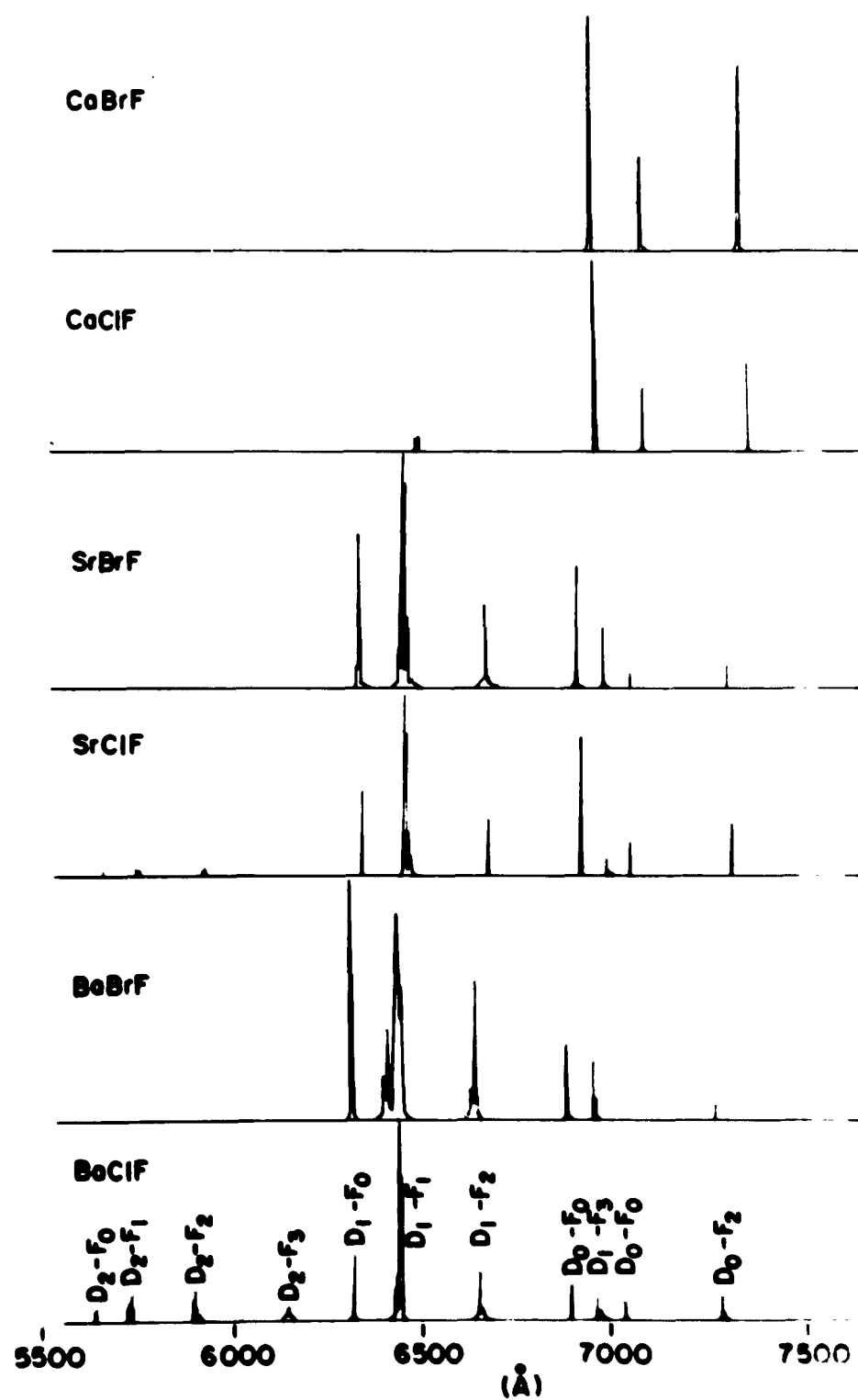


Fig. 28. Fluorescence of $\text{BeClF}:\text{Sm}^{2+}$ in halofluorides at 77 K

for the absence of oscillation in detail, it is possible to understand this behavior qualitatively on the basis of the following arguments. First, although the total fluorescence efficiency is remarkably high, the energy is partitioned among a large number of lines. Further, there is reliable evidence that nonradiative processes are significant. Second, the 4f-5d absorption occurs at energies corresponding to twice that of any of the observed fluorescence lines. It is, therefore, proposed that population inversion of any given pair of states is difficult to achieve because of the broad partition of energy. Also, the effective concentration of rare-earth ions is reduced considerably as a result of the possible transitions from any excited state to the 5d bands and loss of a significant fraction of this reabsorbed energy by nonradiative processes.

The study of samarium has also provided further confirmation of our conclusions regarding the low solubility of trivalent lanthanides in halofluorides. It was observed that, while divalent samarium emission was found in every Sm-containing sample regardless of whether or not deliberate efforts were made to bring about reduction, Sm^{3+} emission was not found. A careful study of many samples grown under various conditions and excited either by 2537-Å light or 3650-Å light failed to reveal any evidence of Sm^{3+} . In all samples at room temperature cathode ray excitation does produce weak Sm^{3+} fluorescence. The intensity of this fluorescence is less in those crystals which are very low in oxide contamination. It follows, then, that the Sm^{3+} concentration is very low but that this oxidized species is much more efficiently excited by cathode rays than is the divalent species, or, alternatively, that Sm^{3+} is initially absent, but is produced in small concentration during excitation by the ionizing action of the cathode ray beam.

B. PEROVSKITES

The perovskites with which we have been concerned are those of the general composition ABF_3 , where A represents a monovalent cation and B, a divalent cation.*

The structure is cubic or slightly distorted therefrom, (tetragonal, orthorhombic, monoclinic, and rhombohedral distortions have been reported) with the B-ion occupying the center of an octahedron of F^- ions lying at the

* For a more complete discussion of the chemical properties of these compounds see Section II.A.

face centers of a cube, the corners of which contain the A-ions (Fig. 29). Compositions which are expected to be chemically compatible with divalent rare earths are those in which the A-ion is an alkali-metal ion, and the B-ion, an alkaline-earth or alkaline-earth-like ion such as Yb^{2+} . We have conducted a study of the melting and crystallization behavior of several members of this class by differential thermal analysis techniques to determine which of the many possible compounds can be crystallized from the melt.* For the purposes of this study, we have selected the following compounds as representative examples with good crystallization properties and desirable optical behavior: RbMgF_3 , KCaF_3 , NaMgF_3 , $\text{KMgF}_3 \cdot \text{KCaF}_3$, RbCaF_3 , KMgF_3 (see Table 2).

1. RbMgF_3

a. $\text{Nd}^{3+} - \text{Nd}^{2+}$ -- Rare earths dissolved in polycrystalline melts of the various perovskites exhibit strong fluorescence, characteristic of the trivalent rare earth. Upon growth of single crystals from these melts, the rare earth is fractionated between the melt and the growing crystals. As would be expected from considerations of charge and ion size, the Mg-containing perovskites reject the trivalent rare earth strongly while in the calcium-containing components, the solubility in the single crystal is relatively high. For example, Nd^{3+} in a polycrystal of RbMgF_3 exhibits sharp line fluorescence which can be related to known transitions in Nd^{3+} (Fig. 30 and Table 7). There is, in addition, a broad band peaking at 7400 \AA which is not related to Nd^{3+} but which contains absorption lines which again can be attributed to the presence of this ion.

When this melt was then grown into a single crystal by the Czochralski technique, the fluorescence spectrum was altered to a broad band containing only vague structure attributable to the Nd^{3+} spectrum (Fig. 31). While the origin of the band both in the melt and in the crystal has not definitely been established, it is possible that it may arise from the presence of a small concentration of Nd^{2+} . McClure and Kiss¹¹ have reported that the lowest $f^n \rightarrow f^{n-1}d$ transition in $\text{CaF}_2:\text{Nd}^{2+}$ lies around 5000 cm^{-1} . In this host it would be expected to be at least as low in energy, perhaps lower, depending on which site the Nd^{2+} ion occupies. It would be expected, then, that transitions in the energy range of this band $\sim 10,000$ to $14,000 \text{ cm}^{-1}$ would

* Semiannual Progress Report No. 2, p. 8.

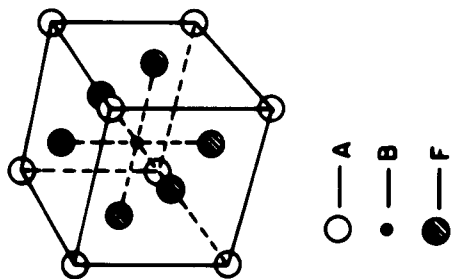


Fig. 29. Crystal structure of ABF_3 perovskites

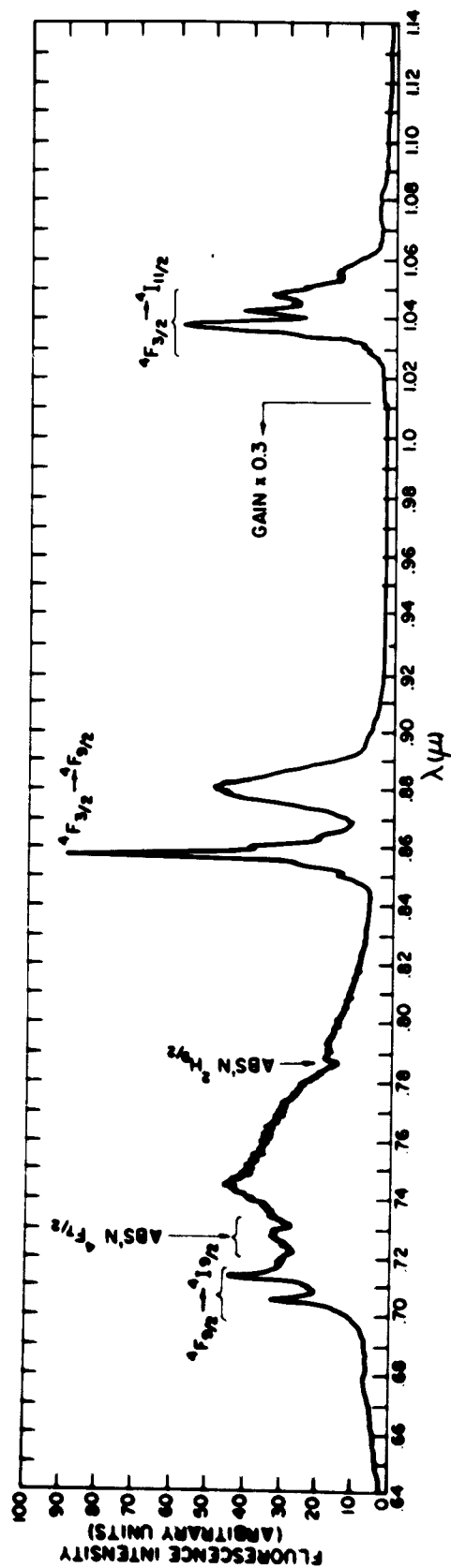


Fig. 30. Fluorescence spectrum of Nd^{3+} in $RbMgF_3$ melt, $77^\circ K$

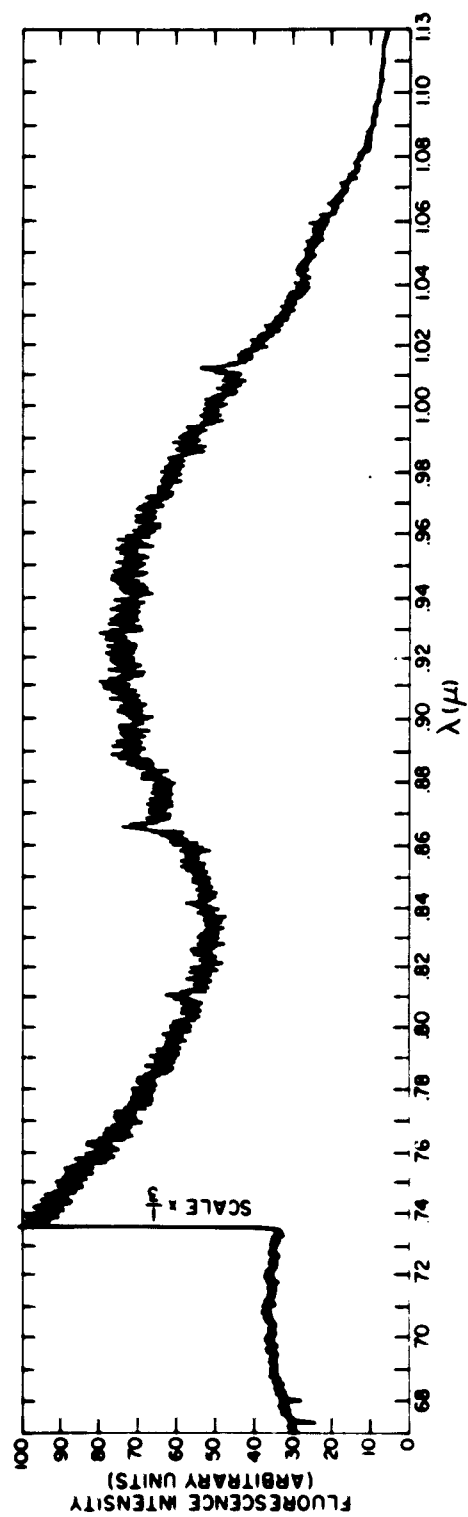


Fig. 31 Fluorescence of Nd^{2+} in RbmgF_3 crystal, 77°K

TABLE 7
FLUORESCENCE TRANSITIONS IN Nd³⁺

Transition	Calculated Energy(cm ⁻¹)*	Experimental Values(cm ⁻¹)
⁴ F _{9/2} → ⁴ I _{11/2}	13975	14184 14031
⁴ F _{3/2} → ⁴ I _{9/2}	11524	11675 11376
⁴ F _{3/2} → ⁴ I _{11/2}	9596	9638 9592 9537 9570 9294
* B. G. Wybourne, J. Chem. Phys. <u>32</u> , 639 (1960).		

occur either between 4f and 5d levels or between 5d levels giving rise in either case to broad emission bands.

From a chemical standpoint, Nd³⁺ is among the ions which are known to exhibit divalency at room temperature (see Section II.C.). In the presence of reducing gas such as H₂ which was present during preparation of the crystal, the relative concentration of Nd²⁺ in the melt would be increased somewhat over the equilibrium concentration. If, as is suspected from the Sm²⁺ observations (vide infra), the divalent ion is soluble in the growing crystal, then as the crystallization proceeds, Nd²⁺ will be continuously extracted at the crystal-melt interface forcing the reaction,



to the right and leading to significant concentrations of Nd²⁺ in the crystal. If this spectrum is indeed representative of the behavior of Nd²⁺ in the perovskites, there is no possibility of observing laser action in this system.

b. Sm³⁺ - Sm²⁺ -- Of all the rare-earth ions of interest, samarium has consistently exhibited the greatest ease of reduction. In all the alkaline-earth halide and halofluoride hosts it has appeared in measurable concentrations as the divalent ion even under conditions where no reducing agent was

added to the system. It was therefore anticipated that similar behavior would be encountered in the perovskites. We found that in many cases this was true to some extent, but that significant concentrations of Sm^{3+} were always present in polycrystalline melts.

A study of samarium in RbMgF_3 supports the hypothesis that the trivalent ion is rejected from the growing crystals in favor of the divalent ion. A sample of RbMgF_3 containing 0.1 mole percent Sm was purified with dry HF gas at a temperature well above the melting point. It was then flushed with flowing pure H_2 and cooled in the hydrogen stream. Upon excitation of the resulting polycrystal at 3650 \AA the fluorescence spectrum (Fig. 32a) shows characteristic Sm^{3+} fluorescence and emission identifiable as originating in the divalent species (Cf. Fig. 26). The intensity of the trivalent emission, however, is considerably greater than that of the divalent. In consideration of the relatively low efficiency of excitation of the trivalent fluorescence as compared with that of the divalent fluorescence, the relative concentration of the divalent species is undoubtedly considerably less than is indicated by its fluorescence intensity. The fluorescence spectrum of a single crystal of good optical quality pulled from a melt of this polycrystalline material (pulled in 2% H_2 , 98% He) was entirely different. Essentially only the divalent spectrum appears (Fig. 32b), the peak intensity of which exceeds that of the divalent species in the original material by more than two orders of magnitude. (This is not apparent in Fig. 32. The illustrations represent normalized spectra and therefore do not reflect adjustments of gain in the detection system or of the monochromator slits.) It is clear from this example that the divalent ion is extracted efficiently by the growing crystal while the trivalent ion, is rejected.

It is to be noted that nearly all the emission originates in transitions from the $^5\text{D}_0$ state of Sm^{2+} . This is to be contrasted with the case of $\text{BaClF}:\text{Sm}^{2+}$ where emission from $^5\text{D}_1$, $^5\text{D}_2$, and $^5\text{D}_3$ is also observed and in $\text{CaF}_2:\text{Sm}^{2+}$ where the 5d levels obscure the $4f \rightarrow 4f$ transitions completely. Apparently, in this host, optical transitions from the higher $^5\text{D}_j$ levels do not occur, the energy being degraded either to the ground state by radiationless (phonon) processes or to the $^5\text{D}_0$ state by similar processes. Because of the high efficiency observed in this sample (the actual Sm concentration according to emission spectroscopy analysis is $< 300 \text{ ppm}$), the latter process appears to

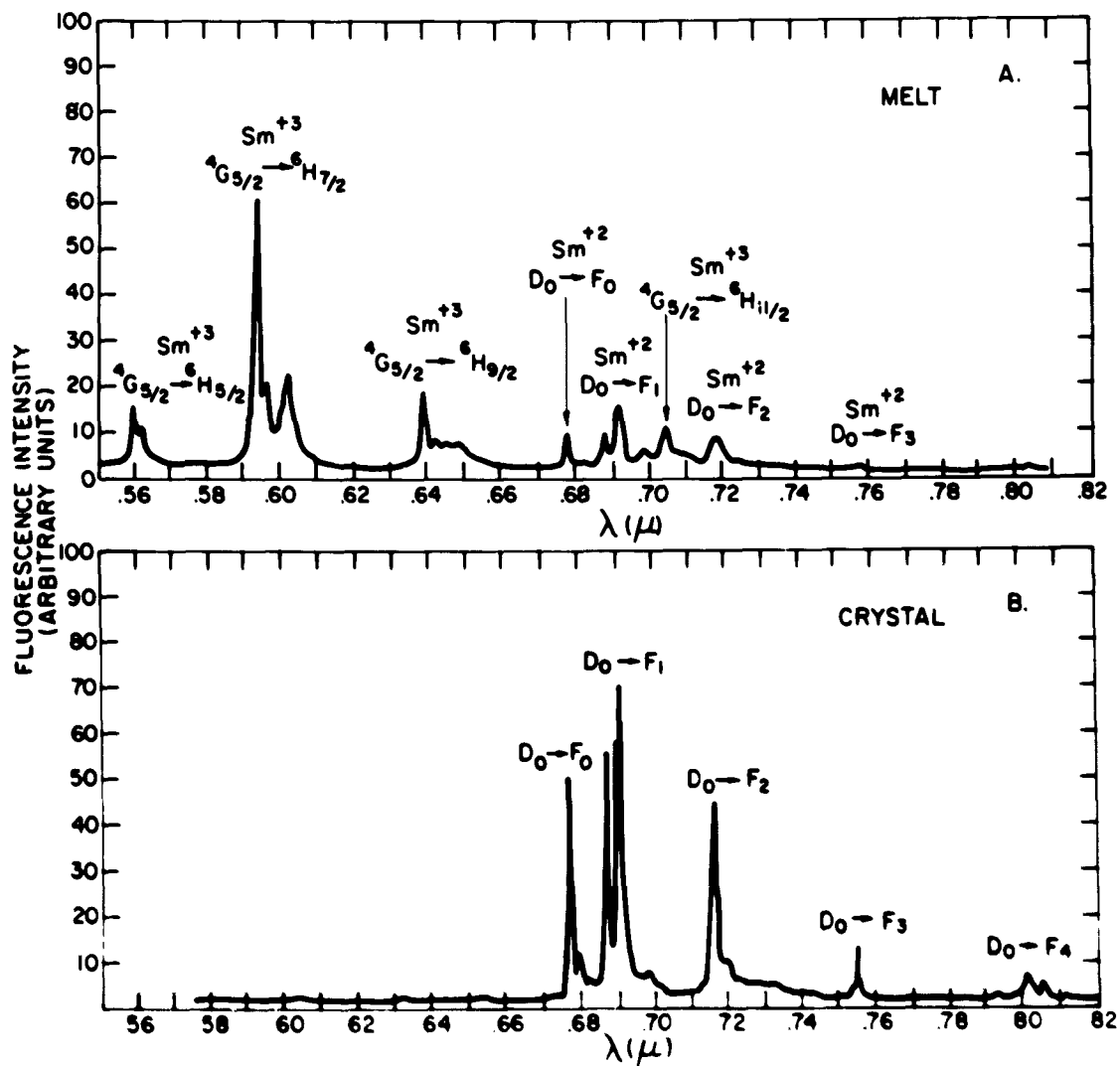


Fig. 32. Fluorescence of Sm in RbMgF₃ melt and crystal, 77° K

be the more probable. We have therefore, in this host, overcome one of the major difficulties encountered with the BaClF:Sm^{2+} system, that of extensive partition of the emission energy among many metastable 4f levels.

Because of the extreme narrowness of the fluorescent spectral lines and the high fluorescence efficiency, this system appears to be a promising candidate for a successful laser. This is especially so in view of the good optical quality of the Czochralski-grown crystals. We therefore proceeded to study the emission lifetime and excitation behavior of the system. Lifetime was measured by exposing the sample to a 2- μsec flash of light from a high-pressure xenon arc while viewing the emission through a monochromator by means of the output pulse produced by the photomultiplier detector (see Section IV.D.). The time dependence of the emission intensity is exponential in character (Fig. 33) and can be represented by a single time constant for each line. While each group of lines can be unambiguously identified as originating in the $^5\text{D}_0$ state of Sm^{2+} and terminating in the $^7\text{F}_j$ levels of the ground state, the various lines examined exhibit different lifetimes (Table 8).

TABLE 8
LIFETIMES FOR Sm^{2+} IN RbMgF_3

Transition	$\lambda(\text{\AA})$	τ
$^5\text{D}_0 \rightarrow ^7\text{F}_0$	6795	$15 \pm 2 \text{ msec}$
$^5\text{D}_0 \rightarrow ^7\text{F}_1$	6930	$21 \pm 2 \text{ msec}$
$^5\text{D}_0 \rightarrow ^7\text{F}_2$	7185	$18 \pm 2 \text{ msec}$

Such behavior is inconsistent with the assumption that all the lines originate in the $^5\text{D}_0$ level unless it is further assumed that each of the transitions viewed represents ions lying in slightly different environments in the crystal. This latter assumption is further supported by the excitation spectra (Fig. 34) which exhibit small differences among the various lines observed, although the spectra for the 6930- \AA and the 7185- \AA lines are indistinguishable within the resolution of the measurements. There is a further inconsistency in the behavior of this system which is related to the

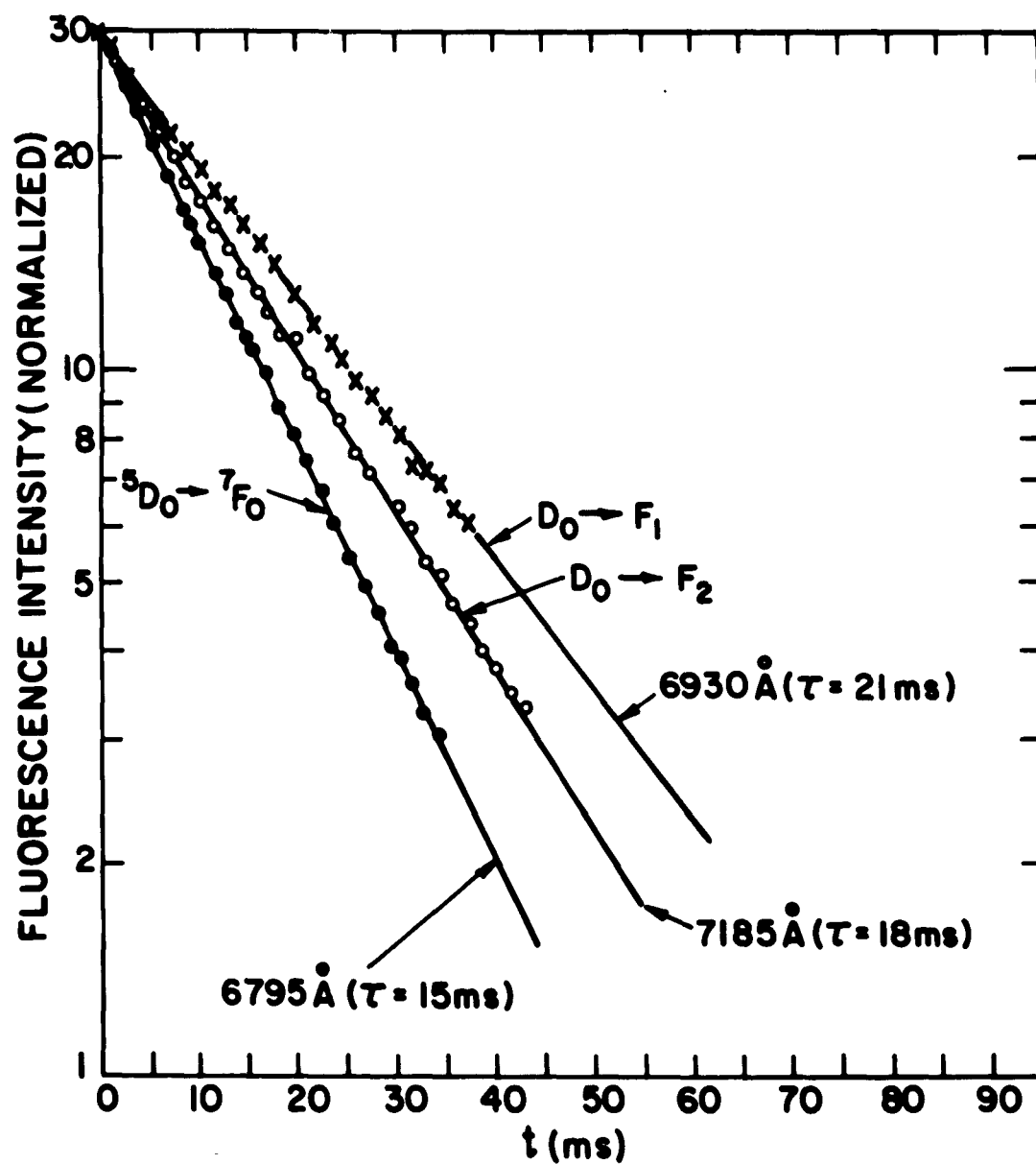


Fig. 33. Lifetime of Sm^{2+} in RbMgF_3 , 77°K

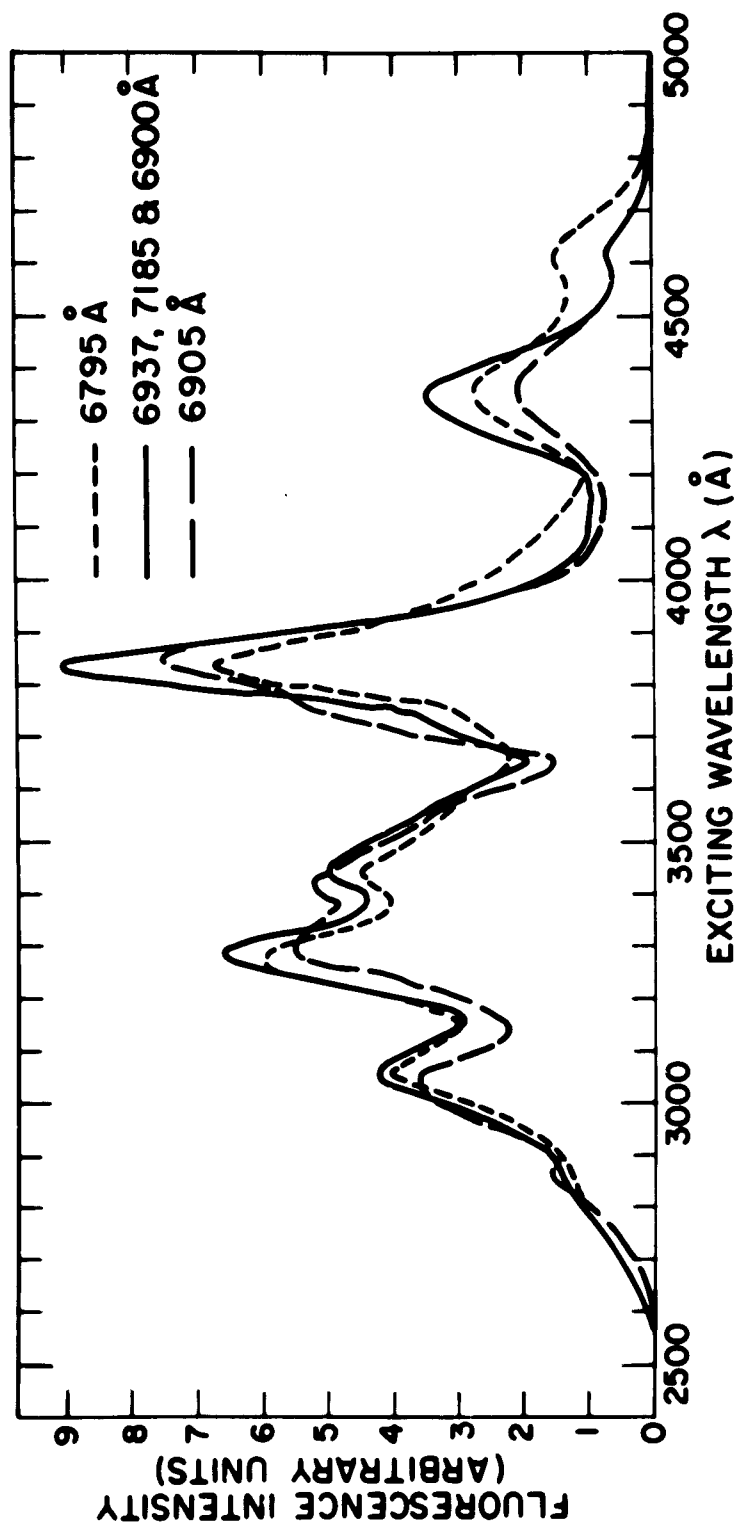


Fig. 34. Excitation spectra in $\text{RbMgF}_3:\text{Sm}^{2+}$, 77°K (Uncorrected)

relatively long lifetimes of the various states. If indeed the transitions are electric dipole in character, one would anticipate that the lifetimes would lie in the 10^{-5} to 10^{-4} second range, while here we are finding lifetimes two orders of magnitude longer. It would appear, then, that the rare-earth ion is located at a site which is symmetrical with respect to inversion. In the absence of more detailed spectroscopic studies, however, this question remains unresolved. In view of these findings, a search for laser action was carried out using the particular crystal reported here. Because of the small size of the available resonators, and because of the low concentration of divalent samarium, the results of the test were inconclusive.

To acquire further information regarding samarium in perovskite hosts, a study similar to that carried out in RbMgF_3 was conducted on the cubic perovskite, KCaF_3 . Here the divalent ion more nearly matches in size that of the rare earth and hence higher solubility would be expected. The polycrystalline melt exhibited approximately the same ratio of divalent to trivalent fluorescence as did the RbMgF_3 melt. Upon pulling a single crystal, however, no significant change in the $\text{Sm}^{3+}/\text{Sm}^{2+}$ ratio was found. The increase in size of the divalent ion by substituting calcium for magnesium has raised the solubility of the rare earth to the point where the charge mismatch is of little consequence. In contrast, then, to the system which contains magnesium and where, evidently, charge matching is of primary importance, no extraction of the divalent species occurs. There is, therefore, no shift to the right in the equilibrium, $\text{Sm}^{3+} + e^- \rightleftharpoons \text{Sm}^{2+}$, and no increase in the amount of available Sm^{2+} in the crystal.

The compound $\text{NaMgF}_3:\text{Sm}$ was also investigated. This experiment was not carried beyond the polycrystalline stage because of lack of time. The sample was prepared by melting the constituents in the usual manner in the presence of SmF_3 and Sm metal slightly in excess of the amount necessary to reduce the material entirely to Sm^{2+} . The product was yellow and strongly luminescent under 3650-Å excitation. The spectrum (Fig. 35) contains only Sm^{2+} emission and like the $\text{RbMgF}_3:\text{Sm}^{2+}$ crystal, all the emission originates in the $^5\text{D}_0$ state. While lifetime measurements were not carried out, the multiplicity of the transitions to $^7\text{F}_j$ levels higher than $^7\text{F}_0$ infers that site multiplicity is present in this compound. The remarkable sharpness of many of the lines in this material indicates that whatever site multiplicity exists, it is not

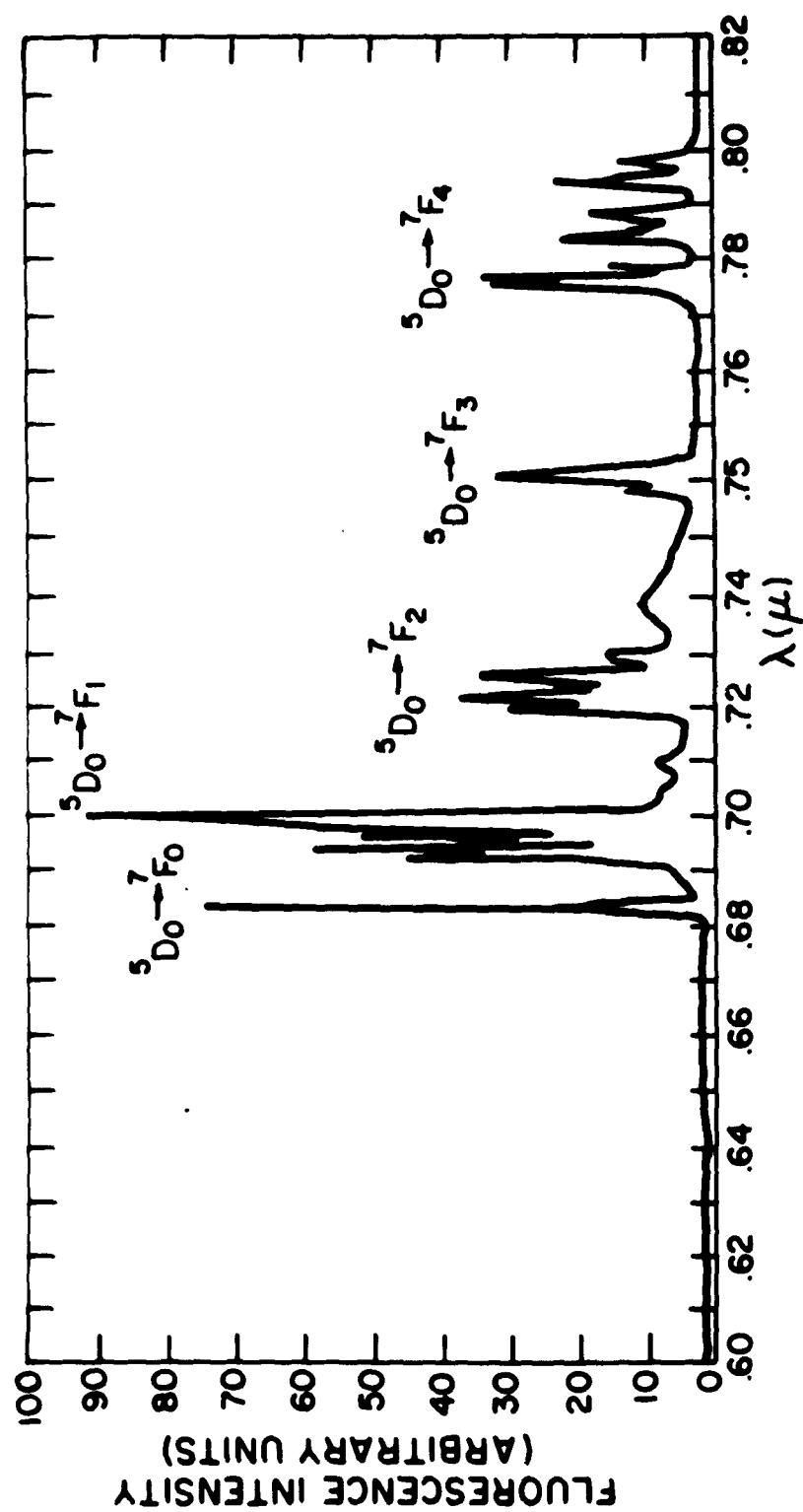


Fig. 35. Fluorescence spectra of $\text{NaMgF}_3:\text{Sm}^{2+}$, 77°K

purely random. Further, the prospect of achieving laser action is good provided high quality crystals can be grown.

The fluorescence of samarium in the system $\text{KMgF}_3 \cdot \text{KCaF}_3$ resembles that of KCaF_3 . Since this compound proved to be extremely difficult to prepare as a single crystal, no further work was conducted on it.

As a consequence of these investigations on samarium, it becomes clear that the most promising systems are $\text{RbMgF}_3:\text{Sm}^{2+}$ and $\text{NaMgF}_3:\text{Sm}^{2+}$. This is true in spite of the unfavorable size of the B site ion. Substantial concentrations of Sm^{2+} can be incorporated provided the crystal is pulled in the presence of samarium metal. Line widths are small, excitation is in the blue-violet region of the spectrum, and indications are that both of these systems form hard crystals of good optical quality. These characteristics, together with the absence of fluorescence from states of higher energy than $^5\text{D}_0$, place these systems among the most promising that we have investigated.

c. Ho^{3+} -- In contrast to the spontaneous reduction in the melt and subsequent extraction of the divalent species into the crystal observed with Sm and Nd, Ho^{3+} proved to be very difficult to reduce at the melting temperature of RbMgF_3 (923°C) even in the presence of Ho metal. Purified RbMgF_3 was melted together with 0.6 mole percent HoF_3 and 0.4 mole percent of Ho metal in the Czochralski apparatus. The metal was observed to dissolve readily, yielding a transparent solution with no evidence of undissolved material. A crystal was pulled from this melt and the fluorescence spectrum studied. Both the melt residue and the single crystal fluoresce in the infrared (only very weak Ho^{3+} fluorescence was observed in the visible region of the spectrum) in the vicinity of $1.93\ \mu$ (Fig. 36). The center of gravity of the more intense group of lines is at $1.939\ \mu$, close to the calculated wavelength of the $^5\text{I}_7 \rightarrow ^5\text{I}_8$ transition of $1.937\ \mu$ in Ho^{3+} (Fig. 19). A crude excitation spectrum indicated that, within the spectral distribution of the Hg-arc exciting light, excitation occurs only at the $4358\text{-}\text{\AA}$ Hg line which lies close to the $^5\text{F}_1$ level of trivalent Ho. The narrowness of the excitation range and the close correspondence of the emission with the $^5\text{I}_7$ energy is adequate evidence that the Ho species present is trivalent. It is clear, therefore, either that Ho^{3+} is not reduced by the corresponding metal at the melting temperature or that residual oxidizing agents in the crystal growing apparatus prevented reduction. That the alternative process, extraction of the divalent

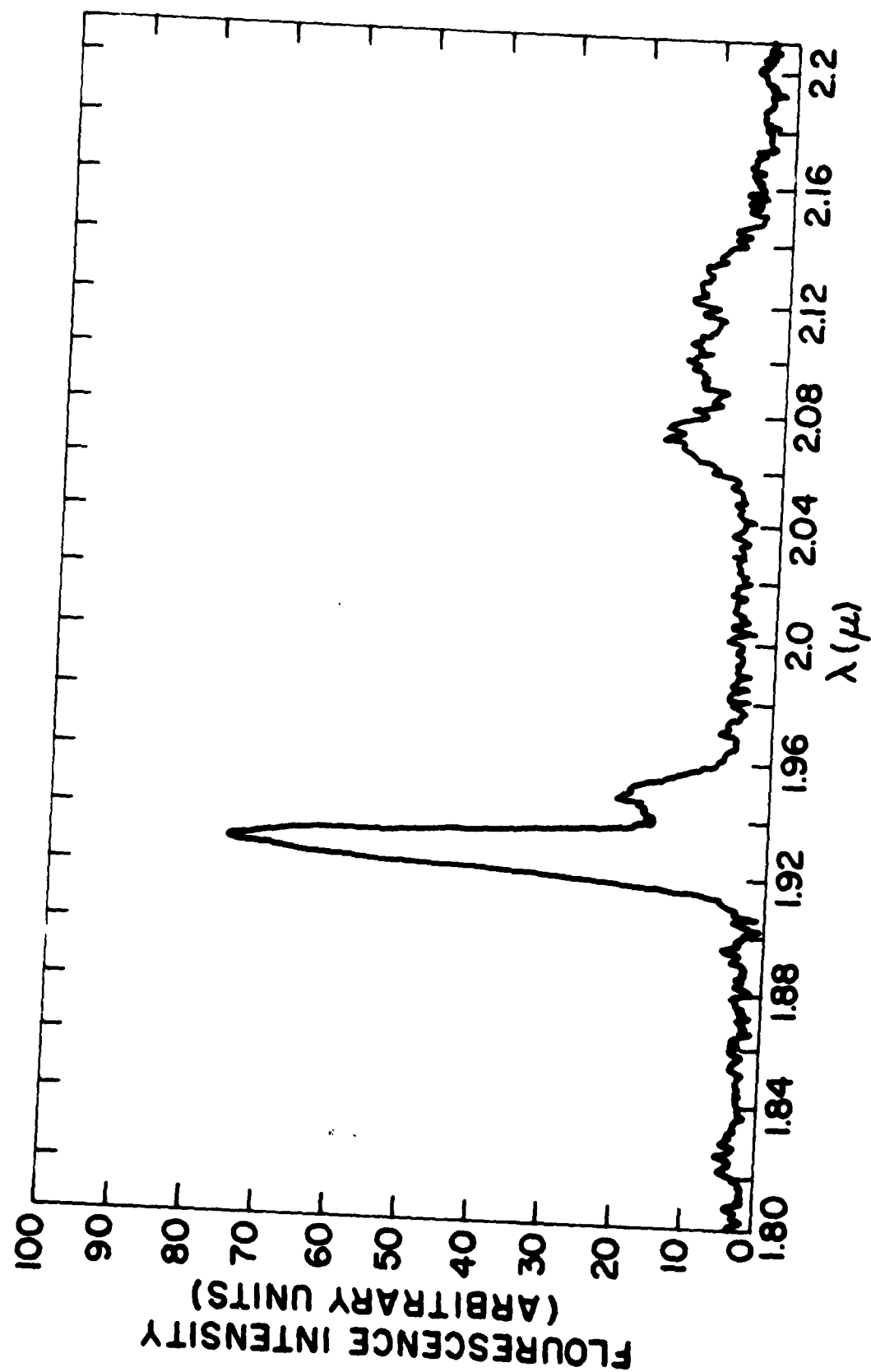


Fig. 36. Fluorescence of Ho^{3+} in RbMgF_3 , 77° K

rare earth into the growing crystal and subsequent disproportionation, does not occur under these conditions is indicated by the lower concentration of Ho^{3+} in the crystal relative to that in the residue. This conclusion was further confirmed by pulling a second crystal from the same melt to which was added an additional quantity of Ho metal. This second crystal exhibited no Ho^{2+} and approximately the same Ho^{3+} concentration as did the original crystal - evidently the saturation concentration under these conditions of solution.

2. Dy^{3+} in KCaF_3 - γ -irradiated

The relatively high solubility of trivalent lanthanides in KCaF_3 raises the possibility of in situ reduction by γ -irradiation. Accordingly, a single crystal of KCaF_3 containing a nominal concentration of 0.1 mole percent of Dy^{3+} was grown by the Czochralski technique. The crystal was of poor quality, opalescent in appearance, with veins of free KF running along the surface. As was anticipated from the results with Sm^{3+} , the concentration of Dy^{3+} in the crystal was sufficiently high to produce intense Dy^{3+} fluorescence (Fig. 37). There was no evidence of spontaneous reduction of the rare earth. The crystal was irradiated with gamma rays to a total dosage of 10^7 rad. After treatment with the gamma radiation, the crystal became brown in color, but no fluorescence was observed in the spectral regions where Dy^{2+} is known to emit. It is therefore concluded that this ion cannot be reduced in KCaF_3 by γ -irradiation, presumably because of the greater stability of the color-center sites relative to that of the trivalent rare-earth ion.

C. SrCl_2

Strontium chloride is a cubic material having the fluorite structure. In its pure state it crystallizes readily forming large single crystals of excellent optical quality. While it is hygroscopic, it takes up moisture slowly and, hence, with appropriate precautions, it can be cut and polished into laser structures. It incorporates trivalent rare earths during growth in the absence of charge compensators, although segregation coefficients are more favorable when Na^+ charge compensation is employed (Fig. 38). Divalent rare earths may be produced both by a priori and in situ methods, and the fluorescence is intense and sharp (Fig. 39). There is evidence that, at

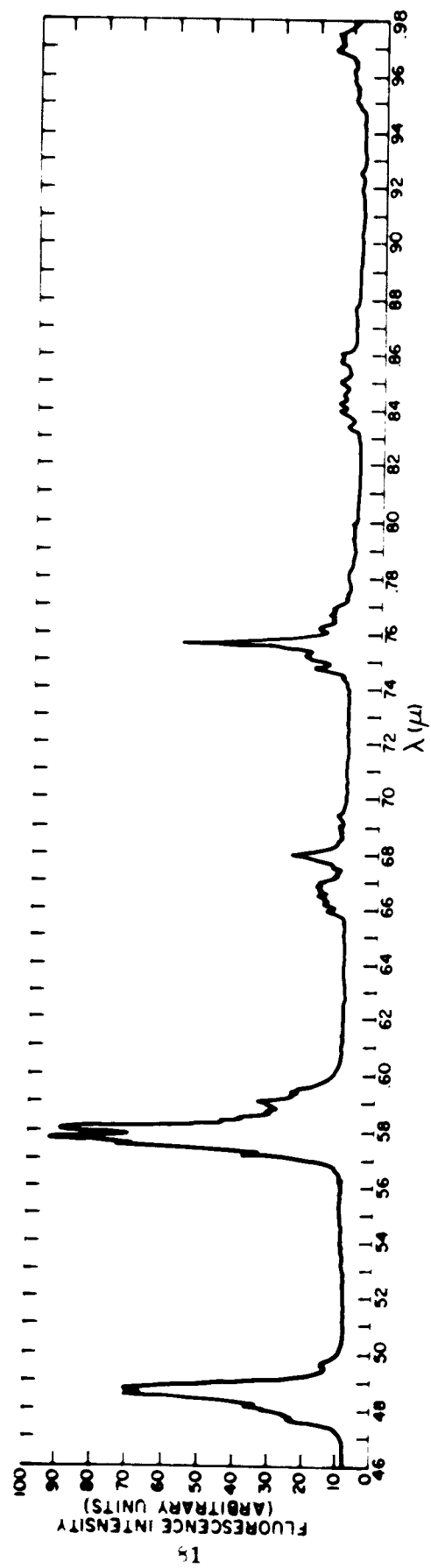


Fig. 37. Fluorescence of Dy^{3+} in KCaF_3 , 77°K

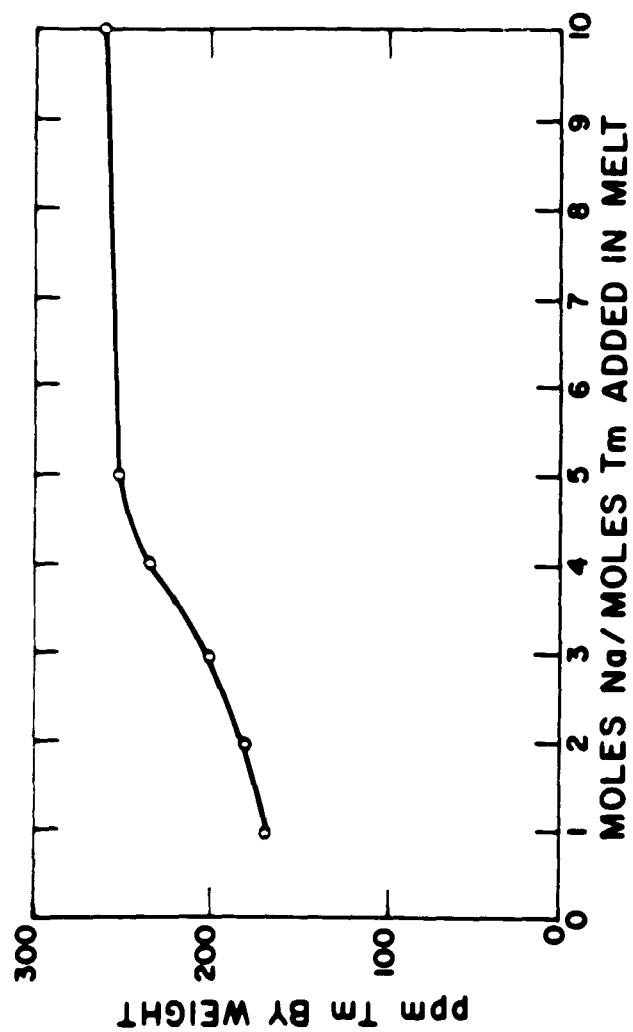


Fig. 38. Influence of charge compensation on Tm concentration in SrCl_2 (Nominal concentration, 0.05 mole %)

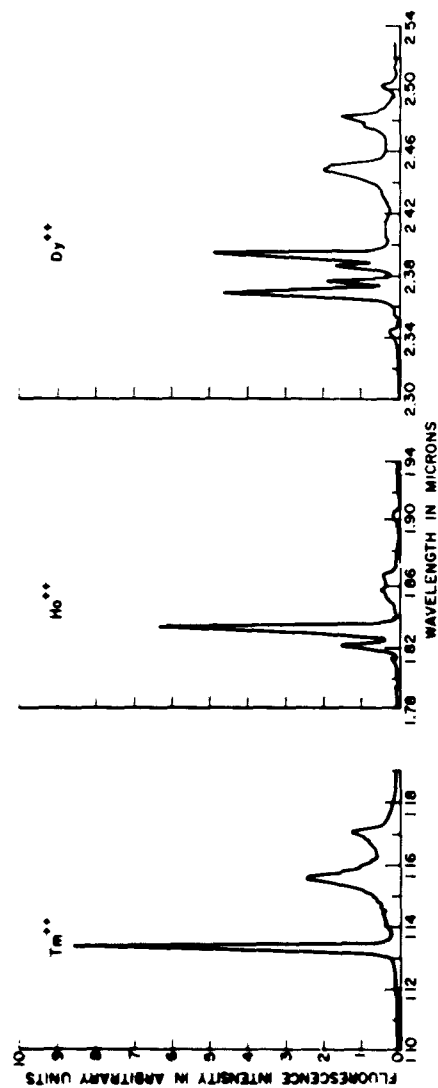


Fig. 39. Fluorescence of divalent rare earths in SrCl_2 at 77°K

least in some instances, the local symmetry is not isotropic and, hence, electric dipole transitions may take place.

In the course of these studies, we have observed important fluorescence behavior in the system $\text{SrCl}_2:\text{Ti}^{2+}$ which had not been previously described in the literature.* In addition to the expected 4f-4f line emission, intense bands appear in the vicinity of 7000 Å and 4800 Å which break up into series of very sharp lines at liquid helium temperature (Fig. 40). These lines represent transitions between vibronic levels of a spin-forbidden 5d band and the ground state. The intensity is high, representing about 90 percent of the total emission energy (the remainder appearing in the $^2F_{7/2} \rightarrow ^2F_{9/2}$ f-f transition), and the lifetime is 200 μsec. Accordingly, it is anticipated that laser action will occur within these transitions.

Fabry-Perot resonators were fabricated from this material and preliminary laser tests were made. Difficulties were encountered in maintaining the reflecting ends and, unfortunately, time did not permit further pursuit of this problem.

* Red Band Fluorescence in $\text{SrCl}_2:\text{Ti}^{2+}$ - Second Semiannual Report, p. 28.

FLUORESCENCE INTENSITY IN ARBITRARY UNITS

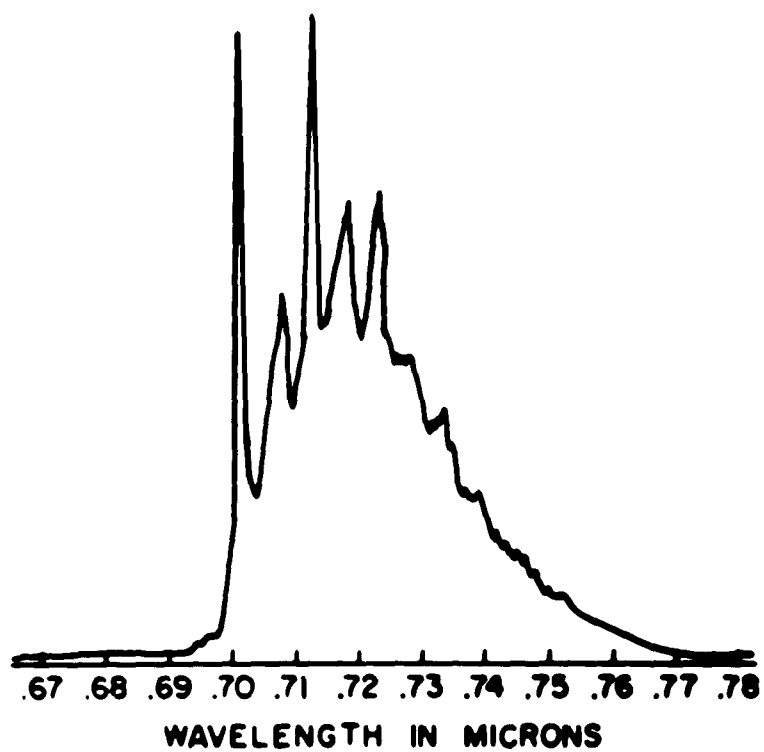
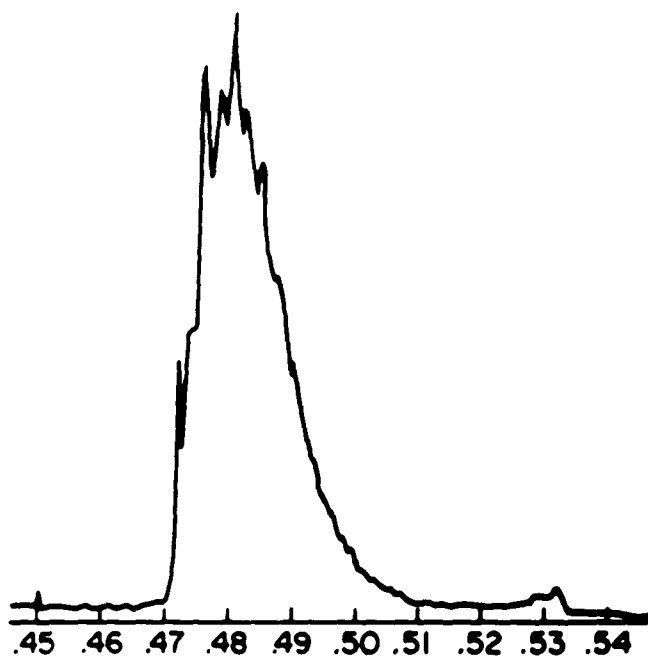


Fig. 40 5d-band fluorescence in $\text{SrCl}_2\text{:Tm}^{2+}$ at 4.2° K

SECTION IV

INSTRUMENTATION

The measurements of fluorescence spectra, excitation spectra, absorption spectra, lifetime, and quantum efficiency, carried out in connection with this study, were performed on a number of different instruments depending upon which was most appropriate for the particular problem. Since most of this equipment is conventional in nature, it is not necessary to discuss it here. Most of the measurements, however, were conducted on two small instruments assembled specifically for this work and found to be of such wide general utility as to warrant a brief description.

A. VISIBLE AND NEAR IR SPECTROMETER

The visible and near infrared spectrometer is mounted as a single integral unit on an optical bench, the axis of which is parallel to the axis of the input slit of the monochromator.

In Fig. 41, the monochromator (A) is a Bausch & Lomb Model 33-86-40, 150-mm quartz grating instrument containing a 600-line/mm reflection replica grating blazed for 7500 Å in first order. The dispersion is 66 Å/mm and the optical aperture, f/4. This monochromator is provided with a sine drive and a calibrated linear wavelength drum having a range of 2000 Å/rev. Attached to the wavelength drum through a ball-race sliding coupling is a commutator of 20 equal segments to provide 100-Å wavelength markers. This commutator is rigidly coupled to an electromagnetic clutch, the opposite end of which carries a ball-chain gear. The gear is driven by a ball chain, the lower end of which engages a ball-chain gear on the paper-drive drum of a Varian G-14 strip chart recorder (E). The gear ratio is arranged so that 0.4 inch of paper travel will move the wavelength drum a distance equivalent to 100 Å. The gears can, of course, be changed to provide different scale factors when required. Normally, the paper is driven at a rate of 1 in./min, giving a wavelength rate of change of 250 Å/min which is suitable for all but very sharp weak lines where electronics cannot follow. In these cases, the chart may be driven at 1/2 in./min.

Actual resolution of the monochromator is limited, not by the theoretical resolution of the grating, but rather by nonparallelism of the slits,

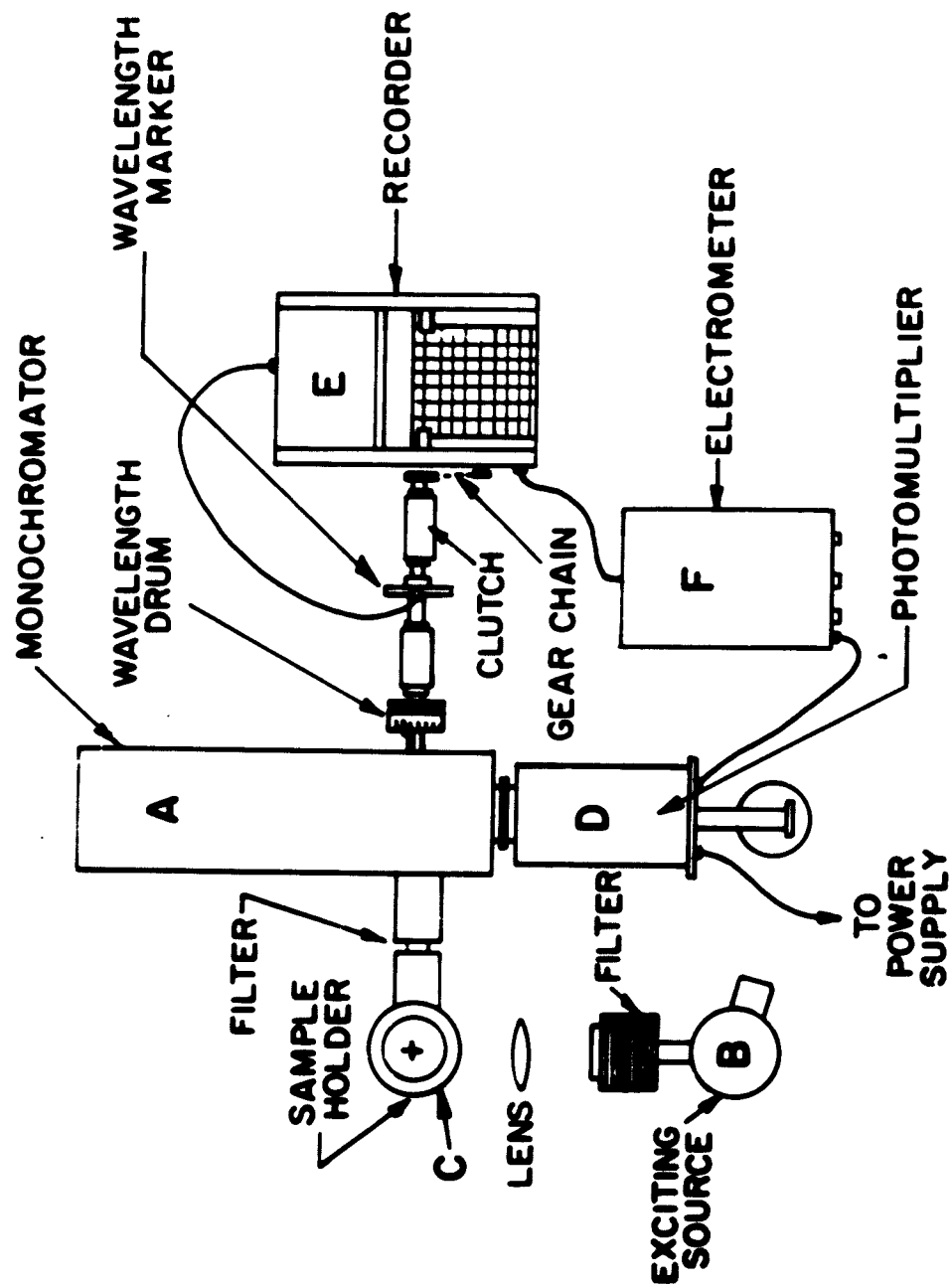


Fig. 41. Visible and near IR spectrometer

adjustment of which is impractical. However, the instrument has wedge-shaped diaphragms located behind each slit which may be employed for reduction of the slit height. With high-intensity signals one can observe spectra while using only the central few millimeters of the slits, in which case the nonparallelism is less important. The sine drive, which provides the linear wavelength scale on the drum, tracks rather well but is subject to some wear and slippage resulting in a calibration shift which can be corrected either by mechanically displacing the wavelength drum or by calibration using known spectral lines. A typical example of the latter procedure is illustrated in Fig. 42 where resolution, tracking, and wavelength precision are measured. In this case, an Osram Hg spectral lamp was used as the source. The mean wavelength correction is $+30.1 \text{ \AA}$ (which has been applied where necessary to spectra in this report) with a deviation from the arithmetic mean of $\pm 2.4 \text{ \AA}$ over the entire scale. The slit setting error is $+ 0.05 \text{ mm}$, and the resolution is within the limit imposed by the width of the ink line in the wavelength scale most usually employed ($100 \text{ \AA}/0.4 \text{ in.}$) and amounts to about 3 \AA .

The detector (D) is a photomultiplier having either S-20 or S-1 response. For most work, the photomultiplier having S-1 response, cooled to liquid nitrogen temperature (see below), was used.

The sample is mounted in a Dewar (C) which is held in a light-tight holder, rigidly fastened to the monochromator and the optical bench, and equipped with access ports for exciting light on the axis of the optical bench and at 90° to it. Excitation sources are mounted separately with appropriate filters and focusing optics.

B. IR SPECTROMETER

The physical arrangement of the infrared spectrometer is identical with that of the visible instrument (Fig. 43). The essential differences are the following. The grating is blazed for 2 \mu in first order and has 300 lines/mm. The first order dispersion is, then, $132 \text{ \AA}/\text{mm}$. The detector (D) is a lead sulfide cell (EK 40-2), cooled to dry-ice temperature. The synchronous detection system operates at 75 cps determined by a chopper located in front of the entrance condenser of the monochromator. The chopper also generates a 75-cps reference signal by means of a small light source and photocell mounted on it. The output of the lead sulfide cell is amplified by a two-stage vacuum tube amplifier which feeds into a PAR Model JB-5 lock-in amplifier.

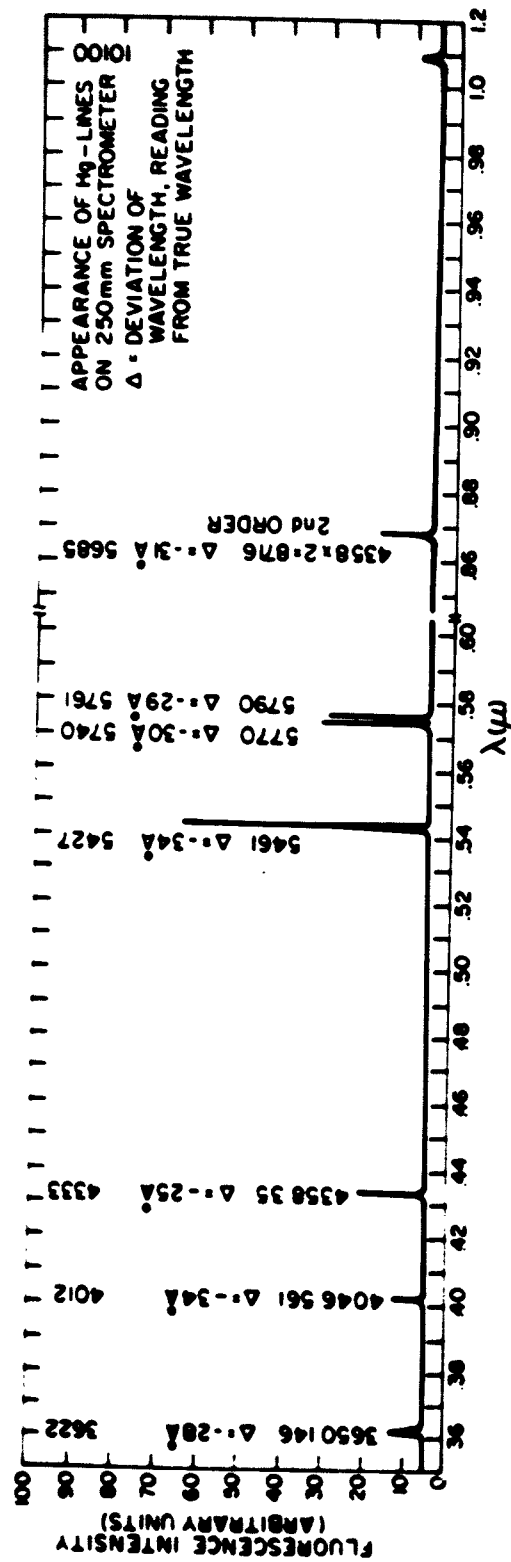


Fig. 42. Tracking and resolution of visible and near IR spectrometer

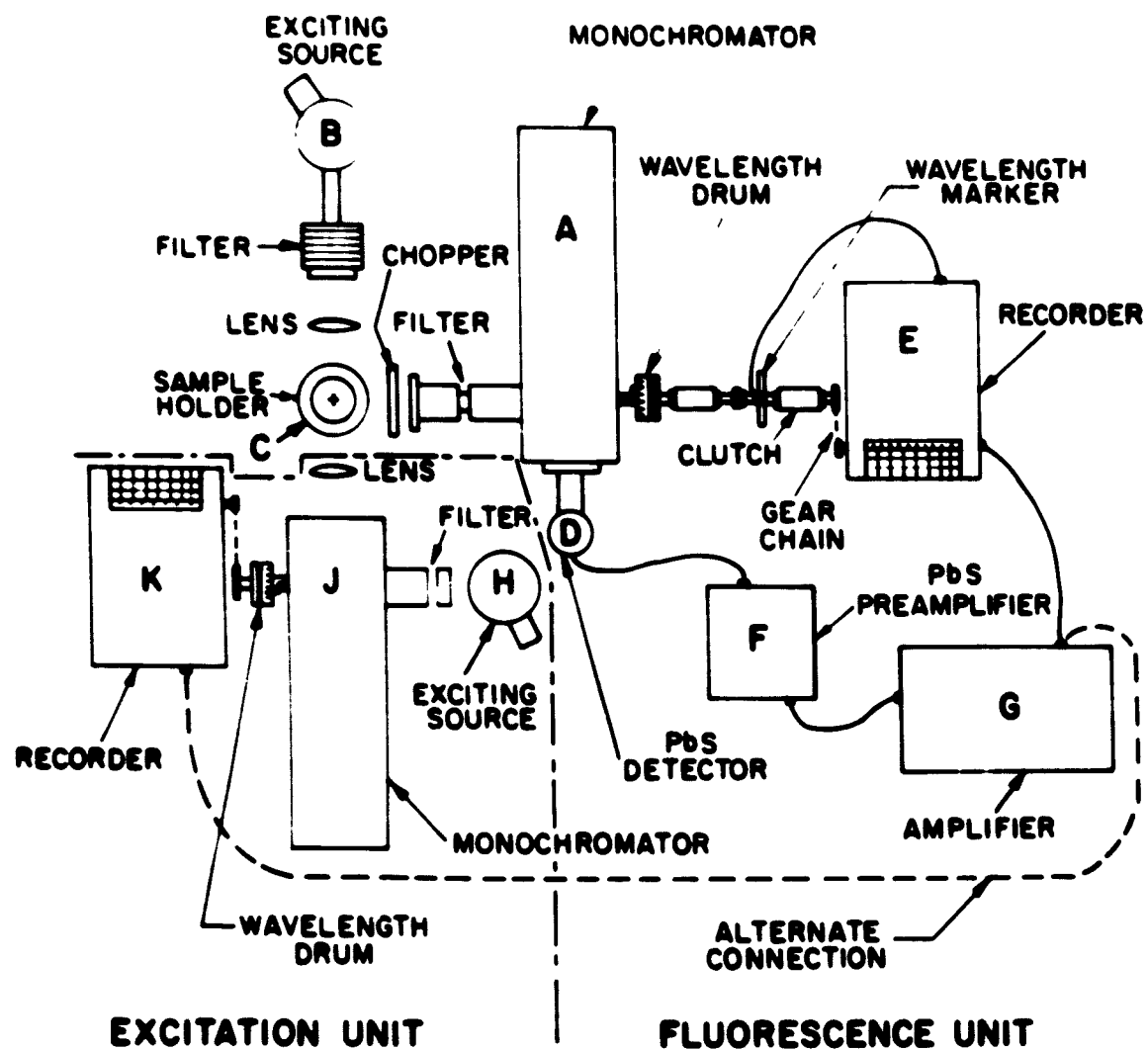


Fig. 43. IR spectrometer

C. EXCITATION SPECTROMETER

The measurement which we designate as excitation spectrometry involves the determination of the dependence of the fluorescence intensity of a given spectral line on the wavelength of the exciting light. These spectra are of particular value because through them one can sort out impurity fluorescence from fluorescence of the ion of interest, detect site multiplicity, distinguish between divalent and trivalent ions, and determine the spectral range over which the selected fluorescent line can be excited. Further, the excitation spectrum usually corresponds closely to the absorption spectrum of the ion of interest. In cases where the material under study is of poor optical quality or where it is very weakly absorbing, the excitation technique is the only way in which information can be obtained regarding the absorption behavior.

The excitation spectrometer is shown in position for measurement of infrared lines in Fig. 43. Because this unit must be moved between the visible and the infrared spectrometer depending on the wavelength of the spectral line of interest, it is considerably less elaborate in design than the fluorescence units. It consists of a 250-mm B & L monochromator (J) having a 600-line/mm grating blazed to peak at 3000 \AA , mounted on a section of optical bench. A bead chain couples the wavelength drum directly to a strip chart recorder (K) chart drive. Wavelength markers are introduced manually. The light source may be either an incandescent tungsten lamp or a high-pressure xenon arc, depending on the spectral range of interest, with filters to minimize scattered light. Detection of the (analyzed) fluorescence is by the appropriate detector through the second monochromator, which remains at a fixed wavelength.

D. LIFETIMES

Fluorescent lifetimes are measured by exciting the sample with a short burst of light from a pulsed xenon arc and viewing the time dependence of the intensity of the selected spectral line on an oscillograph. Selection of the spectral line is by means of the appropriate fluorescence spectrometer, and the fluorescence intensity is recorded photographically. The lifetime is computed graphically by replotting the photographed pulse as $\log I$ vs. t , assuming exponential behavior unless significant deviations are observed, and

defining the lifetime as that time necessary for the intensity to fall by a factor of $1/e$.

The pulsed light source consists of a simple relaxation oscillator composed of a 0.1- μ F capacitor in series with a 10-M Ω resistor and in parallel with a high-pressure (Hanovia type 901C-1) dc xenon arc. The arc lamp is mounted directly on the capacitor with very short heavy leads to minimize inductive effects and radiation. The system is operated by a 15-kV power supply, and trigger pulses are obtained across a small inductance in series with one of the lamp leads. Pulses of 2- μ sec duration and adequate intensity for most purposes are produced by this device.

E. LIGHT SOURCES

The light source which is most generally used for fluorescence measurements is an Osram HBO-500 high-pressure mercury arc. The arc is mounted in a cylindrical shield which is cooled by forced air. The exit port has mounted on it a water-cooled filter cell having quartz windows and which can be filled either with water or CuSO_4 solution depending on the spectral range desired. Additional Corning glass filters may be mounted on the front of this cell. The arc is focused on the sample by a wide-aperture quartz or glass lens, depending on the application. The lamp is powered from the laboratory 130-V dc mains through a water-cooled (Cenco 32965-1) ballast resistor.

Because of the high pressure in the HBO-500, the intensity of the 2537- \AA radiation is very low. Excitation in this range is accomplished by means of a conventional small "germicidal" mercury lamp filtered by a Corning 7-54 filter and focused by means of a quartz lens.

The most useful continuous and quasi-continuous light sources are the PEK X-200 xenon compact arc and the 625-watt Sylvania "Sun-Gun" quartz-iodine tungsten lamp. Mounts for these lamps are similar to that for the high-pressure mercury lamp. In the case of the xenon arc, the integral water-cooled filter may be omitted, and a close-mounted f/1 quartz condenser lens replaces it.

F. DETECTORS

The detectors which were employed are of three types: photomultiplier tubes, PbS photoconductive cells, and a thermopile.

1. Photomultiplier Tubes

The photomultiplier having the highest quantum efficiency and lowest noise over the spectral range from the near ultraviolet to about 8000 \AA is that having an S-20 photosurface such as the RCA 7263. The upper wavelength limit of this tube, however, imposes a limitation which is undesirable for many of the systems of concern in this study. While the PbS cell overlaps this range well and extends into the infrared to beyond 3μ , our arbitrary upper limit, its intrinsically lower sensitivity makes it undesirable in the range where photomultipliers can be employed. The sensitivity of the S-1 photosurface (RCA 7102) extends from the near ultraviolet to 1.2μ . Unfortunately, the quantum efficiency and noise levels are much lower than with the S-20 surface. If, however, the photosurface is cooled, the noise level drops to the point where it is possible in a dc detection system, to make up for the lower sensitivity through external amplification. Accordingly, a cooling mount was designed and constructed for this tube. The mount is illustrated in Fig. 44. It consists of a cylindrical brass shell (A) in which is suspended a second cylindrical shell (B) having a hollow wall. The shell is suspended on a thin-walled stainless steel tube which communicates only between the annulus and the outside (C), and is supported at its back end on three needle points. The photomultiplier (with base removed) (D) is thrust through the opening in the inner cylinder and held in place by phosphor-bronze spring shims. A radiation shield (E) closes the back end of the cylinder, and the photomultiplier leads are brought out through Teflon-lined openings (F). It should be noted that the radiation shield is essential for stable operation in preventing heating of the photocathode by radiation from the voltage divider which is mounted behind it. The voltage divider is made up of ten $50\text{-k}\Omega$ Victoreen glass-encapsulated resistors (G) soldered directly to the photomultiplier leads. The anode connection and the negative high-voltage lead are brought out the back of the mount through glass feedthroughs which are terminated outside in BNC connectors (H). The front port is closed by a $1\text{-}1/2\text{-in.}$ quartz window held in place by O-ring seals. The entire inner

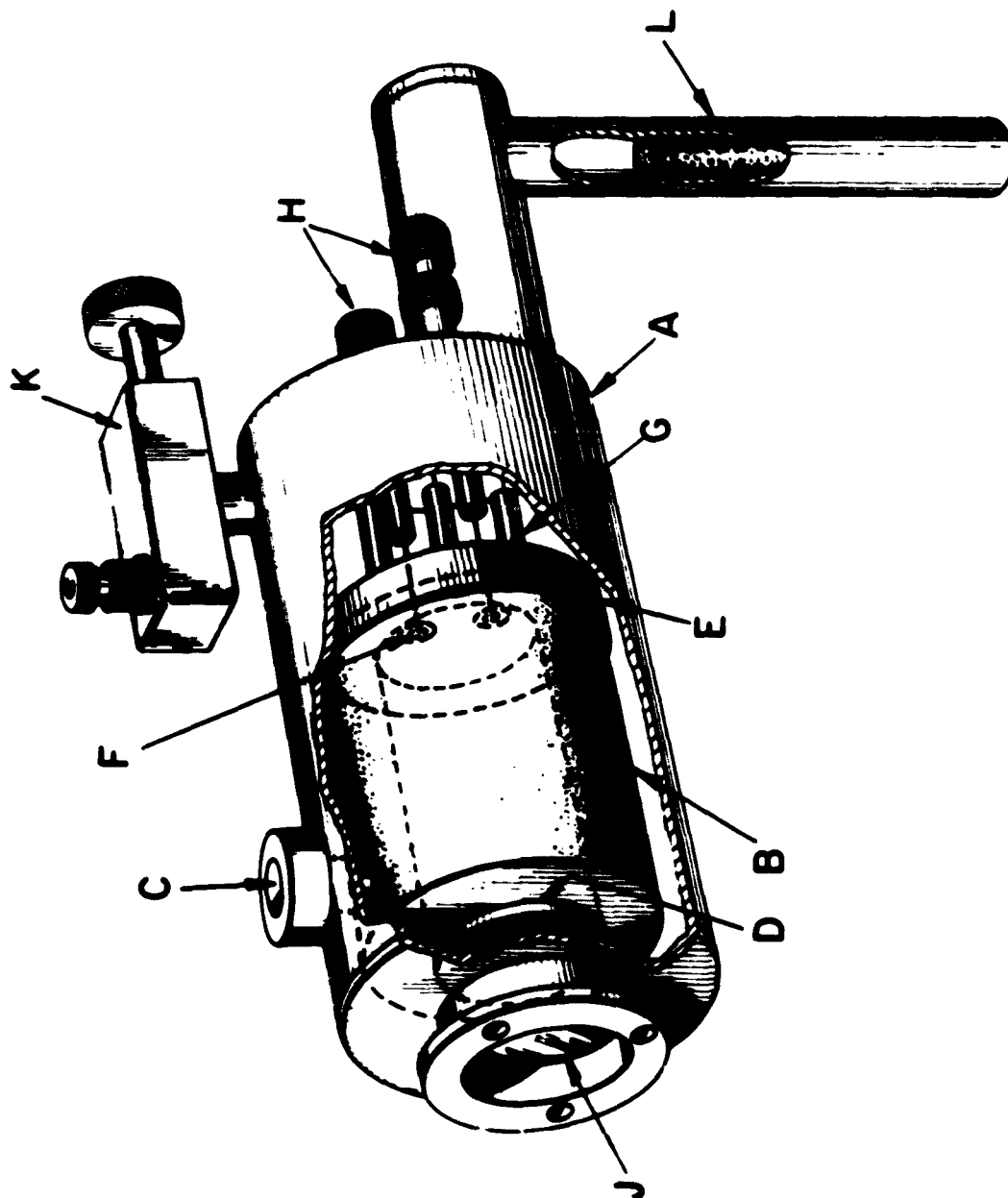


Fig. 44. Cooled photomultiplier

surface of the mount is chrome-plated for additional radiation shielding. The mount is evacuated through a valve and pumping port (K) situated on the top of the outer cylinder. Since it is not possible to outgas the interior of the mount, provision has been made for continuous pumping by means of an absorption pump (L) filled with Linde molecular sieve. It is important to maintain a good vacuum inside the mount, not only for thermal isolation, but also for the prevention of electrical noise caused by ionization of residual gas.

The mount is prepared for use by pumping with a diffusion pump overnight while the sieve finger is held at 350 °C by an electrical heater. The valve is then closed and the system permitted to cool. In operation, the sieve finger is immersed in a Dewar filled with liquid nitrogen, and the annulus filled with liquid nitrogen. [Once pumped down, the mount need not be repumped (except for that produced by cooling of the sieve finger during operation) for at least six months.] When the interior of the mount and the multiplier tube have reached thermal equilibrium with the liquid nitrogen bath, the dark current of the photomultiplier will have dropped from its room temperature value (at 1100 volts overall) of about 10^{-6} ampere to 10^{-13} ampere. This low dark current will remain constant after about 20 minutes of cooling with only occasional replenishment of the nitrogen in the annulus. This value of dark current is one order of magnitude lower than the weakest fluorescence we have observed and at least two orders of magnitude lower than the level of significant fluorescence (i.e., intensities that are clearly above background fluorescence of the Dewars and mounts). It is therefore possible, with this system, to cover continuously the spectral range from 3500 Å to 1.2 μ using a simple electrometer (e.g., Kiethley Model 610A) as the photomultiplier amplifier.

2. PbS Cell and Thermopile

For measurements beyond 1.2 μ a PbS cell was employed (EK, type O-2) mounted on a copper block in the vacuum space of a small Dewar. Cooling was by means of a dry-ice acetone mixture.

Energy calibration of the spectrometers and light sources was accomplished with the aid of a Reeder type O-7 thermopile, the output of which was measured directly on a Kiethley Model 150A microvoltmeter.

G. FILTERS

Optical filters were employed throughout this study for separation of orders in the spectrometers, for removal of heat from light sources, for isolation of exciting light from fluorescence, and for reduction of scattered light in the spectrometers. Frequently, these filters were simply selected from among the commercially available Corning glass filters. Most often, however, the Corning filters were used in conjunction with either of two liquid filters, saturated CuSO_4 solution or distilled water.

The copper sulfate filter served two purposes. First, with the HBO-500 lamp it was necessary to remove the large amount of heat generated by the lamp to protect associated optical equipment from overheating. Second, all the Corning ultraviolet filters exhibit an additional pass band in the visible red and infrared. The copper sulfate filter with its strong cut-off in the red (Fig. 45) eliminates the danger of confusing fluorescence spectra in this spectral region with lamp light scattered from the sample.

Under circumstances where red light was required, as in excitation spectra, for example, but where high-temperature light sources were involved, a filter of distilled water was employed. This filter has the disadvantage of moderately strong absorption around 0.97μ (Fig. 46), but the absorption is not so intense as to preclude correction for it.

Two additional filters were found to be useful as order separators above 1μ . This is an especially critical range since our infrared grating is blazed to peak at 2μ in first order and 1μ in second order. These filters consist of polished, 3-mm-thick pieces of high-purity silicon and germanium. Absorption spectra for these filters are illustrated in Fig. 47.

H. CALIBRATION

In general, for these studies, intensity calibration of the fluorescence spectrometer is not considered important, since the essential analytical information rests in line locations and relative widths. Further, because of the limited resolving power of the instruments, the precision of absolute intensity and efficiency measurements is questionable, and such studies should be carried out on a higher-quality spectrometer. In the measurement of excitation spectra, however, particularly where broad excitation bands are

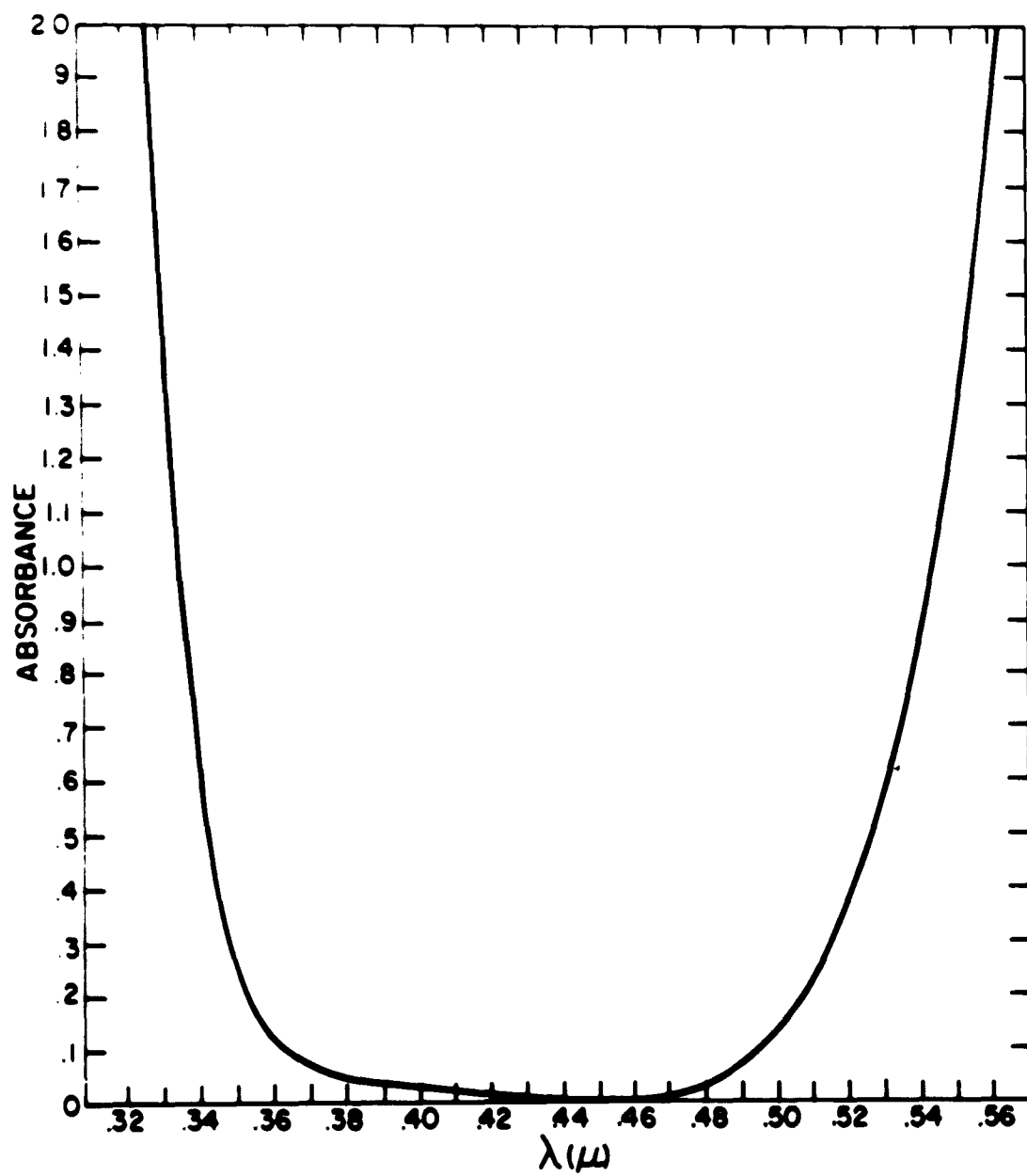


Fig. 45. Absorption spectrum of 5 cm saturated CuSO_4 solution

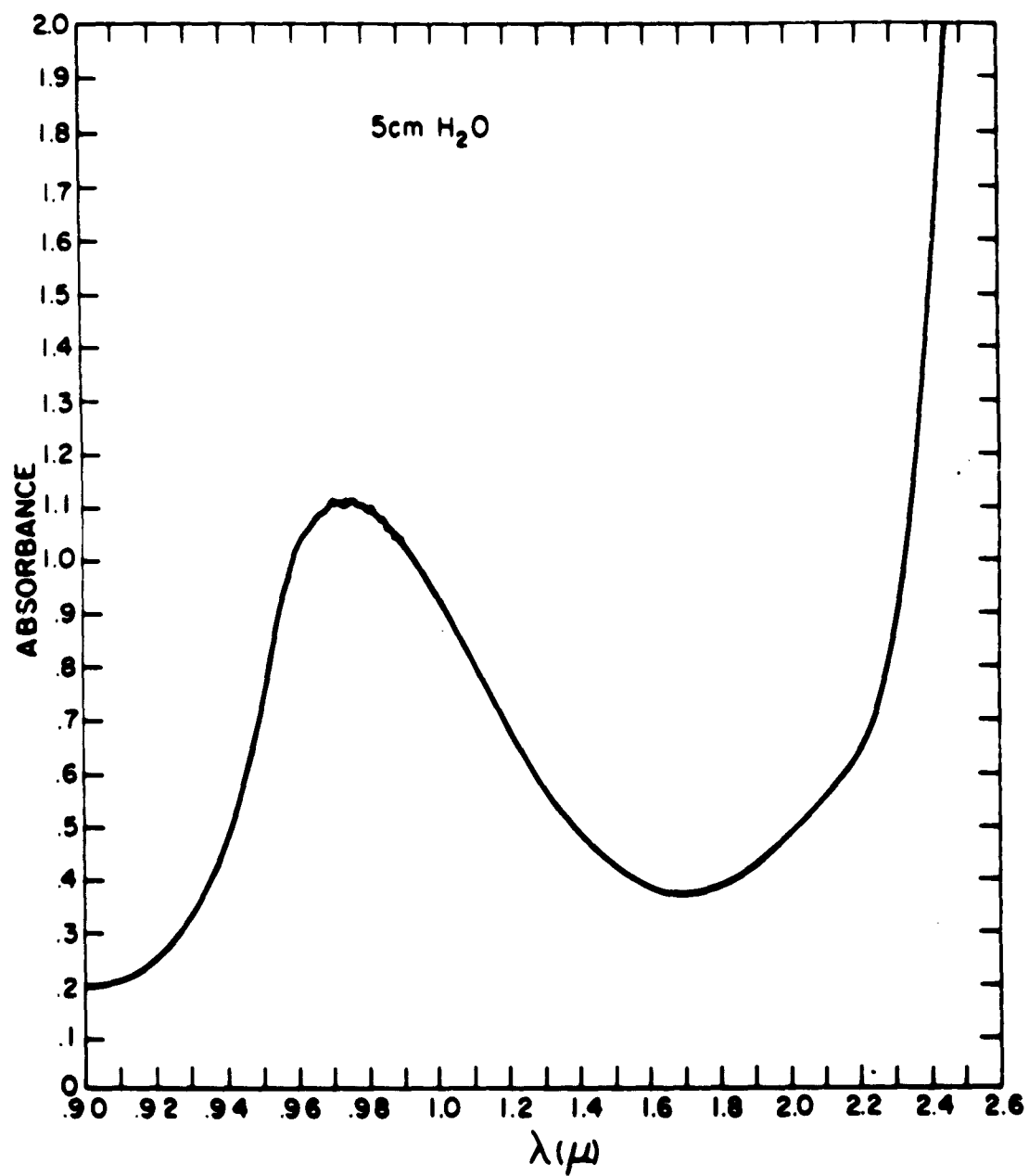


Fig. 46. Absorption spectrum of H₂O

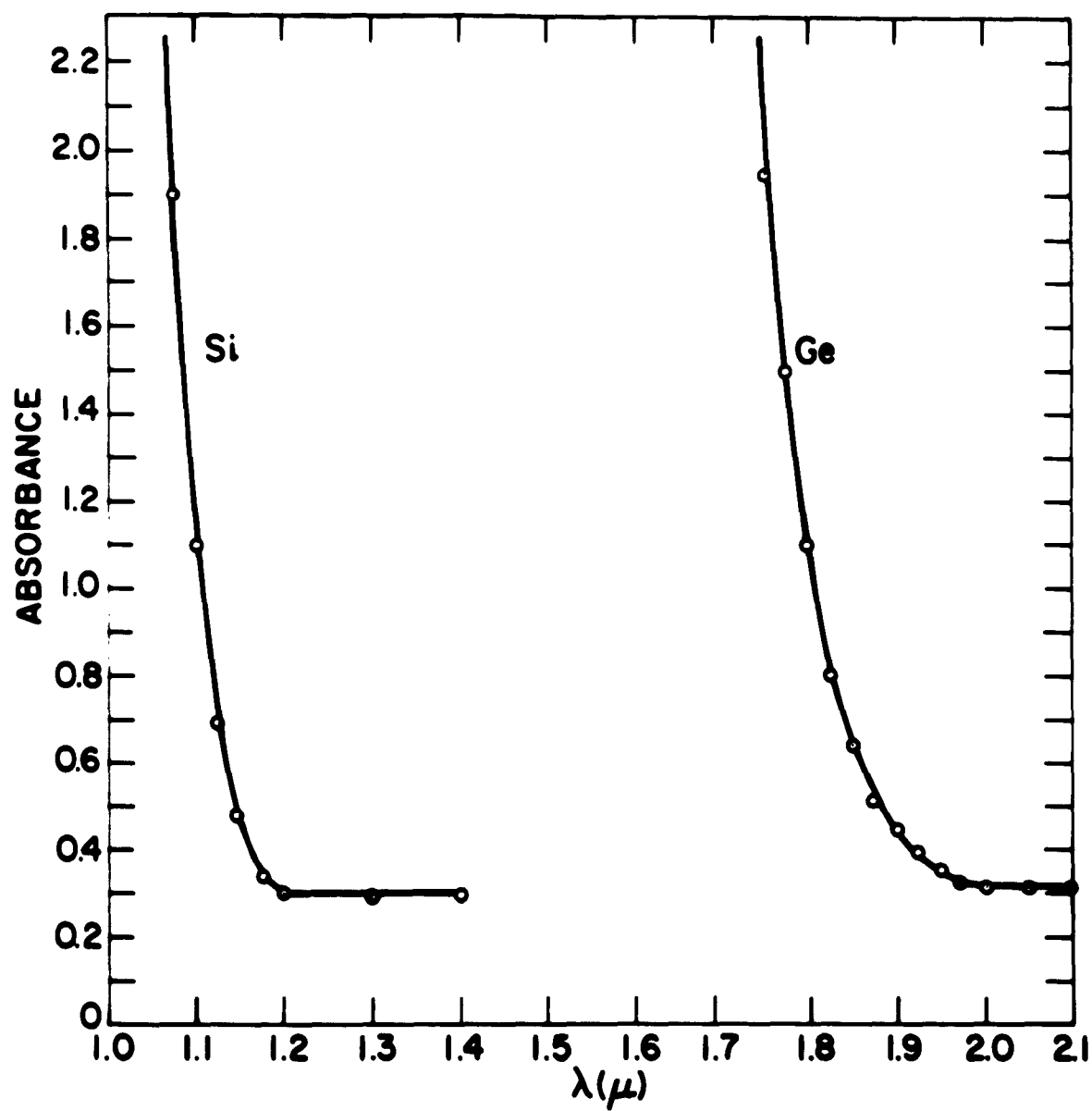


Fig. 47. Absorption spectra of Si and Ge filters

involved, it is necessary to have information concerning the wavelength dependence of the intensity of the exciting light.

Two different light sources were employed in taking excitation spectra, a 625-watt Sylvania "Sun-Gun" quartz-iodine tungsten lamp, and a 200-watt FEN X-200 xenon compact arc. The former source is useful above 3500 Å, and the latter, below this wavelength. Calibration of the tungsten lamp-monochromator combination was performed through the use of the thermopile in a point-by-point measurement of the total energy. This was then converted to relative numbers of photons per unit time and so plotted (Fig. 48b).

In the region below 3500 Å, with the xenon lamp, advantage was taken of the fluorescence properties of the compound sodium salicylate which has constant quantum efficiency between 1800 and 3500 Å. The calibration curve for this system is illustrated in Fig. 48a.

The relative response of the combination 7500-Å blaze monochromator and cooled S-1 photomultiplier was then determined by impinging the output of the calibrated excitation spectrometer on the entrance slit of the second monochromator. The output for each wavelength was then recorded and normalized for equal numbers of photons. The resulting curve is illustrated in Fig. 49. It is of interest to note that the changes in sensitivity over the range studied are smooth without large changes in slope. It is therefore valid to assume that for sharp lines, there is no appreciable shift in the recorded spectra.

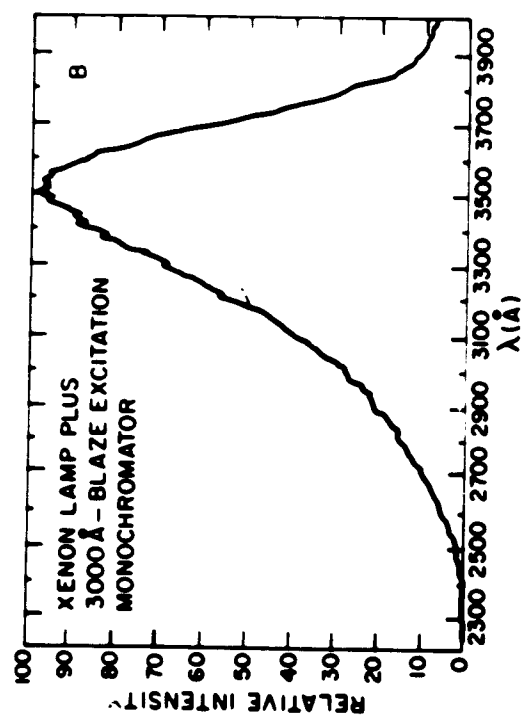
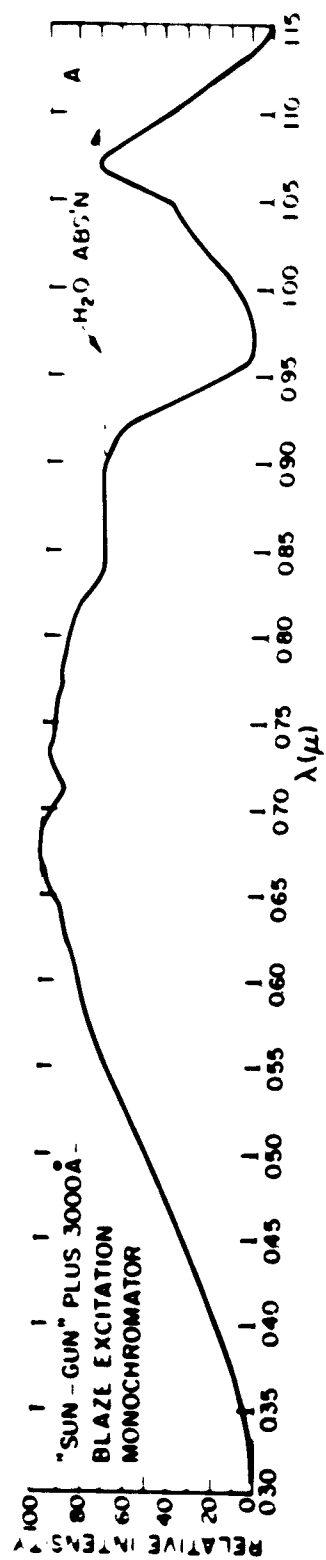


Fig. 48. Output calibration of excitation spectrometer

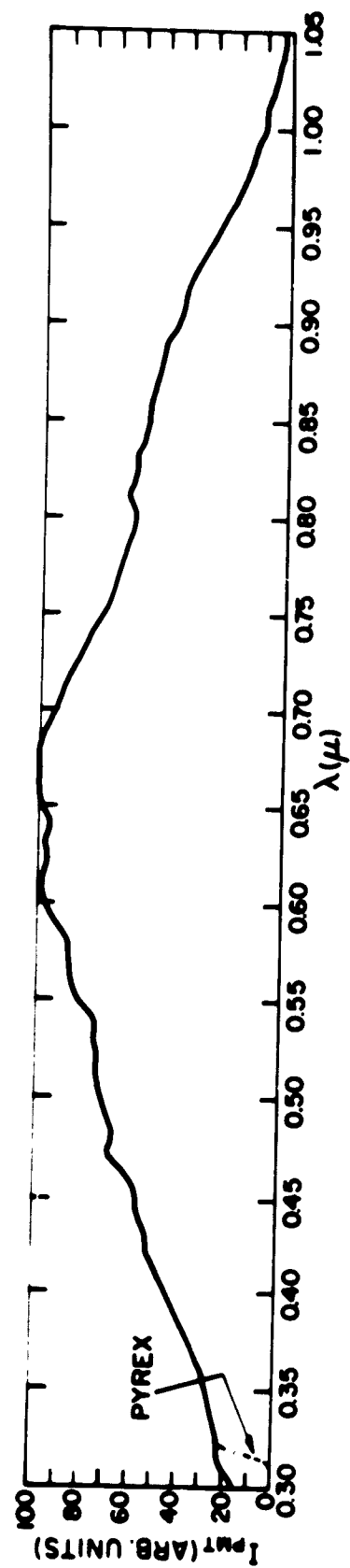


Fig. 49. Spectral sensitivity of 7500 Å-blaze spectrometer and S-1 photomultiplier tube

SECTION V

RECOMMENDATIONS FOR FURTHER WORK

As a consequence of the studies reported herein, a clear pattern for future work on divalent rare earth emerges. It should, at the outset, be recognized that with the exception of Sm^{2+} and the 5d-4f transitions in $\text{SrCl}_2:\text{Tm}^{2+}$, the ions which offer promise of exhibiting 4f-4f laser action, Dy^{2+} , Ho^{2+} , Er^{2+} , and Tm^{2+} , emit principally in the infrared. There is, then, little likelihood of producing laser action in the visible with these ions. The question of the oxidation-reduction mechanism is tentatively solved, but many questions remain unanswered. On the basis of our present understanding of the mechanism, however, crystal growth conditions which will optimize the incorporation of divalent rare earths can be specified. Of the hosts we have studied, BaClF , RbMgF_3 , and SrCl_2 stand out as the most satisfactory. Logical completion of these studies require the following experimental investigations.

A. GROWTH OF CRYSTALS IN SEALED METALLIC SYSTEMS

Either Bridgman or Czochralski techniques should be employed in systems which are as free of oxidizing impurities as the present state-of-the-art permits. In the Bridgman method, the technique of Miller et al.²⁵ should be employed in which the crystallization is carried out in welded tantalum or molybdenum capsules which have been manipulated, filled, and welded shut in a dry box containing scrupulously dried and deoxidized inert gas. An excess of pure rare-earth metal reducing agent adequate to bring about reduction and to remove residual oxidizing agents should be used.

In the Czochralski technique, the apparatus should be tight and free of sources of oxidizing agents and again, preferably all metal. An advantage of this method lies in the ability to dope the melt very heavily with rare earth and rare-earth metal, thus maximizing the concentration of divalent rare earth in the melt which could then be extracted into the growing crystal.

B. DETAILED SPECTROGRAPHIC AND METALLOGRAPHIC STUDIES OF CRYSTALS GROWN UNDER THE ABOVE-MENTIONED CONDITIONS

Since the questions of disproportionation or electron trapping are not satisfactorily answered, investigations of crystals grown under the most

nearly ideal conditions attainable for the presence of color centers or free metal would shed much light on these problems.

C. QUENCHING STUDIES

Quenched samples of a priori reduced rare earth have always resulted in Ln^{2+} . This fact could be used as a check on the direct oxidation or disproportionation processes. In these experiments, samples as identical as possible, using rare-earth metal as the reducing agent, would be heated to the molten state and quenched under identical conditions after varying periods of time in the molten state. If disproportionation is operative, then the Ln^{2+} concentration is relatively unchanged as a function of heating time. If direct oxidation is the mechanism of Ln^{2+} loss, then a progressive decrease and possible total absence of Ln^{2+} with time of heating would be found.

D. HIGH-TEMPERATURE AND MOLTEN-STATE ABSORPTION SPECTROSCOPY

Direct and unequivocal answers to the problems of retention and stability of divalent rare earths can best be obtained with the aid of high-temperature absorption spectroscopy. This approach is useful in the study of the re-oxidation of Ln^{2+} in both the solid and liquid state. With this technique, the appearance and disappearance of either Ln^{2+} or Ln^{3+} as a function of temperature, time concentration of rare earth, host composition, and other conditions can be determined. The rate and extent of the reaction of the different lanthanides with externally introduced oxidizing or reducing agents can also be pursued. Specifically, the question of the formation of divalent rare-earth ions of the more difficult to reduce ions in the perovskites is a case in point. The conditions for self-reduction of samarium in various hosts is another problem which high-temperature absorption spectroscopy could help solve.

The equilibrium constants for the reduction of trivalent rare earth by hydrogen, as in the case of Dy and Ho in BaClF is another problem which is amenable to this technique. From observations on the kinetics of the loss of Ln^{2+} during annealing or cooling from the molten state, the mechanism of the oxidation process could be deduced.

Although the methods of high-temperature absorption spectroscopy are difficult, a mark of the progress of the state of research in this field is the commercial availability of a semi-automatic recording spectrophotometer specifically designed for measurements to 1450°C.²⁶ Morrey and Madsen²⁷ have reviewed the problems of furnace design, and Gruen and coworkers²⁸ have investigated the oxidation states of transition metal ions and actinide ions in fused salts by absorption spectroscopy.

E. 5d FLUORESCENT STATES, VIBRONIC TRANSITIONS AND COLOR CENTERS

The promise for new laser mechanisms held out by our observations of sharp vibronic levels in forbidden 5d transitions of Tm^{2+} suggests that considerably more exploratory work should be carried out on systems of this nature. Further spectroscopic and resonance studies should be pursued in order to gain a deeper understanding of these phenomena.

Yet another source of fluorescent states and pumping bands which we have encountered in the course of our studies are color centers of various kinds, the nature of which is not known. These centers may play a significant role in the luminescent phenomena of interest.

F. DIVALENT RARE-EARTH-CONTAINING PEROVSKITES

A family of perovskites which were not investigated but which would readily incorporate divalent rare earth with almost perfect size match is $AYbF_3$. A is an alkali metal ion. The ytterbium here is divalent and the compound is readily prepared by fusing AF and YbF_3 under hydrogen. Calculation of the tolerance factors for this group of compounds shows that $NaYbF_3$ would probably not form, $KYbF_3$ and $RbYbF_3$ would be cubic perovskites and $CsYbF_3$ would be noncubic. The congruently melting compound $KYbCl_3$ has been prepared.²⁹

G. GENERAL RARE-EARTH STUDIES

Finally, it should be recognized that rare earths are becoming of increasing importance in other classes of electronically active solids such as magnetics, cathodoluminescent materials, infrared quantum counters, semiconductors, and dielectrics. It is, therefore, basic to further progress in these areas that a complete understanding of the chemistry of these elements be obtained.

REFERENCES

1. L. F. Johnson, G. D. Boyd, K. Nassau, and R. R. Soden, *Phys. Rev.* 126, 1406 (1962).
2. Z. J. Kiss and R. C. Duncan, *Appl. Phys. Letters* 5, 200 (1964).
3. A. L. Shawlow and C. H. Townes, *Phys. Rev.* 112, 1940 (1958).
4. Z. J. Kiss and P. N. Yocom, *J. Chem. Phys.* 41, 1511 (1964).
5. F. K. Fong, *RCA Review* 25, 303 (1964).
6. H. Guggenheim and J. V. Kane, *Appl. Phys. Letters* 4, 172 (1964).
7. H. L. Pinch, *J. Amer. Chem. Soc.* 80, 3167 (1964).
8. D. S. McClure and Z. J. Kiss, *J. Chem. Phys.* 39, 3251 (1963).
9. H. A. Klasens, P. Zalm, and F. O. Huysman, *Philips Res. Rep.* 8, 441 (1953).
10. R. E. Thoma, *Inorg. Chem.* 1, 220 (1962).
11. B. V. Strum, Reactor Chem. Div., Ann. Prog. Rep., January 31, 1962, ORNL 3262, p. 19.
12. P. F. Weller, J. D. Axe, and G. O. Pettit, *J. Electrochem. Soc.* 112, 74 (1965).
13. L. Ekstrom and L. R. Weisberg, *J. Electrochem. Soc.* 109, 321 (1963).
14. F. J. Norton and S. A. Seybolt, *Trans. Met. Soc. AIME* 230, 595 (1964).
15. L. F. Druding and J. D. Corbett, *Inorg. Chem.* 2, 869 (1963).
16. L. F. Druding and J. D. Corbett, *J. Am. Chem. Soc.* 83, 2462 (1961).
17. G. J. Novikov and O. G. Polyachenok, *Russ. J. Inorg. Chem.* 8, 545 (1963).
18. O. G. Polyachenok and G. J. Novikov, *Russ. J. Inorg. Chem.* 8, 816 (1963).
19. L. B. Asprey and F. H. Kruse, *J. Inorg. Nuclear Chem.* 13, 32 (1960).
20. J. Arends, *Phys. Stat. Solidi* 7, 805 (1964).
21. D. S. McClure, "Electronic Spectra of Molecules and Tons in Crystals, Part II. Spectra of Tons in Crystals" in Advances in Solid State Physics, Vol. 9, p. 469 (1959).
22. Z. J. Kiss, *Proc. IRE* 50, 1531 (1962).
23. G. J. Goldsmith et al., in A Research Program on The Utilization of Light, Technical Documentary Report No. ASD-TDR-63-529, p. 105, April 1963.
24. Z. J. Kiss et al., Solid State Laser Explorations, Interim Engineering Report No. 1, p. 32, February 1, 1964.
25. A. E. Miller et al., *Rev. Sci. Instr.* 34, 644 (1963).
26. Cary Model 14-H, Bulletin No. 114-H, Applied Physics Corporation, Monrovia, California.
27. J. R. Morrey and A. W. Madsen, *Rev. Sci. Instruments* 32, 799 (1961).

REFERENCES (Cont'd)

28. D. M. Gruen, R. L. McBeth, J. Kooi, and W. T. Carnall, Ann. N.Y. Acad. Sci. 79, Art. 11, 941 (1960).
29. G. I. Novikov, O. G. Polyachenok, and S. A. Frid, Zh. Neorg. Khim 9, 472 (1964).

UNCLASSIFIED

Security Classification

DOCUMENT CONTROL DATA - R&D		
<i>(Security classification of title, body of abstract and indexing annotation must be entered when the overall report is classified)</i>		
1. ORIGINATING ACTIVITY (Corporate author) Radio Corporation of America RCA Laboratories Princeton, New Jersey		2a. REPORT SECURITY CLASSIFICATION UNCLASSIFIED
		2b. GROUP N/A
3. REPORT TITLE Divalent Rare-Earth Ions in Optical Maser Materials		
4. DESCRIPTIVE NOTES (Type of report and inclusive dates) Final Report for the period July 1, 1963 to January 15, 1965		
5. AUTHOR(S) (Last name, first name, initial) Goldsmith, George J., and Pinch, Harry L.		
6. REPORT DATE April 1965	7a. TOTAL NO. OF PAGES 112	7b. NO. OF REFS 29
8a. CONTRACT OR GRANT NO. AF33(657)-11221	9a. ORIGINATOR'S REPORT NUMBER(S) FINAL REPORT	
b. PROJECT NO. 7371		
c. Task No. 737101	9b. OTHER REPORT NO(S) (Any other numbers that may be assigned this report) AFML-TR-65-115	
10. AVAILABILITY LIMITATION NOTICES Qualified users may obtain copies of this report from DDC. DDC release to CPSTI is not authorized.		
11. SUPPLEMENTARY NOTES		12. SPONSORING MILITARY ACTIVITY Air Force Materials Laboratory Research and Technology Division, AFSC Wright-Patterson Air Force Base, Ohio
13. ABSTRACT This report describes a study of divalent rare earths in dilute solid solution in hosts suitable for fabrication into optical maser oscillators. Previous Semiannual Progress Reports under this Contract are summarized. As the program progressed, the effort continually converged on the materials and problems which appeared to be most critical and which offered the highest probability of success. Therefore, this report concentrates primarily upon the systems $BaClF:Ln^{2+}$ and $ABF_3:Ln^{2+}$ (where A = alkali-metal ion, and B = alkaline-earth ion), those compounds selected as best suited to our objectives. The problems were in three major categories: reduction of the rare earth from the normal trivalent to divalent, incorporation of the desired ion into the host with retention of the desired valence state, and the growth of single crystals of suitable optical quality. The first and third categories were satisfactorily solved in many cases, while the second was solved only to a limited extent. On the basis of these studies, one can specify in some detail the materials in which, and the conditions under which, this second aspect of the problem can be successfully solved. While most of the studies involved conventional physical and chemical measurements and procedures, some apparatus were designed and constructed which became of sufficiently general utility throughout the laboratories to warrant a brief description of their construction and performance. Also included are the relevant calibration measurements necessary for a thorough understanding of the experimental procedures and results.		

DD FORM 1473

UNCLASSIFIED

Security Classification

UNCLASSIFIED
Security Classification

KEY WORDS	LINK A		LINK B		LINK C	
	ROLE	WT	ROLE	WT	ROLE	WT
Optical masers Crystal growth Lasers Rare earth elements Lanthanides Fluorescence Divalent lanthanides						

INSTRUCTIONS

1. ORIGINATING ACTIVITY: Enter the name and address of the contractor, subcontractor, grantee, Department of Defense activity or other organization (*corporate author*) issuing the report.

2a. REPORT SECURITY CLASSIFICATION: Enter the overall security classification of the report. Indicate whether "Restricted Data" is included. Marking is to be in accordance with appropriate security regulations.

2b. GROUP: Automatic downgrading is specified in DoD Directive 5200.10 and Armed Forces Industrial Manual. Enter the group number. Also, when applicable, show that optional markings have been used for Group 3 and Group 4 as authorized.

3. REPORT TITLE: Enter the complete report title in all capital letters. Titles in all cases should be unclassified. If a meaningful title cannot be selected without classification, show title classification in all capitals in parenthesis immediately following the title.

4. DESCRIPTIVE NOTES: If appropriate, enter the type of report, e.g., interim, progress, summary, annual, or final. Give the inclusive dates when a specific reporting period is covered.

5. AUTHOR(S): Enter the name(s) of author(s) as shown on or in the report. Enter last name, first name, middle initial. If military, show rank and branch of service. The name of the principal author is an absolute minimum requirement.

6. REPORT DATE: Enter the date of the report as day, month, year, or month, year. If more than one date appears on the report, use date of publication.

7a. TOTAL NUMBER OF PAGES: The total page count should follow normal pagination procedures, i.e., enter the number of pages containing information.

7b. NUMBER OF REFERENCES: Enter the total number of references cited in the report.

8a. CONTRACT OR GRANT NUMBER: If appropriate, enter the applicable number of the contract or grant under which the report was written.

8b, 8c, & 8d. PROJECT NUMBER: Enter the appropriate military department identification, such as project number, subproject number, system numbers, task number, etc.

9a. ORIGINATOR'S REPORT NUMBER(S): Enter the official report number by which the document will be identified and controlled by the originating activity. This number must be unique to this report.

9b. OTHER REPORT NUMBER(S): If the report has been assigned any other report numbers (*either by the originator or by the sponsor*), also enter this number(s).

10. AVAILABILITY/LIMITATION NOTICES: Enter any limitations on further dissemination of the report, other than those imposed by security classification, using standard statements such as:

- (1) "Qualified requesters may obtain copies of this report from DDC."
- (2) "Foreign announcement and dissemination of this report by DDC is not authorized."
- (3) "U. S. Government agencies may obtain copies of this report directly from DDC. Other qualified DDC users shall request through _____."
- (4) "U. S. military agencies may obtain copies of this report directly from DDC. Other qualified users shall request through _____."
- (5) "All distribution of this report is controlled. Qualified DDC users shall request through _____."

If the report has been furnished to the Office of Technical Services, Department of Commerce, for sale to the public, indicate this fact and enter the price, if known.

11. SUPPLEMENTARY NOTES: Use for additional explanatory notes.

12. SPONSORING MILITARY ACTIVITY: Enter the name of the departmental project office or laboratory sponsoring (*paying for*) the research and development. Include address.

13. ABSTRACT: Enter an abstract giving a brief and factual summary of the document indicative of the report, even though it may also appear elsewhere in the body of the technical report. If additional space is required, a continuation sheet shall be attached.

It is highly desirable that the abstract of classified reports be unclassified. Each paragraph of the abstract shall end with an indication of the military security classification of the information in the paragraph, represented as (TS), (S), (C), or (U).

There is no limitation on the length of the abstract. However, the suggested length is from 150 to 225 words.

14. KEY WORDS: Key words are technically meaningful terms or short phrases that characterize a report and may be used as index entries for cataloging the report. Key words must be selected so that no security classification is required. Identifiers, such as equipment model designation, trade name, military project code name, geographic location, may be used as key words but will be followed by an indication of technical content. The assignment of links, rules, and weights is optional.

UNCLASSIFIED
Security Classification